

THESIS

THE IMPACT OF REFORESTATION IN THE NORTHEAST UNITED STATES ON
PRECIPITATION AND SURFACE TEMPERATURE

Submitted by

Allyson Clark

Department of Atmospheric Science

In partial fulfillment of the requirements

For the Degree of Master of Science

Colorado State University

Fort Collins, Colorado

Spring 2013

Master's Committee:

Advisor: David Randall

A. Scott Denning
Dan Binkley

ABSTRACT

THE IMPACT OF REFORESTATION IN THE NORTHEAST UNITED STATES ON PRECIPITATION AND SURFACE TEMPERATURE

Since the 1920s, forest coverage in the northeastern United States has recovered from disease, clearing for agricultural and urban development, and the demands of the timber industry. Such a dramatic change in ground cover can influence heat and moisture fluxes to the atmosphere, as measured in altered landscapes in Australia, Israel, and the Amazon. In this study, the impacts of recent reforestation in the northeastern United States on summertime precipitation and surface temperature were quantified by comparing average modern values to 1950s values. Weak positive (negative) relationships between reforestation and average monthly precipitation and daily minimum temperatures (average daily maximum surface temperature) were found. There was no relationship between reforestation and average surface temperature. Results of the observational analysis were compared with results obtained from reforestation scenarios simulated with the BUGS5 global climate model. The single difference between the model runs was the amount of forest coverage in the northeast United States; three levels of forest were defined – a grassland state, with 0% forest coverage, a completely forested state, with approximately 100% forest coverage, and a control state, with forest coverage closely resembling modern forest coverage. The three simulations were compared, and had larger magnitude average changes in precipitation and in all temperature variables. The difference in magnitudes between the model simulations observations was much larger

than the difference in the amount of reforestation in each case. Additionally, unlike in observations, a negative relationship was found between average daily minimum temperature and amount of forest coverage, implying that additional factors influence temperature and precipitation in the real world that are not accounted for in the model.

ACKNOWLEDGEMENTS

I would like to thank Dr. David Randall for his invaluable guidance and support and Drs. Scott Denning and Dan Binkley for their advice and time as members of my committee. Additionally, I would like to thank Dr. Ian Baker and Don Dazlich for their assistance in setting up and running the BUGS model simulation.

I would like to extend my thanks to my friends and parents who have supported my time dedicated to this project, with special thanks given to James Carpenter.

This research was supported in part by the National Science Foundation Science and Technology Center for MultiScale Modeling of Atmospheric Processes, managed by Colorado State University under cooperative agreement ATM-0425247.

TABLE OF CONTENTS

ABSTRACT..... ii

ACKNOWLEDGMENTS..... iv

TABLE OF CONTENTS..... v

LIST OF TABLES..... vii

LIST OF FIGURES..... viii

Chapter 1: Introduction..... 1

 1.1: Effects of Ground Cover on Atmospheric Quantities..... 1

 1.2: Global Reforestation Studies..... 5

 1.3: On the Northeast United States..... 14

 1.4: Summary of Literature..... 20

 1.5: Description of Project..... 22

Chapter 2: Methodology..... 24

 2.1: Historical Observations in the Northeast United States..... 24

 2.2: Modeling Reforestation in the Northeast United States..... 31

Chapter 3: Results of Observational Analysis..... 37

 3.1: Ground Cover Changes..... 37

 3.2: Precipitation..... 39

 3.3: Surface Temperature..... 43

 3.4: Summary..... 49

Chapter 4: Results of Model Analysis..... 52

 4.1: Analysis of the Effects of Ground Cover on Atmospheric Quantities 52

 4.2: Surface Fluxes..... 52

 4.3: Surface Temperature..... 62

4.4: Precipitation.....	68
4.5: Circulation Changes.....	70
4.6: Summary.....	80
Chapter 5: Discussion.....	93
5.1: Discussion.....	93
5.2: Future Work.....	97
REFERENCES.....	99
APPENDIX A.....	109

LIST OF TABLES

Table 2.1: Years of released inventory reports for each of the eight states included in the region of study.....	27
Table 3.1: Summary of relationships between listed variables and the fractional forest cover change between the present (2005-2010) and the 1950s (1950-1955). Each relationship was described as strong positive (negative), weak positive (negative), or no relationship. For example, having a 'strong positive' relationship indicated that a variable increased as forest coverage increased. A strong relationship was defined as having a positive (negative) regression coefficient and a correlation coefficient with an absolute value greater than 0.5. A weak relationship was defined as having a positive (negative) regression coefficient and a correlation coefficient with an absolute value between 0.2 and 0.5. Having no relationship was defined as having a correlation coefficient with an absolute value less than 0.2.....	51
Table 4.1: Summary of relationships between listed variables and the prescribed ground cover change in the forest-grass comparison, forest-control comparison, and control-grassland comparison. In this analysis, surface latent heat fluxes, surface sensible heat fluxes, total precipitation rate, evaporation minus precipitation, average surface temperature, average daily maximum surface temperature, average daily minimum surface temperature, surface wind speed, and surface pressure, all averaged over the JJA season, were studied. Each relationship was described as strong positive (negative), weak positive (negative), or no relationship. For example, having a 'strong positive' relationship in the forest-grassland comparison indicated that a variable increased as forest coverage increased. A strong relationship was defined as over 75% of grid cells in the study region had a significant positive (negative) change. A weak relationship was defined as between 20 and 75% of grid cells had a significant positive (negative) change. Having no relationship was defined as less than 20% of grid cells had a significant change.....	92

LIST OF FIGURES

Figure 1.1: A schematic of the surface heat budget of bare soil (a) and vegetation (b) (Pielke 2001, Avissar and Pielke 1990)..... 3

Figure 1.2: A schematic of the surface moisture budget of bare soil (a) and vegetation (b) (Pielke 2001, Avissar and Pielke 1990)..... 3

Figure 1.3: Southwestern Australia from the Geostationary Meteorological Satellite visible channel as seen on January 3, 1999 at 1500 LST. The line of demarcation between the clouded area and the clear area occurs approximately at the location of the rabbit-proof fence, with the clouded boundary layer found over the native vegetation and the clear skies over the agricultural crops (from Pielke et al. 2011)..... 6

Figure 1.4: Potential loss in Amazon forest land by 2050, in brown, as predicted by “business as usual” (a) and “increased governance” (b) situations with the probability of a >20% decrease in dry-season rainfall contoured. Here the dry season is defined as December through February when south of the Equator and June through August when north of the Equator. Precipitation scenarios from the IPCC Fourth Assessment Report’ mid-range global greenhouse gas emissions scenarios were used (from Malhi et al. 2008)..... 11

Figure 2.1: Modern fractional forest coverages (here the averaged JJA seasons for 2005-2010) gridded to the 1x1 degree grid..... 30

Figure 2.2: Global map of biome types (noted as 1-12) as used in the control run..... 35

Figure 2.3: Region of interest as used in model run. Cells outlined in red were modified for the forest and grasslands runs..... 35

Figure 2.4: The LAI index (equation 2.1) for the control simulation. Having an LAI index closer to 1 (0) indicated having nearly 100% (0%) forest coverage, as in the entirely forested (grassland) run..... 36

Figure 3.1: The absolute change in fractional forest coverage, calculated by subtracting the fractional forest coverage from the 1950-1955 period from the fractional forest coverage of the 2005 – 2010 period..... 38

Figure 3.2: The relative fractional change in forest coverage, computed by dividing the absolute change in forest coverage (figure 3.1) by the fractional coverage of the 1950-1955 period..... 39

Figure 3.3: Changes in average JJA monthly precipitation in inches between the 2005-2010 time period and the 1950-1955 time period.....	40
Figure 3.4: Changes in average JJA monthly precipitation in inches significant at the 95% confidence level between the 2005-2010 time period and the 1950-1955 time period.....	41
Figure 3.5: Change in average JJA monthly precipitation (inches) versus the change in fractional tree coverage. The red line is the linear regression of the plotted data, and is equal to $y = 4.1x - 0.47$. The blue circles represent non-significant changes in monthly precipitation and the red squares represent significant changes in monthly precipitation.....	42
Figure 3.6: Changes in average JJA surface temperature (K) between the 2005-2010 time period and the 1950-1955 time period.....	44
Figure 3.7: Changes in average JJA surface temperature (K) versus the absolute change in fractional tree coverage. The red line is the linear regression of the plotted data, and is equal to $y = -0.84x + 0,1$ (as in equation 3.4).....	44
Figure 3.8: Changes in average JJA daily maximum temperature (K) between the 2005-2010 time period and the 1950-1955 time period.....	46
Figure 3.9: Change in average JJA surface daily maximum (K) versus the absolute change in fractional tree coverage. The red line is the linear regression of the plotted data, and is equal to $y = -2.6x + 0.23$ (as in equation 3.5).....	46
Figure 3.10: Changes in average JJA daily minimum temperature (K) between the 2005-2010 time period and the 1950-1955 time period.....	48
Figure 3.11: Change in average JJA surface daily minimum temperature (K) versus the absolute change in fractional tree coverage. The red line is the linear regression of the plotted data, and is equal to $y = 4.7x+0.086$ (as in equation 3.6).....	49
Figure 4.1: Changes globally (top) and in the study region (bottom) in average JJA surface latent heat fluxes (W/m^2) between the entirely forested run and the grassland run. All colored areas are a change significant at the 95% confidence level.....	56
Figure 4.2: Changes globally (top) and in the study region (bottom) in average JJA surface latent heat fluxes (W/m^2) between the entirely forested run and the control run. All colored areas are a change significant at the 95% confidence level.....	57
Figure 4.3: Changes globally (top) and in the study region (bottom) in average JJA surface latent heat fluxes (W/m^2) between the control run and the grassland run. All colored areas are a change significant at the 95% confidence level.....	58

Figure 4.4: Changes globally (top) and in the study region (bottom) in average JJA surface sensible heat fluxes (W/m^2) between the entirely forested run and the grassland run. All colored areas are a change significant at the 95% confidence level..... 59

Figure 4.5: Changes globally (top) and in the study region (bottom) in average JJA surface sensible heat fluxes (W/m^2) between the entirely forested run and the control run. All colored areas are a change significant at the 95% confidence level..... 60

Figure 4.6: Changes globally (top) and in the study region (bottom) in average JJA surface sensible heat fluxes (W/m^2) between the control run and the grassland run. All colored areas are a change significant at the 95% confidence level..... 61

Figure 4.7: Changes globally (top) and in the study region (bottom) in average JJA surface temperature (K) between the entirely forested run and the grassland run. All colored areas are a change significant at the 95% confidence level..... 64

Figure 4.8: Changes in the study region in average JJA surface daily minimum surface temperature (K, top) and average JJA surface daily maximum surface temperature (K, bottom) between the entirely forested run and the grassland run. All colored areas are a change significant at the 95% confidence level..... 65

Figure 4.9: Changes globally (top) and in the study region (bottom) in average JJA surface temperature (K) between the entirely forested run and the control run. All colored areas are a change significant at the 95% confidence level..... 66

Figure 4.10: Changes globally (top) and in the study region (bottom) in average JJA surface temperature (K) between the entirely forested run and the grassland run. All colored areas are a change significant at the 95% confidence level..... 67

Figure 4.11: Changes globally (top) and in the study region (bottom) in average JJA total precipitation rate (mm/day) between the entirely forested run and the grassland run. All colored areas are a change significant at the 95% confidence level..... 71

Figure 4.12: Changes globally (top) and in the study region (bottom) in average JJA total precipitation rate (mm/day) between the entirely forested run and the control run. All colored areas are a change significant at the 95% confidence level..... 72

Figure 4.13: The relative fractional change in forest coverage, computed by dividing the absolute change in forest coverage (figure 3.1) by the fractional coverage of the 1950-1955 period..... 73

Figure 4.14: Changes globally (top) and in the study region (bottom) in average JJA total precipitation rate (mm/day) between the control run and the grassland run. All colored areas are a change significant at the 95% confidence level..... 74

Figure 4.15: Changes globally in average JJA evaporation - precipitation (mm/day) between the entirely forested run and the control run. All colored areas are a change significant at the 95% confidence level..... 75

Figure 4.16: Changes globally (top) and in the study region (bottom) in average JJA evaporation - precipitation (mm/day) between the control run and the grassland run. All colored areas are a change significant at the 95% confidence level..... 76

Figure 4.17: Changes globally (top) and in the study region (bottom) in average JJA surface wind speed (m/s) between the entirely forested run and the grassland run. All colored areas are a change significant at the 95% confidence level..... 81

Figure 4.18: Changes globally (top) and in the study region (bottom) in average JJA surface wind speed (m/s) between the entirely forested run and the control run. All colored areas are a change significant at the 95% confidence level..... 82

Figure 4.19: Changes globally (top) and in the study region (bottom) in average JJA surface wind speed (m/s) between the control run and the grassland run. All colored areas are a change significant at the 95% confidence level..... 83

Figure 4.20: Changes globally in average JJA sea level pressure (Pa) between the entirely forested run and the grassland run. All colored areas are a change significant at the 95% confidence level..... 84

Figure 4.21: Changes globally in average JJA sea level pressure (Pa) between the entirely forested run and the control run. All colored areas are a change significant at the 95% confidence level..... 85

Figure 4.22: Changes globally in average JJA sea level pressure (Pa) between the control run and the grassland run. All colored areas are a change significant at the 95% confidence level..... 86

Figure 4.23: Variance explained by the first ten EOFs..... 87

Figure 4.24: (a) The response of mean sea level pressure to change in ground cover, calculated by the averaged JJA mean sea level pressure subtracted from the averaged JJA mean sea level pressure from the forested run for the area of 20 latitude to 90 latitude; (b) The first EOF, as computed in appendix A, projected onto the response in 4.24a; (c) The residual, calculated by subtracting the projection from the response. All plots are in units Pa and the 95% confidence level filter was not applied..... 88

Chapter 1: Introduction

1.1. Effects of Ground Cover on Atmospheric Quantities

1.1.1. Introduction

As a response to increased human demand, native vegetation and forests have been transformed into urban and agricultural regions. These changes have varied in size and scope; in the Amazon, rainforests have been cleared for increased pasture and farmland. Natural encroachment and reforestation efforts in the northeast United States have revitalized diseased and cleared native forests.

Altering a landscape from its natural vegetation has many direct implications for and influences on surface climate (Pielke et al. 2011). Atmospheric turbulence; momentum, heat, moisture, aerosol, and trace gases fluxes; and absorption and reflection of incoming and outgoing radiation are all influenced by surface conditions. The direct global radiative impact of land use and land cover change have been estimated to be small, a decrease of $0.2 \pm 0.2 \text{ W m}^{-2}$ (Forster et al. 2007). Because of this, land use change has largely been omitted from previous Intergovernmental Panel on Climate Change assessments and predictions (Pielke et al. 2011). However, ground cover change is a highly localized phenomenon and thus a global assessment was not an accurate depiction of the local influences of the changes. In this analysis, the impacts of reforestation in the northeast United States were analyzed with respect to changes in temperature and precipitation as seen in observations and model simulations.

1.1.2. The Surface Energy Budget

The energy budgets for both bare and vegetated soil are set forth in equations 1.1 and 1.2 (Pielke2001) (figures 1.1, 1.2).

$$R_N = Q_o + H + L(E + T) \text{ (Equation 1.1)}$$

$$P = E + T + RO + I \text{ (Equation 1.2)}$$

Here, R_N is the net of all radiative fluxes, Q_o is the soil heat flux, H is the turbulent sensible heat flux, and $L(E+T)$ is the turbulent latent heat flux based on the latent heat of vaporization (L), evaporation (E), and transpiration (T). The precipitation budget P is controlled by evaporation, the conversion of liquid water to water vapor by nonbiological processes; transpiration, biological processes that represent the conversion to water vapor; excess water flow over land (runoff RO); and infiltration, the rate at which water enters the soil (I). The budgets discussed here do not act independently of each other; for example, if R_N remains constant while evaporation and transpiration decrease, turbulent sensible heat fluxes must increase. An increase (reduction) in latent heat can cool (warm) surface temperatures due to changes in evaporative cooling (Ban-Weiss 2011, Claussen et al 2001, DeFries et al 2002, Davin and de Noblet-Ducoudre 2010). One method of decreasing evapotranspiration is by deforestation, which increases runoff (Pielke 2001).

Equation 1.3 was the definition of the Bowen Ratio (B), which is the ratio of sensible heat fluxes to latent heat fluxes at the surface.

$$B = \frac{H}{L(E+T)} \text{ (Equation 1.3)}$$

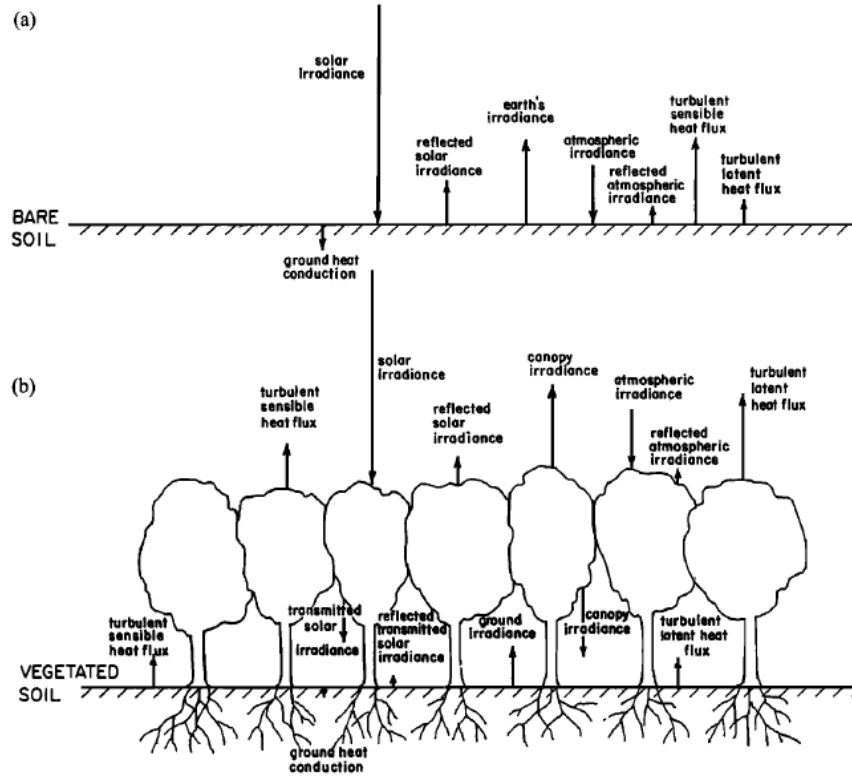


Figure 1.1 A schematic of the surface heat budget of bare soil (a) and vegetation (b) (Pielke 2001, Avissar and Pielke 1990)

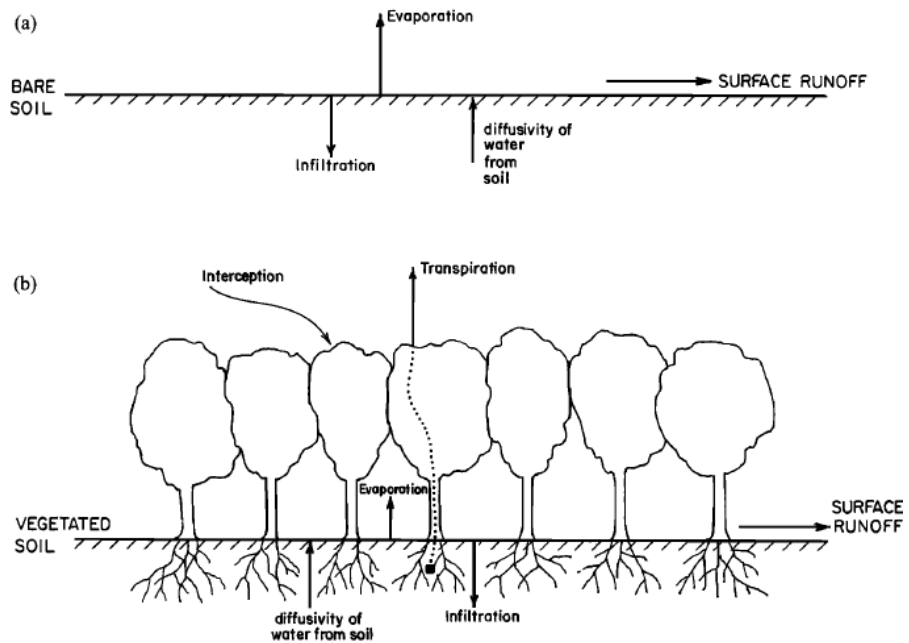


Figure 1.2 A schematic of the surface moisture budget of bare soil (a) and vegetation (b) (Pielke 2001, Avissar and Pielke 1990)

As the Bowen ratio decreases, for a constant value of R_N , the boundary layer becomes a more supportive environment for cumulus development. Forests and irrigated croplands have a lower Bowen ratio or a greater latent heat flux relative to sensible heat flux (Ban-Weiss, et al. 2011). Thus, a change in land use and the resulting impacts on variables such as surface albedo, leaf area, and intercepted rainfall may have local and regional impacts on the potential precipitation rates and cumulus development. Deforestation and the removal of native vegetation in favor of crops will influence the sensible and latent heat fluxes.

1.1.3. Effects in the Boundary Layer

Forests are naturally rough boundaries between the atmosphere and the earth. By changing ground cover, surface moisture and heat fluxes will be influenced. An increase in turbulence resulting from increased forest coverage is important for any quantities transported through turbulent diffusion, such as water vapor, gases, or aerosols (Veen et al., 1996). As land is deforested, the albedo of the region increases (Schrieber et al. 1996). The resulting decrease in absorbed solar radiation leads to cooler surface temperatures and enhanced subsidence in the area. If the region of subsiding air is large enough, precipitation will be suppressed, creating a positive feedback mechanism for increase drying in the area (Schrieber et al. 1996, Ban-Weiss et al. 2011).

The changes in surface moisture, heat, and momentum fluxes will impact the development of the planetary boundary layer. When sensible heat fluxes are higher, the planetary boundary layer depth increases and is more likely to exceed the lifting condensation level, increasing the potential for cumulus development (Nair et al. 2011).

Regional cumulus potential is also dependant on local atmospheric conditions. For example, in a relatively moist environment, cloud development is more likely in locations with a low Bowen ratio, typically forested regions. In region with a dry lower troposphere, however, areas with high Bowen ratios are the first to have convective cloud development (Rabin et al. 1990, Schrieber et al. 1996). Thus, changes in native vegetation and land use have significant impacts on the spatial distribution of convective cloud development.

On a global scale, when the atmosphere and surface are considered together, a change in latent or sensible heating will not significantly alter the global energy balance because changes in evaporation will be balanced by changes in water vapor condensation. Instead, changes in global temperatures are linked to changes in water vapor content, low clouds, and the vertical temperature profile (Ban-Weiss et al. 2011).

1.2. Global Reforestation Studies

1.2.1. Australia

Large amounts of land in southern Australia have been converted for agricultural use. In this region, approximately 50% of the native forest and 65% of the native woodlands have been altered. In southwest Australia, over 13 million ha of land has been cleared for winter crops during the past seventy years (Pielke et al. 2011). Several studies have analyzed the impact of this land use change both through the impacts of ground cover change and associated irrigation activity.

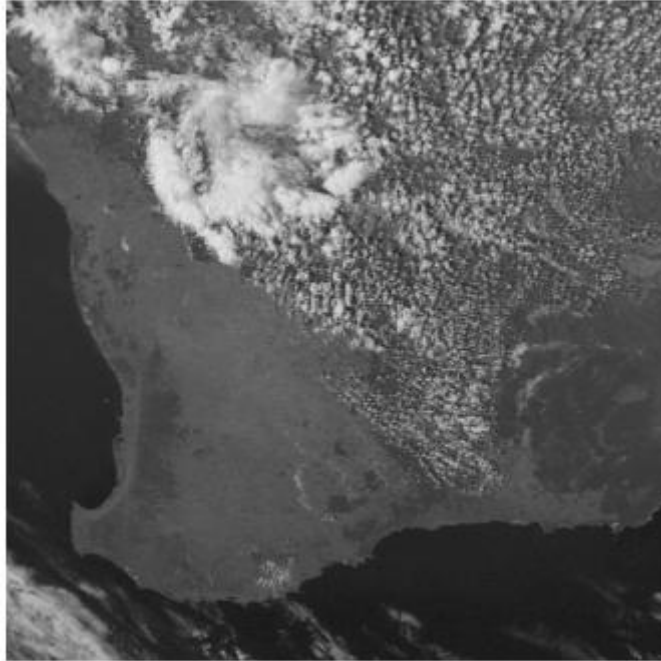


Figure 1.3 Southwestern Australia from the Geostationary Meteorological Satellite visible channel as seen on January 3, 1999 at 1500 LST. The line of demarcation between the clouded area and the clear area occurs approximately at the location of the rabbit-proof fence, with the clouded boundary layer found over the native vegetation and the clear skies over the agricultural crops (from Pielke et al. 2011).

A 750 km long rabbit-proof fence was built to separate agricultural land and native vegetation in southwest Australia (figure 1.3). From 2005 to 2007, the Bunny Fence Experiment compared atmospheric conditions on the two sides of the fence (e.g., Nair et al. 2011, Pitman et al. 2004). In the agricultural areas, there has been approximately a 20% decrease in wintertime rains with preferential cloud formation over the native vegetation as seen in observations. The causes of this decrease in rainfall are hypothesized to be due to changes in large-scale circulation and regional-scale land cover.

Compared to the native-vegetation side of the fence (the east side), the agricultural side of the fence (the west side) has large seasonal variations in ground cover. While there

was little change in the natural vegetation during the course of the year, the west side has periods of growth and dormancy. During the austral summer, the west side of the fence has high albedo and surface roughness. These decrease dramatically after harvest. Overall, native vegetation land has higher sensible heat fluxes compared to the agricultural fields, as confirmed in observations (Lyons et al., 1993, 2002). Aircraft observations confirmed an increase in depth of the planetary boundary layer as a response to the sensible heat flux differences. Because of this, cloud formation, and thus an increased propensity for rainfall, was favored on the eastern side of the fence. Additionally, the western, agricultural fields have large seasonal variability in latent heat fluxes. Large latent heat fluxes were measured during the austral summer, when the crops were still in growth. In winter, the flux rate can drop by 60% (Nair et al. 2011). In comparison, the latent heat fluxes over the native vegetation stay approximately constant during the entire year. Native plants have deeper roots than agricultural crops and thus have more access to underground water supplies and provide an important link between ground water and the atmosphere.

One dominant circulation pattern in the region is the west coast trough, a quasi-permanent surface heat low over western Australia (Nair et al. 2011). The trough brings warm continental air masses into southwest Australia, generating large cloud fields. When the position of the west coast trough changes, the locations of surface convergence and convective development shift. Changes in planetary boundary layer development and surface roughness shifted the west coast trough (Nair et al. 2011). Thus, conditions on the eastern, native-vegetation side both increased sensible heat fluxes enhancing boundary level development and aided convergence associated with the west coast trough to prompt the formation of convective rainstorms.

Changes in latent and sensible heat fluxes have been linked to present day decreases in precipitation. Studies have analyzed a sudden decrease in austral winter rainfall over southwestern Australia during the 1970s (Pitman and Narisma 2004). In the authors' model analysis, rainfall was reduced in the region of interest and enhanced further inland. The authors concluded that the reduction in surface roughness length reduced surface drag in the region. This increased moisture divergence inland over southwest Australia and increased moisture convergence inland. The change in wind patterns was the primary driver of changes in precipitation in this case study where, similar to the Bunny Fence experiment, changes in location of moisture convergence will have a direct effect on the location of rainfall.

1.2.2. Israel

For nearly sixty years, Israel has been irrigating agricultural land in the south with water from Lake Tiberias during the dry season (de Ridder et al. 1998). The dry season lasts from April to October and was the result of subtropical high pressure systems. The irrigation program was part of the National Water System and large parts of naturally dry southern Israel were now cultivated agricultural land due to the program's success. Early studies on the local climate impacts of this land cover change concluded that the increased irrigation decreased the sensible heat flux in the region. This change in the sensible heat flux, along with the increase in surface roughness was associated with a decrease in diurnal surface wind and temperature variability (e.g., Alpert and Mandel (1986)).

Additionally, Otterman et al. (1990) also studied the local changes of increased agricultural cultivation on precipitation. Increased precipitation rates were observed during the month of October, the transition period between the dry and wet seasons. The precipitation during this period was normally the result of convective storms. The region naturally has high-albedo soil; surface albedo was thus decreased with this land cover change. The decrease in albedo and day-to-night soil heat storage increased the daytime sensible heat flux. The authors argued that the increase in daytime sensible heat flux would intensify convection in the region. Enhanced advection would bring in moist air from the Mediterranean Sea while enhanced daytime convection would allow for increased convective storm development. In combination, the changes in convection and advection would account for the observed increase in October rains.

de Ridder et. al (1998) also investigated the connection between changing sensible heat fluxes due to land cover change and increased October rainfall amounts. Their study was limited to dark soil areas; the effects of changing albedo were not considered. Instead, the impacts of change in roughness length and moisture availability due to the increase in agricultural land were emphasized. The authors concluded that in their simulations the land cover change in southern Israel was responsible for a decrease in diurnal wind speed and temperature. Additionally, the increase of moisture at the surface would create conditions favorable for moist convective activity. However, this was an indirect effect from decreased surface sensible heat fluxes and associated decrease in the coastal circulation.

Overall, the yearly precipitation total in Israel has declined while the frequency of extreme rain events has increased. As agricultural irrigation continues in the region, the local and regional impacts of the projects will be a persistent impact of the projects.

1.2.3. The Amazon

In the Amazon, there has been large scale deforestation for pasture land on the order of 10,000 km² per year (Malhi et al. 2008). Observational studies from the past thirty years agree that this deforestation has decreased the amount of rainfall in the region, but the magnitude of influence of the deforestation was still unconfirmed. The positive feedback between vegetation and local convective rainfall has been well-documented but the impacts on large scale circulations were also debated.

Following deforestation in the region, the new pastureland typically has an albedo of 0.18, an increase of 0.05 compared to the previous forests (Gash and Nobre 1997). Net radiation has decreased by approximately 11%. Transpiration and latent heat flux have also decreased over the pastureland. The new vegetation has comparatively shallower roots, resulting in a soil moisture deficit during the dry season (Pielke et al. 2011, Gash and Nobre 1997). Eastern Amazonia is particularly prone to enhanced dry seasons. Comparatively, northern and western Amazonia are more resilient to changes in ground cover as precipitation in the region is primarily orographically driven (figure 1.4) (Malhi et al. 2008). Sensible heat fluxes have increased over these regions, which, as discussed previously, enhances boundary layer development. Planetary boundary layer depths are reported to be as much as 600m higher over pasture lands compared to forests (Pielke et

al. 2011). Thus on the small scale, deforestation is hypothesized to produce mesoscale circulations favorable to cloud and precipitation development (Bonan 2008).

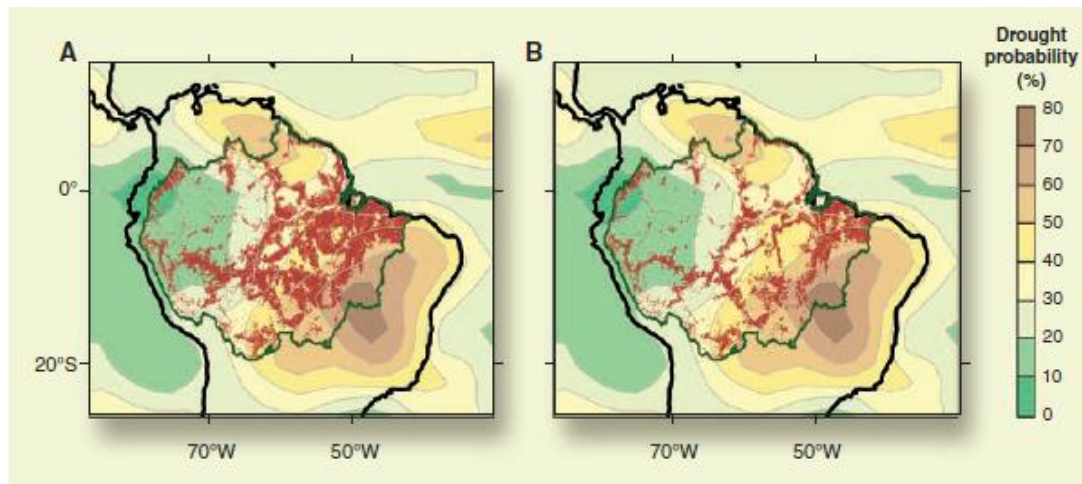


Figure 1.4 Potential loss in Amazon forest land by 2050, in brown, as predicted by “business as usual” (a) and “increased governance” (b) situations with the probability of a >20% decrease in dry-season rainfall contoured. Here the dry season is defined as December through February when south of the Equator and June through August when north of the Equator. Precipitation scenarios from the IPCC Fourth Assessment Report’ mid-range global greenhouse gas emissions scenarios were used (from Malhi et al. 2008).

Observational studies in the region are difficult to compare. Studies have made use of observations from a specific site and have then compared the effects of deforestation on that location alone. Another method used was to compare rainfall from forested and deforested sites in the same time frame. However, it is difficult to determine the exact influence of topographic variations and biases present in data from different collection methods impact these studies (Meher-Homji 1991, Pielke et al. 2007). In observational studies such as Meher-Homji (1991); Pielke (2001); Duriex et al. (2003); and Ray et al., (2006), there are reported annual rainfall decreases ranging from 1-20%.

Sud et al. (1996) noted that there was no significant signal detectable in observational rainfall data. The inherent noise drowned out the small signal in the precipitation data, but the authors noted a significant decline in evapotranspiration over deforested areas. The authors ran 5-year numerical simulations to investigate the impacts of reforestation on the large-scale circulation. The only difference between simulations was that the region typically dominated by tropical forests was instead prescribed to be savanna. In this study, only a small region was deforested and no major climate drift was seen in response to the deforestation. The annual mean rainfall was approximately the same in both the control and deforested cases with no significant change reported. Net moisture transport in the Amazon increased in the simulations due to warming in the PBL and enhanced winds. The noted reduction in evapotranspiration was compensated for by increased moisture convergence. The authors noted that global changes were indistinguishable from natural variability.

Due to the size of the Amazon forests, the deforestation has been hypothesized to impact global circulation patterns. Avissar (2004) used a global climate model (GCM) without interannual sea surface temperature variability to better analyze any altered global connections. The authors reported connections between tropical deforestation and rainfall in other locations. For example, there were significant decreases in precipitation over coastal Pacific Ocean, parts of Arica, and Indonesia. There was no consistent global temporal trend; while the summer (wet season) was adversely affected in the Amazon, precipitation rates throughout the entire year were lower in Indonesia (Avissar 2004). In central Africa, the dry season was the most affected. Because of these global effects,

changing land use in the Amazon could lead not only to the loss of diverse ecosystems locally but may have far-reaching impacts.

1.2.4 Africa

The use of reforestation to possibly mitigate impacts of climate change has been suggested for Africa in general and particularly west Africa . The IPCC (2007) predicted that, as a result of climate change, between 75 and 250 million people could experience more water stress by 2020. For over seventy years, geoengineering practices like reforestation have been proposed to alter meteorological processes favorably in the region. Stebbings (1935) argued for afforestation in west Africa. By establishing forests in land previously unforested, precipitation and soil retention would increase. Additionally, forest plantations have been proposed (e.g., Enger and Tjernstrom 1991) that would radically increase precipitation to the point where irrigation would no longer be required.

Abiodun et al. (2012) ran regional climate model simulations to analyze local and regional effects of reforestation in west Africa. West Africa was defined in terms of three zones: the Sahel, the Savanna, and the Guinea zones. Nine numerical studies were then done with one control followed by eight different scenarios with different amounts of reforestation in the zones (e.g., Sahel zone fully reforested, 100% reforestation in Nigeria) to study the impact of reforestation in different regions of west Africa.

The authors reported that in their simulations, reforesting western Africa impacted regions beyond the initial reforestation. In all simulations, temperatures cooled in the

reforested area but the area bordering the reforestation experienced warming. In the reforested zone, monsoon winds slowed as a result of increased surface roughness and weakened meridional temperature gradient. These alterations introduced a cooling within and upwind of the reforested area but warmed downwind of the area. The impact on precipitation and temperature patterns varied based on the location of the reforested area. For example, with reforestation in the Savanna, rainfall was reduced north of the region due to delays in monsoon flow. In comparison, when the Sahel was reforested, rainfall was reduced south of the region as a result of a delayed monsoon.

Overall, the authors concluded that while the cooling temperatures or increased precipitation may mitigate some impacts of global climate change in the altered regions, area beyond the reforested land would have enhanced warming and decreased precipitation. Thus additional studies are needed to further investigate impacts of large-scale reforestation in western Africa.

1.3. On the Northeast United States

1.3.1. A History of Forest Use in the Northeast

In the early 1500s, explorers from Eastern Europe landed on the eastern coast of North America. These initial explorers started a deforestation process that would continue for centuries. Steyaert and Knox (2008) estimated that since 1650, over 2/3 of the land in eastern United States has undergone drastic changes in albedo and surface roughness. Early settlers' need for agricultural land and timber products required clearing much of the

natural forests and conversion of natural wetlands in the region (Steyart and Knox 2008). For example, by 1820 in Connecticut, only 25% of the land area remained forestland, compared to the virgin forests that had previously covered approximately all of the state (Wharton et al. 2004).

By 1850, agricultural use of land in the Northeast had peaked. The growth of the railroads enabled cheap crops from the Midwest to be imported into the region; farmers abandoned farms in the northeast in favor of fertile Midwest land. Timber was still in demand for charcoal production, but by 1925 coal was a cheaper alternative (Wharton et al. 2004). The timber industry continued to decline; by 1950 the Massachusetts timber product industry was one third of the same industry in 1900 (Ferguson and Howard 1956). In land around the Great Lakes and mid-Atlantic, large scale commercial logging was still underway during the late 1800s and 1900s (Steyart and Knox 2008). Pennsylvania, the highest producer of lumber in the country at the time, manufactured over 2.3 billion board-feet between 1889 and 1899. By the early 1900s, Pennsylvania began importing lumber for use; by 1922, 84% of the lumber being used in Pennsylvania was imported (Ferguson 1958). Land cleared for agricultural and industrial uses slowly reverted back to forest. Still chestnut blight, Dutch elm disease, and natural pests, including the gypsy moth, continued to stress the forestland coverage (Wharton et al. 2004).

Along with changing industrial demand in the northeast, environmental conservation movements in the 1880s lobbied extensively for reforestation. Continued soil and water quality degradation and decline of saw timber and industrial-grade lumber were looming concerns (Russell and Davis 2001). Use of forestland changed from industrial to

recreational. New forest management policies, including additional tree planting and fire suppression, were introduced (Russell and Davis 2001). By the 1950s in Rhode Island, it was estimated that the timber growth rate was over six times larger than the cut rate (Ferguson and McGuire 1957). Today, much of the previously deforested land has once again become grown over. There are, however, new challenges to forestland in the northeast. As urbanization, population, and suburban development continue to grow, forests continue to be cleared in the region (Diffenbaugh 2009).

Additionally, even though forests have continued to grow over abandoned land, there has yet to be a return to a pristine state. The new forests are still young and human intervention has fundamentally altered forest composition across the region. Effectively 100% of the land area in the region has evidence of human disturbance (Steyaert and Knox 2008). For example, the present extent of wetlands in the region is approximately half of the area covered by wetlands in 1650 (Steyaert and Knox 2008). Deforestation, disease and pests have decimated the populations of American elms, native chestnuts, and chinquapins. In place of such trees and old-growth pine forests cleared for logging, populations of aspen, birch, and primarily deciduous trees have increased (Steyaert and Knox 2008). Changing forest composition can impact many physiognomical factors including, but not limited to: surface roughness; surface albedo; average leaf area index, or the measurement of leaf area in a given area; canopy height; and land-atmospheric interactions.

1.3.2. Previous Studies in the Region

Previous modelling studies in eastern and central United States have identified a number of shifts in regional atmospheric and surface characteristics. When vegetation, and thus the leaf area index (LAI), was increased, simulated impacts include a decreased albedo, summertime warming, and wintertime cooling (Pielke 2007, Bounua et al. 2000, Xue 1996). There is qualitative agreement on how changing LAI impacts summertime maximum and minimum temperatures and precipitation.

Strack et al. (2008) estimated that, since 1920, summer maximum temperatures have remained approximately constant in the eastern United States. Present minimum temperatures, in comparison, have cooled by around 0.1 K compared to the 1920 temperatures. Compared to the 1650 temperatures, both maximum and minimum temperatures have risen overall. Summer minimum temperatures have warmed by about 0.3 K, and summertime maximums by around 0.4 K (Strack et al. 2008). The authors argued that the increase since 1650 is related to changes in surface roughness in the same time period. Soil moisture contents have been reduced in the eastern United States since the 1600s, reducing the amount of evaporation. However, compared to 1920, there has been reforestation and both maximum and minimum June temperatures cooled slightly as soil moisture contents and forest coverage increased (Strack et al. 2008). Bounua et al. (2000) also reported a cooling of temperatures during the summer in the northern latitudes. Their models simulated a cooling of approximately 1.8K in reforested areas. The authors also noted a decrease in the warm season diurnal temperature range (DTR) as a

result of increased daytime evapotranspiration. The authors also noted that seasonal changes in DTR are, in large part, controlled by insolation and cloudiness.

As documented in Asner et al. (2004), when midlatitude deciduous forests were converted to grasslands, croplands, and pasture, there were numerous hydrological impacts. The new agricultural land sees a reduction in spring snow melt, a lowering of cloud base, and increased runoff, soil evaporation, and reduced transpiration. This results in higher soil moisture fluxes over the deforested land. However, when forest land was changed to croplands, there was no clear trend in moisture availability due to variable crop transpiration rates and irrigation (Asner et al. 2004). Strack et al. (2008) found little change in precipitation in time in the eastern United States. Bounua et al. (2000) found increases of almost 10 mm/month in both precipitation and evaporation in simulations with increased vegetation. Evaporation increased slightly more than precipitation, resulting in soil-water deficiencies. Xue (1996) reported results consistent with Strack et al. (2008) while Pinty et al. (1989) described a nonlinear relationship between soil moisture availability and higher region precipitation (Pielke et al. 2011).

In Xue et al. (1996)'s modeling simulation, a change in land area index altered regional qualities and also had broader implications for global circulation. Bounua et al. also reported an increase in low-frequency variability in weather patterns in simulations with increased vegetation.

1.3.3. Issues with Studies in the Region

In the northeast United States, several variables could influence the results of atmospheric change analysis. These include, but are not limited to, variable changes in ground cover, complex circulation patterns, and a variety of influences on precipitation sources in the region. Changes in land use vary in time and space. Although a forest may be cleared systematically, encroachment and recovery will occur sporadically over the region. Urbanization also occurs at variable rates in space and time as human demand for land evolves. There are also issues with time-varying spatial and temporal data coverage. Major reforestation in the region occurred prior to 1920 and there was limited information available with high resolution forest coverage and composition or meteorological records.

In general, this part of the world has a complex meteorological system. Compared to tropical regions, the midlatitudes have a larger variety of air mass source regions and more frequent passing of frontal systems (Pielke et al. 2007). In such a complex circulation system, the changes in the precipitation signal are nearly indistinguishable from background noise. It was also more difficult to determine the sources of the changes in precipitation fields. Pielke et al. (2007) suggested using unconventional means to determine changes in total precipitation. One such example was Swank and Vose (2004), which studied the impacts of changing mixed deciduous hardwood forests to forests of primarily eastern white pine. For the study, the authors analyzed annual streamflow in local watersheds. Over a period of ten years, the streamflow decreased in time. The authors concluded that the white pine trees had a greater leaf area index and greater

transpiration rate that led to increased water loss. Modeling studies must be used in order to detect signals and changes attributable to land cover changes.

1.4. Summary of Literature

By altering ground cover, several components of the energy budget are changed (equations 1.1, 1.2), which will further impact other atmospheric processes. For example, when reforestation (deforestation) occurs, latent heat fluxes and atmospheric moisture availability will increase (decrease) (Pielke 2001). Enhanced latent heat fluxes can cool surface temperatures due to an increase in evaporative cooling. Similarly, sensible heat fluxes will decrease (increase) with reforestation (deforestation), decreasing (increasing) boundary layer depth. Additionally, deforested land has a lower albedo compared to forested land, leading to relatively less absorbed solar radiation, cooler surface temperatures, and enhanced subsidence (Schrieber et al. 1996, Ban-Weiss et al. 2011). Cumulus development, and thus precipitation, is typically more favored in the moist environments seen over forested land compared to the drier environments over deforested land (Rabin et al. 1990). Also, increased surface roughness slows surface wind speeds. Thus, by changing ground cover, surface weather conditions and the potential for cumulus development aloft will be changed substantially.

Studies analyzing recent ground cover changes around the globe, including Australia and the Amazon, confirmed theoretical impacts of altering native vegetation. In Australia, agricultural and native vegetation fields are separated by a rabbit-proof fence. On the eastern, native-vegetation side, relatively higher sensible heat fluxes and increased

boundary layer depths are observed (Lyons et al. 1993, 2002). While austral summer latent heat fluxes are higher over the agricultural fields, when crops are in growth, wintertime latent heat fluxes are 60% of the summer rate (Nair 2011). In comparison, surface latent heat fluxes over the deeper-rooted native vegetation stay constant year round. Overall, precipitation and cumulus development was favored over the native vegetation (Pitman and Narisma 2004).

In the Amazon, native forests are cleared to create pastureland. In these clearings, albedo is increased, while net radiation, transpiration, and surface latent heat fluxes are decreased. Surface sensible heat fluxes, and thus boundary layer depths, were also enhanced over the deforested land. Eastern Amazonia is more prone to enhanced dry seasons when deforestation resulted in a soil moisture deficit. In comparison, precipitation in the northern and western regions of the Amazon is primarily orographically driven and more resilient to changes in ground cover (Malhi et al. 2008). Overall, only small shifts in precipitation, with decreases ranging from 0-20%, were detected over the Amazon and any changes outside of the region were indistinguishable from natural variability (e.g., Sud et al. 1996, Meher-Homji 1991, Ray et al. 2006, Duriex et al. 2003).

Forest coverage in the northeast United States has increased since the 1920s despite increasing urban and suburban development, disease, and population growth. Natural regrowth, a reduction in the timber industry and agricultural use, and human intervention have all contributed to the reforestation. Previous studies suggest that deforestation (reforestation) since 1650 (the 1920s) has resulted in a slight warming (cooling) in both maximum and minimum summertime temperatures in the eastern United States (e.g.,

Strack et al. 1996, Bounua et al.). Findings on the connections between precipitation and ground cover are mixed. Studies such as Strack et al. (2008) found no relationship between reforestation and precipitation, while in Bounua et al. (2000)'s study, reforestation was linked in increases in both precipitation and evaporation. However, the midlatitudes region is much more complex than other case studies presented here, with issues like frequent weather patterns making it hard to distinguish a signal.

1.5. Description of Project

In this study, a combination of observational data analysis and model simulations are utilized to study impacts of ground cover change in the northeast United States summer. Historical data from a variety of sources are used to compare precipitation and temperature patterns from the period of 1950 (low forest coverage) to 2010 (high forest coverage).

Additionally, three runs of the BUGS5 climate model were prepared. A control run and two idealized cases were used. In the experiments, the area of interest was either completely deforested or completely forested. This eliminated spatial and temporal variation in regrowth and other variable quantities to reduce the amount of noise in the results. Eigenorthogonal functions were also used to analyze responses in atmospheric circulation due to reforestation in the model data (Appendix A).

Goals of the study include first defining any changes in precipitation and temperature that have occurred during this period of reforestation in the northeast United

States. Additionally, to determine the amount of reforestation necessary to have shifts in temperature and precipitation in the region the changes in the observations will be compared to difference between the model simulations. Finally, the amount of agreement between the influences of ground cover on precipitation and temperature changes in this region, the theory, and previous studies will be ascertained.

Chapter 2: Methodology

2.1. Historical Observations in the Northeast United States

2.1.1. Meteorological Observations

The region chosen for the study included eight northeastern states: Pennsylvania, New York, Connecticut, Rhode Island, Massachusetts, New Hampshire, Vermont, and Maine. The analysis investigated the impacts of reforestation on precipitation and temperature during the Northern hemisphere warm season of April through October, with the ‘summer months’ defined as June, July, and August for the years 1950 through 2010. The observational data used in the analysis came from four individual data products released by the National Climatic Data Center (NCDC). Reporting sources for the products included the National Weather Service reporting stations, the Federal Aviation Administration, and cooperative observers. Due to the use of both historical and modern observations, there are inconsistencies in measurement methods. All data has undergone quality control measures and checks by the NCDC to ensure the best possible internal consistency. These included comparing monthly sums to entered daily data and assuring spatial consistency between neighboring stations. Additionally, the data was checked for internal inconsistencies such as daily maximum temperatures less than the same day daily minimum and a daily minimum temperature higher than the previous day’s daily maximum temperature. If inconsistencies were found, data was compared with secondary data

sources and nearby stations to determine if the data were reasonable or needed to be adjusted to achieve consistency.

The four separate data sets were chosen for best possible spatial and temporal coverage. Data sets were arranged by station location, with associated latitude, longitude, and elevation recorded. These individual stations were both binned by United States county and gridded on a 1x1 degree grid. Individual stations had their own temporal resolutions ranging from a minimum frequency of 24 hours to a maximum of 15 minutes. At each time, a variety of local meteorological variables were recorded including (but not limited to): precipitation accumulated since the last observation, temperature at time of observation, dew point temperature, sea-level pressure, cloud cover, wind speed and direction, and the presently observed weather.

Precipitation

From the higher resolution data sets, monthly total precipitation for a grid box (and county) was calculated. First, the unique stations from the data sets were identified. For each station, the high-resolution observations were summed to create a monthly total for all months in the chosen time range. If there was less than 80% temporal coverage for any station in a particular month, the month was omitted from the sample. After the station monthly totals were computed, an overall grid box (county) average per month was found by averaging together all of the individual stations monthly totals.

Temperature

Similarly, for each grid box (county), the monthly averaged daily minimum and maximum temperature were calculated. In a data set, minimum (maximum) temperatures for each day were calculated only when the temporal resolution was equal to or better than hourly. The stations were gridded as previously described for precipitation; for each station, if an individual day met the temporal resolution criteria, the maximum and minimum temperatures were found. The average monthly daily maximum and minimum temperature were only computed if there was, again, at least 80% coverage in a month. If not, the data point was excluded from the sample. The grid box (county) monthly average was again found by averaging together the included stations' monthly averages. Of the 197 counties included in the sample domain, 158 had precipitation data meeting the coverage controls from 1950 to 2010.

2.1.2 Forest Survey Inventory Reports

In addition to precipitation and temperature data, ground cover descriptions for the region in question were needed. Here, the amount of land covered by trees in one county (grid box) is the 'forest-land area' and the fraction of total county (grid box) area covered by forest is hereafter the 'fractional coverage'. Many modern types of measurements, such as satellite imagery, do not go back far enough in time for the analysis. For this study, the forest coverage data used was tabulated from Forest Service reports. The U.S. Forest Service, with the cooperation of the individual states, conducts the forest inventories. For

each state, a new survey is typically completed once every decade. Inventory release dates for each state are listed in table 2.1.

Table 2.1: Years of released inventory reports for each of the eight states included in the region of study.

State	Inventory Years
Connecticut	1953 ¹ , 1972 ² , 1985 ² , 1998 ³ , 2005 ³⁹ , 2006 ³⁹ , 2007 ³⁹ , 2008 ³⁹ , 2009 ³⁹ , 2010 ³⁹
Maine	1959 ⁵ , 1971 ^{6,7} , 1982 ^{7,8} , 1995 ⁹ , 2003 ¹⁰ , 2005 ³⁹ , 2006 ³⁹ , 2007 ³⁹ , 2008 ³⁹ , 2009 ³⁹ , 2010 ³⁹
Massachusetts	1928 ¹¹ , 1953 ¹¹ , 1972 ¹² , 1985 ^{12,13} , 1998 ¹³ , 2005 ³⁹ , 2006 ³⁹ , 2007 ¹⁴ , 2008 ³⁹ , 2009 ³⁹
New Hampshire	1948 ¹⁵ , 1960 ¹⁶ , 1972 ¹⁷ , 1983 ^{17,18} , 1997 ¹⁸ , 2005 ³⁹ , 2006 ³⁹ , 2007 ¹⁹ , 2008 ³⁹ , 2009 ³⁹ , 2010 ³⁹
New York	1950 ²⁰ , 1968 ²¹ , 1980 ²² , 1993 ²² , 2005 ³⁹ , 2006 ³⁹ , 2007 ³⁹ , 2008 ²³ , 2009 ³⁹ , 2010 ³⁹
Pennsylvania	1955 ²⁴ , 1965 ²⁵ , 1978 ²⁶ , 1989 ²⁶ , 2004 ²⁷ , 2005 ³⁹ , 2006 ³⁹ , 2007 ³⁹ , 2008 ³⁹ , 2009 ²⁸
Rhode Island	1935 ^{29,30} , 1953 ³⁰ , 1972 ³¹ , 1985 ^{31,32} , 1998 ³² , 2005 ³⁹ , 2006 ³⁹ , 2007 ³³ , 2008 ³⁹ , 2009 ³⁹
Vermont	1948 ³⁴ , 1966 ³⁵ , 1973 ³⁶ , 1983 ^{36,37} , 1997 ³⁷ , 2005 ³⁹ , 2006 ³⁹ , 2007 ³⁹ , 2008 ³⁹ , 2009 ³⁹ , 2010 ³⁸

¹Griswold and Ferguson 1957 ²Dickson and McAfee 1988a ³Alerich 2000a ⁴Butler et al. 2011 ⁵Ferguson and Longwood 1960 ⁶Ferguson and Kingsley 1972 ⁷Powell and Douglas 1984 ⁸Powell 1985 ⁹Griffith and Alerich 1996 ¹⁰McWilliams et al. 2005 ¹¹Ferguson and McGuire 1957 ¹²Dickson and McAfee 1988b ¹³Alerich 2000b ¹⁴Butler et al. 2010a ¹⁵Larson et al. 1954 ¹⁶Ferguson and Jensen 1963 ¹⁷Frieswyk and Malley 1985a ¹⁸Frieswyk and Widmann 2000a ¹⁹Morin et al. 2010 ²⁰Armstrong and Bjorkbom 1956 ²¹Ferguson and Mayer 1970 ²²Alerich and Drake 1995 ²³Widmann et al 2010 ²⁴Ferguson and Longwood 1960 ²⁵Ferguson 1968 ²⁶Alerich 1993 ²⁷McWilliams et al. 2007 ²⁸McCaskill et al. 2011 ²⁹Brooks et al. 1993 ³⁰Kingsley 1976 ³¹Dickson and McAfee 1988c ³²Alerich 2000c ³³Butler et al 2010b ³⁴McGuire and Wray 1952 ³⁵Kingsley and Barnard 1968 ³⁶Frieswyk and Malley 1985b ³⁷Frieswyk and Widmann 2000b ³⁸Morin et al. 2011. ³⁹Accessible via Forest Service online tables

Forest Service Inventory Reports

While surveys are released by individual state agencies, consistent information is contained within them. Inventory reports often include a summary of statewide changes in forest-land, a report on the health of a state's timber industry, and statistical tables describing state forest characteristics on a state and county level. These tables include information such as: forest composition, forest ownership, stand-size class, forest-land area, total county land area, and output of wood products at the time of the survey. These descriptions are often reported in terms of thousands of cubic feet or 'board feet'. One board foot is equivalent to a volume of one-foot length, one-foot wide, and one-inch thick. Forest-land area is given in unit of thousands of acres.

In these surveys, forest inventory estimates are calculated based on collected forest condition samples. A variety of sampling procedures are utilized during the survey process including: aerial photography, measurement of specific ground plots established in early surveys, and in later surveys, the measurement of additional ground plots. Data summaries were created using the FINSYS computer system, as developed at the Northeastern Forest Experiment Station (Dickson and McAfee 1988). The preliminary summaries are then reviewed by outside agencies and experts exclusive to an individual state to undergo data quality checks. Estimates of precision for the inventories are available upon request from the individual state agencies.

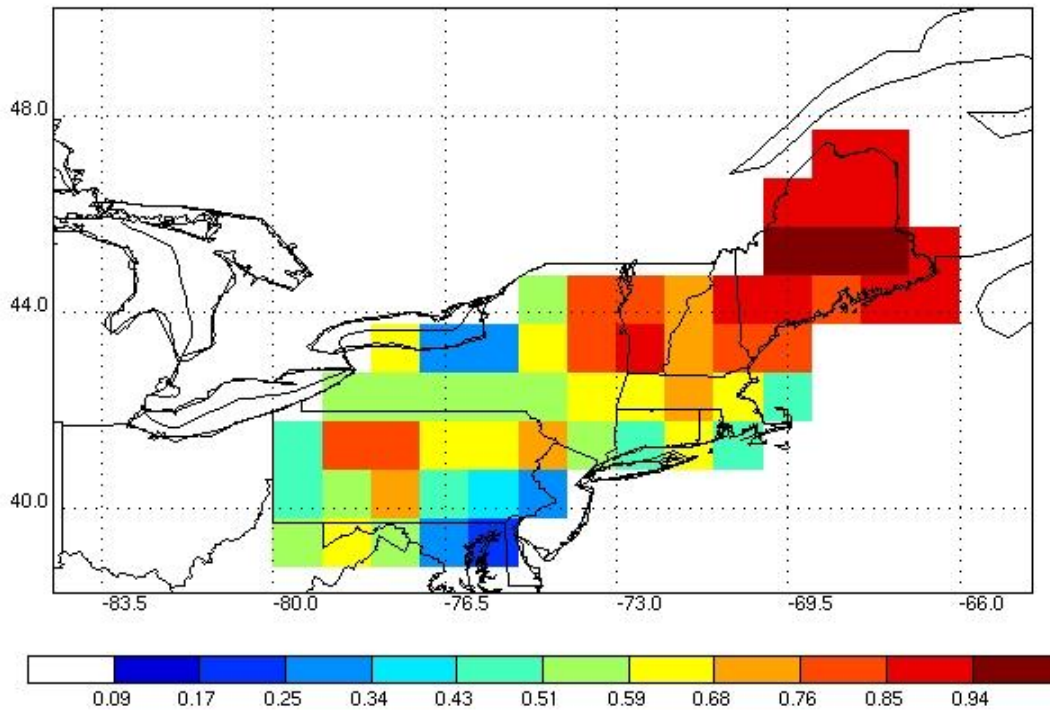
For the purpose of this study, deciduous and conifer trees are both included in calculation of forest acreage. No distinction was made in forest make-up in the data used in the analysis. 'Forest-land area' is defined as the sum of commercial and non-commercial

land. These categories can be broken up into more specific bins including timberland, productive reserved, urban forest, and unproductive forest-lands.

Tree Coverage

Following the tabulation of each county's historical forest-land area, the data were prepared for gridding on a 1x1 degree grid. First, linear regressions were used for consecutive 'pairs' of survey data to estimate trends in yearly forest-land areas for each county. This procedure was made based on the assumption that, on a yearly time scale, the rate of tree growth was constant. County boundaries were then assigned latitude and longitude coordinates and interpolated to the same 1x1 degree grid as used in the precipitation and temperature data. For the interpolation, weighted averages were used to assign a forest coverage to the grid box based on the relative area of each county within the grid box. In figure 2.1, the fractional forest coverage as calculated for the 2005 to 2010 time period and gridded to the 1x1 degree grid was plotted.

2005-2010 Fractional Tree Coverage



Dec 14, 2012

Figure 2.1 Modern fractional forest coverages (here the averaged JJA seasons for 2005-2010) gridded to the 1x1 degree grid.

2.1.3. Assumptions

Several assumptions had to be made to use the available historical observations and forest coverage data in the analysis. Coverage in space and time for both sets varied greatly. In the precipitation and temperature data sets, very few stations have collected data for the sixty years represented in the chosen sample. The methods of data collection, frequency of collection, location of stations, and frequency of reports have all varied over the years. Generally, modern data is reported more frequently, often hourly, whereas historical data was only reported once or twice a day. Thus, only months from any one

station that had recorded observations for at least 80% of the month were included in the data set to mitigate bias from stations that underreported in the early years compared to the later years. The stations were also not evenly distributed throughout the region. Instead, the stations tended to be clustered around population centers, airports, and the coasts. In less populated regions, such as central Pennsylvania, there were fewer collecting stations and less coverage. It is assumed that the spatial coverage of the stations is adequate to describe precipitation and temperature patterns.

Forest coverage records were not published frequently and each state completed the survey of tree coverage at different times. Over time, the statistical analysis used to calculate forest coverage also became more refined (e.g., Griswold and Ferguson 1957, Dickson and McAfee 1988a, Alerich 2000a) with a reduction in the error of the estimates. It is assumed that, on the scale of a U.S. county, forest growth (depletion) occurred linearly on the time scale of a decade and that all estimates represented the state of forest growth at the time of sampling. Tree coverage was also recorded based on the overall total coverage for each county. To interpolate the data to the 1x1 degree grid, it was assumed that the coverage was constant in space over a county. That is, if 50% of a county was forested, then every part of the county had 50% coverage.

2.2. Modeling Reforestation in the Northeast United States

To isolate the signal associated with ground cover change from the noise from other variable elements, including increased carbon dioxide, changes in global circulation patterns, and biases present in observations, three different simulations were run in the

global climate model BUGS (formerly the CSUGCM, Randall et al, 1996). For each of the runs, all model parameters were identical with only one change: the amount of forest-land area in the Northeast United States. The global model was run once in a 'control state', with ground cover approximating the current realistic forest-land area; once in a 'grasslands state', where the Northeast has been completely deforested; and once in a 'forested state', where the forest-land area in the Northeast was maximized. All other parameters remained the same. The model was run for six years, including one year of spin up, for each of the three scenarios.

2.2.1. Model Description and Set Up

BUGS5 is a general circulation model that has evolved from the University of California Los Angeles GCM. It uses a geodesic grid and modified sigma coordinate (Suarez et al. 1983; Randall et al. 1985; Ringler et al. 2000; <http://kiwi.atmos.colostate.edu/BUGS/BUGSoverview.html>). A unique aspect of the model is that the planetary boundary layer (PBL) depth changes due to horizontal mass flux divergence, entrainment, and convective mass flux. The entrainment rate is predicted by integrating the turbulent kinetic energy (TKE) conservation equation over the depth of the PBL (Randall and Schubert, 2004). BUGS5 uses a modified Arakawa-Schubert cumulus parameterization with a prognostic cumulus kinetic energy (Ding and Randall, 1998; Pan and Randall 1998), which relaxes the quasi-equilibrium closure of the models original Arakawa-Schubert parameterization. The stratiform cloud parameterization includes prognostic variables for cloud water, cloud ice, rain, snow, and water vapor (Fowler et al.

1996), and was directly coupled to the cumulus parameterization. The microphysics parameterization followed Fowler and Randall (2002). The radiation scheme was adopted from the Community Atmosphere Model (CAM).

The dynamical core is based on a spherical geodesic grid (Ringler et al., 2000) and solves the vorticity and divergence equations with second-order accuracy. The horizontal grid has 10242 grid cells, with a horizontal grid spacing of about 240 km.

The land-surface model is version 2 of the Simple Biosphere Model developed by Piers Sellers and colleagues (Sellers et al., 1996; Randall et al. 1996). Twelve distinct vegetation classes are defined in SiB2; SiB2 also includes different soil types through properties such as heat capacity and moisture storage capacity. Based on prescribed biome and Normalized Difference Vegetation index (NDVI) values, the fraction of photosynthetically active radiation (FPAR) is determined. Surface roughness is a function solely of vegetation type and is based on canopy height and leaf-area index, a measure of plant density. Surface albedo is computed based on the prescribed leaf-area index, biome type, and soil reflectance (Sellers et. al 1996). SiB2 includes a 'patchy-snow' parameterization to allow surface albedo to vary with snow depth. These variables are used to calculate the exchange of energy, momentum, carbon, and water between the land surface and the atmosphere.

The control run used prescribed realistic surface conditions based on the NDVI climatological mean for the period of 1982 to 1998 (Los et al. 1994) (figure 2.2). For the grassland (forested) extreme case, the 39 points, outlined in figure 2.3, were modified to a biome class of 12 (2 and 3) with appropriate canopy heights and fractional leaf coverage.

For the forested run, fractional leaf coverage peaked during the early summer months of May and June. In the months that follow, it is assumed that, for deciduous trees, dead leaves remain in the canopy for a month before being removed from the canopy and decreasing the canopy greenness (Sellers et al. 1996). In figure 2.4, the land area index (LAI) index of the control run is plotted. The index (equation 2.1) compares the LAI of the control run (LAI_c) to those of the entirely forested run and the grassland run (LAI_f and LAI_g respectively). In this index, having an LAI index close to 1 (0) means that the grid cell had nearly 100% (0%) forest coverage, as seen in the entirely forested (grassland) run.

$$LAI\ index = (LAI_c - LAI_g) / (LAI_f - LAI_g) \quad (\text{Equation 2.1})$$

Overall, the control run was more similar to the entirely forested simulation than to the grassland simulation, with nearly all grid cells having an LAI index of greater than 0.5 (figure 2.4). When comparing the control simulation (figure 2.4) to the 2005-2010 gridded observation forest coverage (figure 2.1), the two estimates were qualitatively similar. Compared to the modern observations, the forest coverages prescribed in the control simulations were underestimated in Maine and overestimated in eastern New York, Vermont, and western New Hampshire.

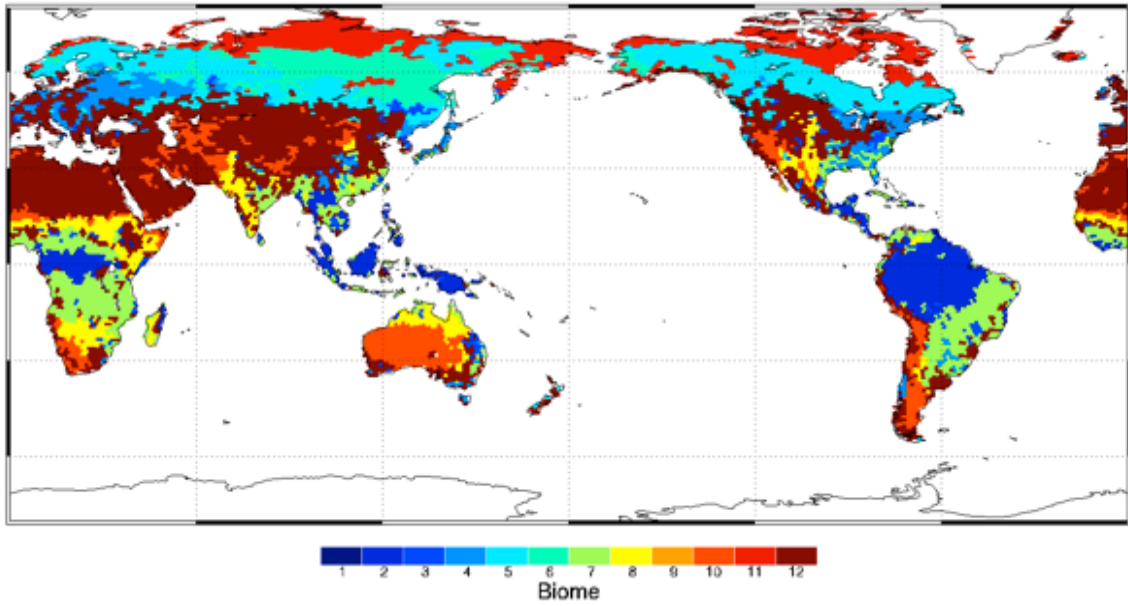


Figure 2.2 Global map of biome types (noted as 1-12) as used in the control run.

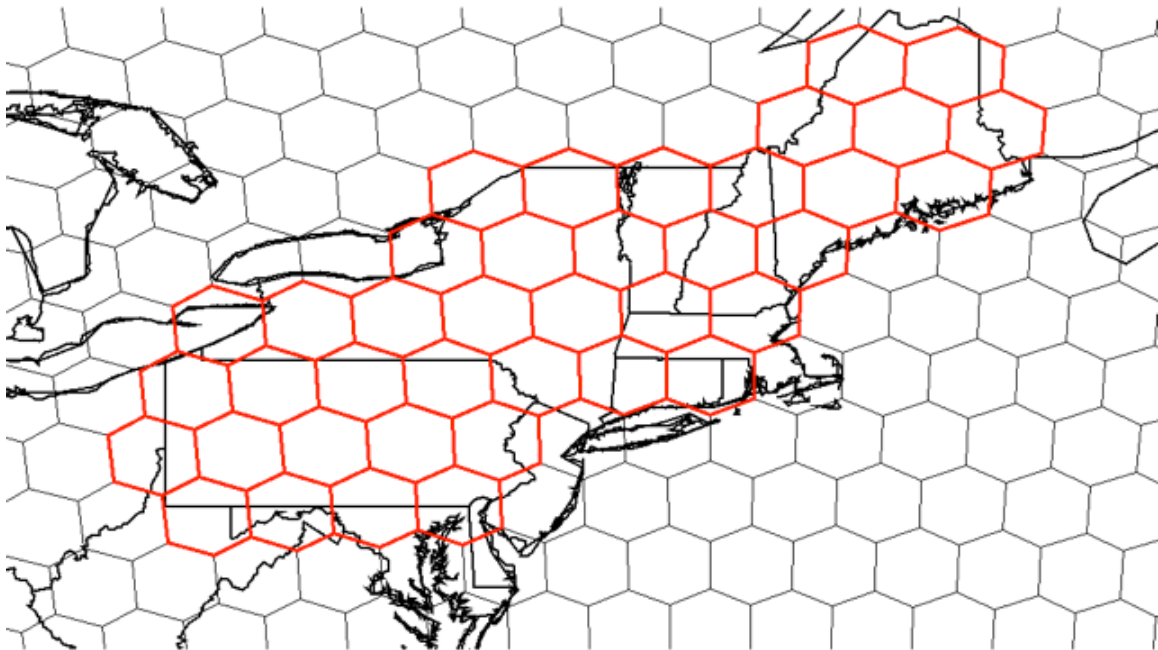


Figure 2.3 Region of interest as used in model run. Cells outlined in red were modified for the forest and grasslands runs.

LAI Index

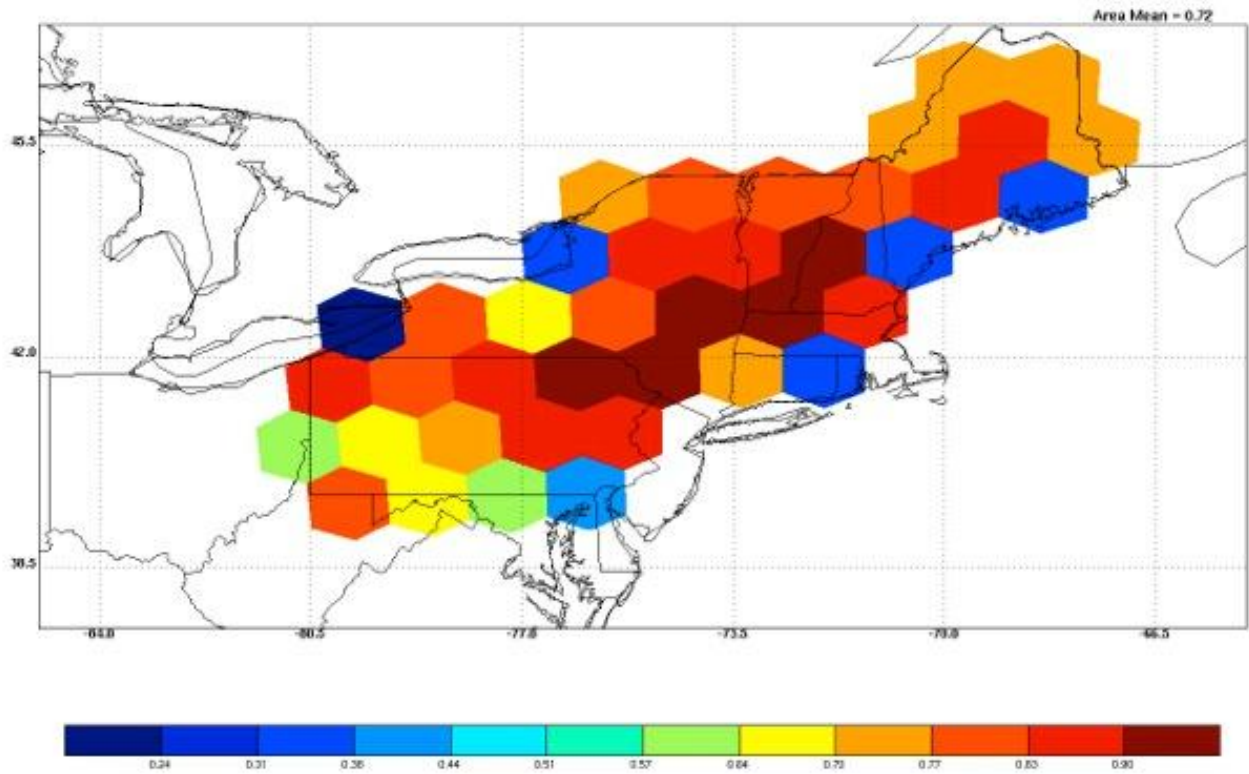


Figure 2.4 The LAI index (equation 2.1) for the control simulation. Having an LAI index closer to 1 (0) indicated having nearly 100% (0%) forest coverage, as in the entirely forested (grassland) run.

Chapter 3: Results of Observational Analysis

3.1. Ground Cover Changes

In this analysis, the modern time period, here defined as the average of the summer seasons from 2005 through 2010, was compared to the historical time period. The historical time period was chosen as the average of the summer seasons between 1950 and 1955, where the summer season was defined as June, July, and August. The absolute change in fractional forest coverage was computed by subtracting the historical fractional forest coverage from the modern fractional forest coverage (figure 3.1). Overall, the average change in fractional forest coverage between the 2005-2010 time period and the 1950-1955 time period was 0.075 and a majority of the region of study had an increase of fractional forest coverage. The largest increases in the absolute change in fractional forest coverage in the modern era were found in eastern New York and southwestern Pennsylvania, with a maximum increase of 0.32 in southwest Pennsylvania. Decreases in fractional forest coverage, with the greatest decrease of 0.15, were located in Connecticut, Rhode Island, and on the coasts of Massachusetts and Maine.

The areas of the northeast United States had large or small changes relative to the historical period were also calculated with the relative fractional forest coverage change (figure 3.2). For example, in Maine and southern Pennsylvania, absolute forest changes were large compared to the rest of the domain. However, this change was small compared to the historical forest coverage for Maine. In contrast, absolute changes of a similar

magnitude in New York resulted in nearly doubling the 1950-1955 fractional forest coverage by 2005-2010.

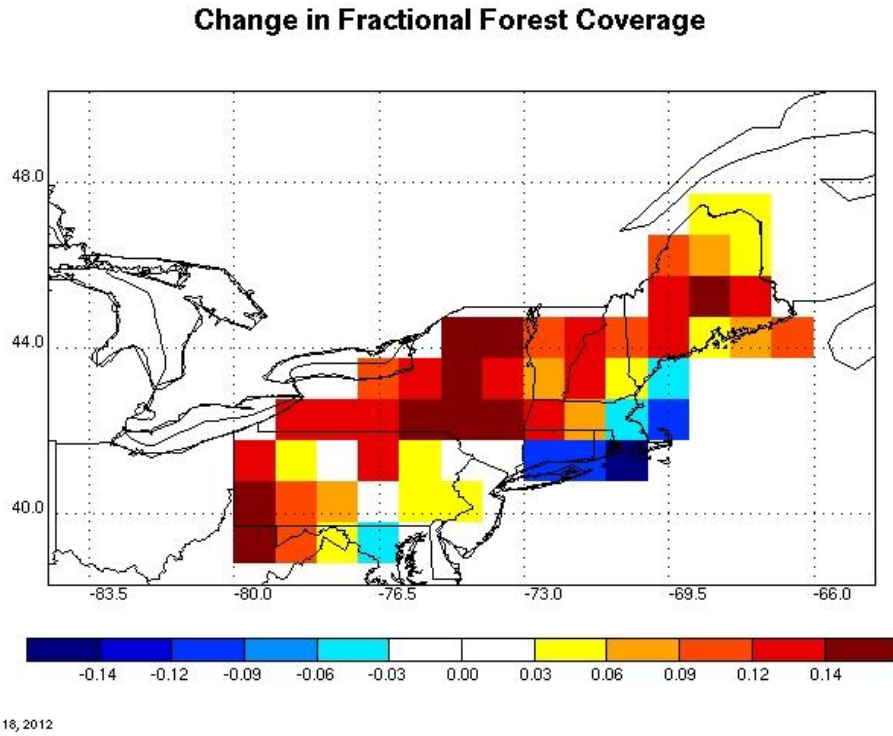
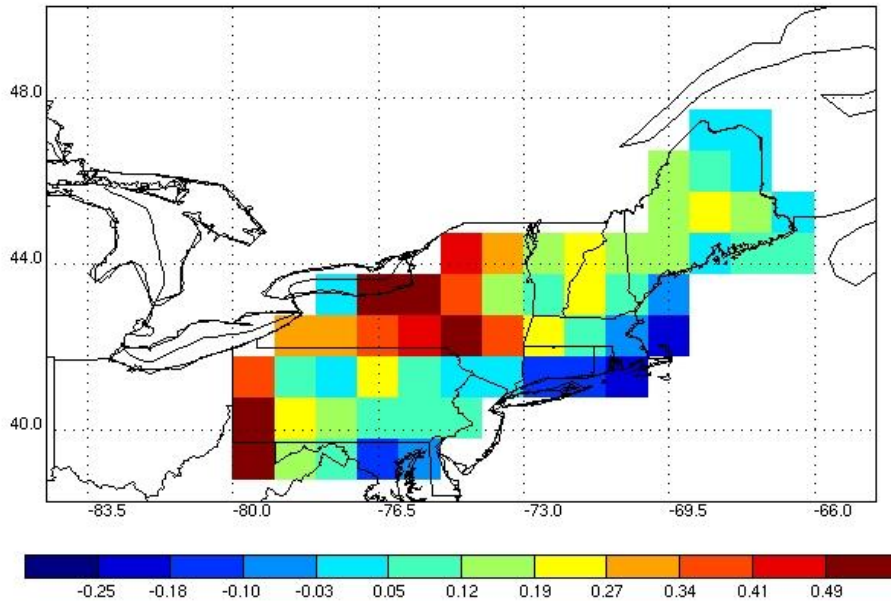


Figure 3.1 The absolute change in fractional forest coverage, calculated by subtracting the fractional forest coverage from the 1950-1955 period from the fractional forest coverage of the 2005 – 2010 period.

Relative Change in Fractional Forest Coverage



Dec 18, 2012

Figure 3.2 The relative fractional change in forest coverage, computed by dividing the absolute change in forest coverage (figure 3.1) by the fractional coverage of the 1950-1955 period.

3.2. Precipitation

Precipitation changes between the present (2005-2010) and the 1950s are displayed in figures 3.3, 3.4, and 3.5. Overall, the average precipitation change in the northeast United States was a slight decrease of 0.18 inches/month. Large sections of the area of interest, including most of Pennsylvania, Vermont, New Hampshire, and Massachusetts had a decrease in average summer season monthly precipitation (figure 3.3). Thus, overall precipitation rates declined in the 2000s compared to the 1950s, with a maximum decrease of 2.28 inches/month found in Massachusetts and Rhode Island. However, there were areas of increased precipitation in the area of study. The maximum precipitation increase of 3.67 inches/month was located in Maine. Positive anomalies in

monthly precipitation rates were primarily located in western New York, Maine, and western Massachusetts (figure 3.3).

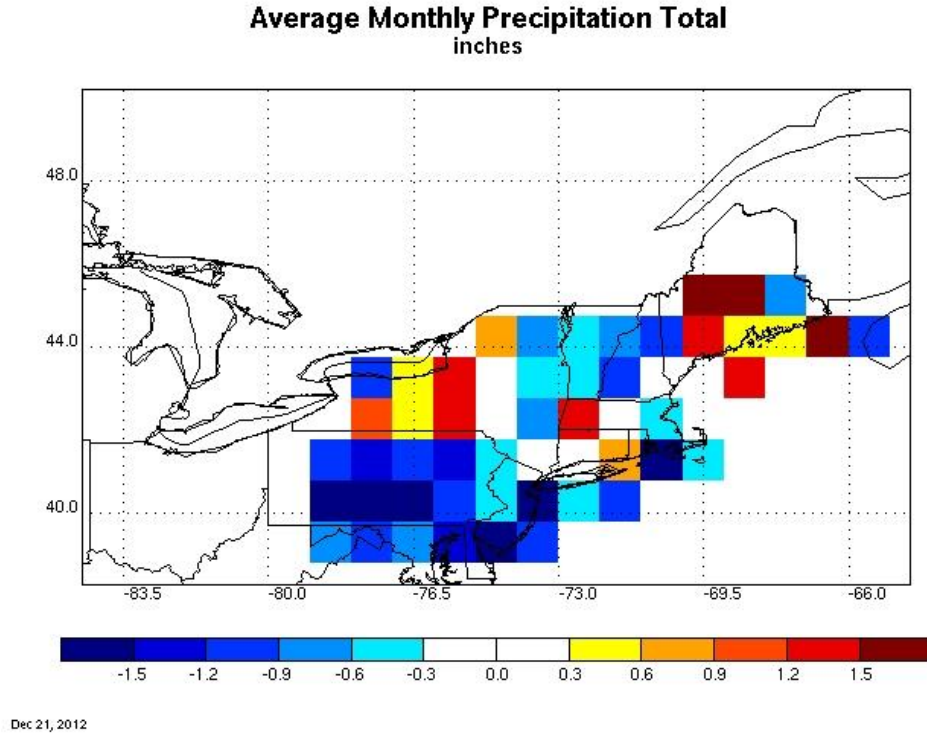


Figure 3.3 Changes in average JJA monthly precipitation in inches between the 2005-2010 time period and the 1950-1955 time period.

Additionally, the significance of the change in each grid box was evaluated using the difference of means t-test (equation 3.1, 3.2), where \bar{X} is the mean of each sample, s^2 is an unbiased estimate of the variance of each sample, and n is the number of data points in each sample. For the degrees of freedom in the sample, the number of months included, 18, was used.

$$t = \frac{\bar{X}_1 - \bar{X}_2}{s_{\bar{x}_1 - \bar{x}_2}} \quad \text{(Equation 3.1)}$$

$$s_{\bar{x}_1 - \bar{x}_2} = \sqrt{\frac{s_1^2}{n_1} + \frac{s_2^2}{n_2}} \quad \text{(Equation 3.2)}$$

Significant changes in precipitation were plotted in figure 3.4. Out of the grid boxes with significant changes, the differences were more evenly distributed between positive and negative changes (figure 3.4). Again, the precipitation decreases were found in Pennsylvania, along the Appalachian Mountains, and off the coast of Maine. Precipitation increases were located again in Maine and off of Lake Ontario, in western New York. The mean of the significant precipitation changes was -0.15 inches/month, a small increase in the modern time period precipitation totals compared to the 1950s.

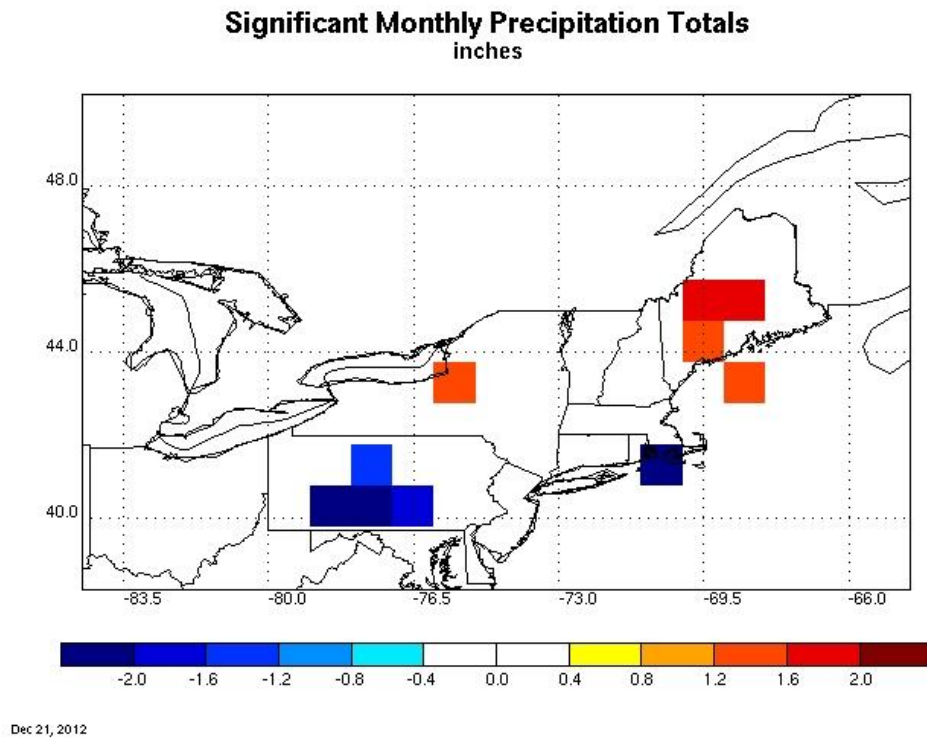


Figure 3.4 Changes in average JJA monthly precipitation in inches significant at the 95% confidence level between the 2005-2010 time period and the 1950-1955 time period.

The spread of all changes in average monthly precipitation, including both significant and insignificant changes as a function of fractional forest coverage is plotted in figure 3.5. Overall, a weak positive relationship between changes in precipitation rate and changes in tree coverage is recorded. Increasing the amount of land area covered by

forests increases the amount of precipitation in general within the region. The relationship can be modeled with linear regression (equation 3.3), where y represents the change in average summer season monthly precipitation and x is the fractional forest coverage for a certain grid box.

$$y = 4.1x - 0.47 \quad \text{(Equation 3.3)}$$

However, the data had a large spread around the regression line, with a correlation coefficient of 0.302 (figure 3.5). When only the significant changes are considered, the correlation coefficient increases 0.75.

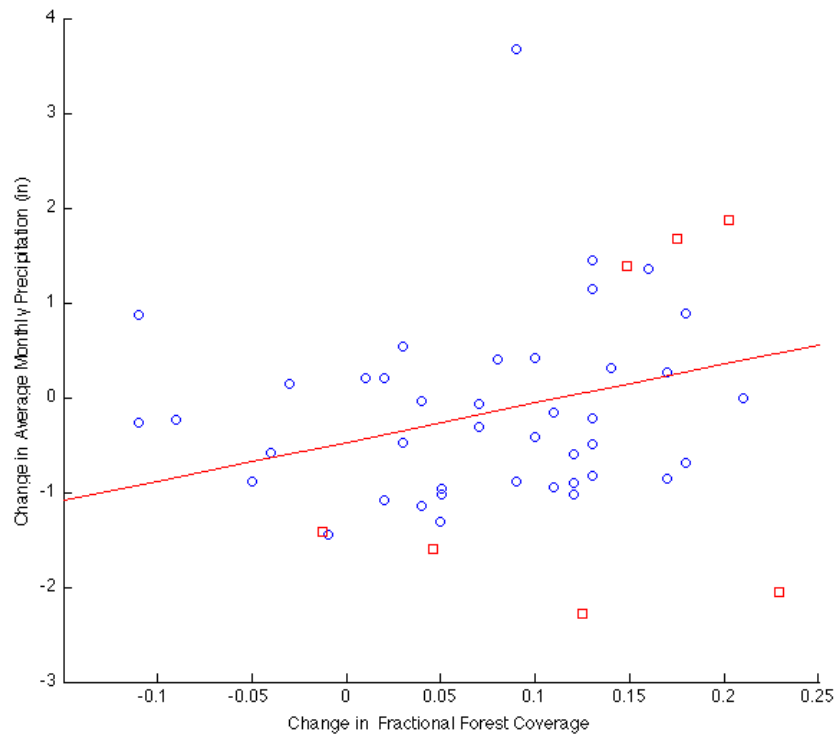


Figure 3.5 Change in average JJA monthly precipitation (inches) versus the change in fractional tree coverage. The red line is the linear regression of the plotted data, and is equal to $y=4.1x - 0.47$. The blue circles represent non-significant changes in monthly precipitation and the red squares represent significant changes in monthly precipitation.

3.3. Surface Temperature

Changes in average summer season surface temperature were typically located along the Atlantic coast (figure 3.6). Overall, the differences in temperature between the modern and historical time periods were small, ranging from 1.56 K to -1.36 K. There was no structure in the distribution of positive and negative shifts in average temperature, with positive shifts in average JJA temperature occurring in Pennsylvania, Massachusetts, New Hampshire, Vermont, and Maine. Negative changes in surface temperature were also located in Pennsylvania, Massachusetts, and Maine, with no qualitative connection to topography or the relative and absolute changes in forest coverage (figure 3.1). The average change in the region of interest was 0.05 K. None of the changes were significant at the 95% confidence level.

There was a negative linear relationship between the changes in average surface temperature and absolute or relative changes in tree coverage (equation 3.4).

$$y = -0.84x + 0.1 \quad \text{(Equation 3.4)}$$

However, the spatial correlation coefficient between temperature and both measurements of forest coverage change was only -0.11 (figure 3.7), thus the linear relationship between the two variables was weak.

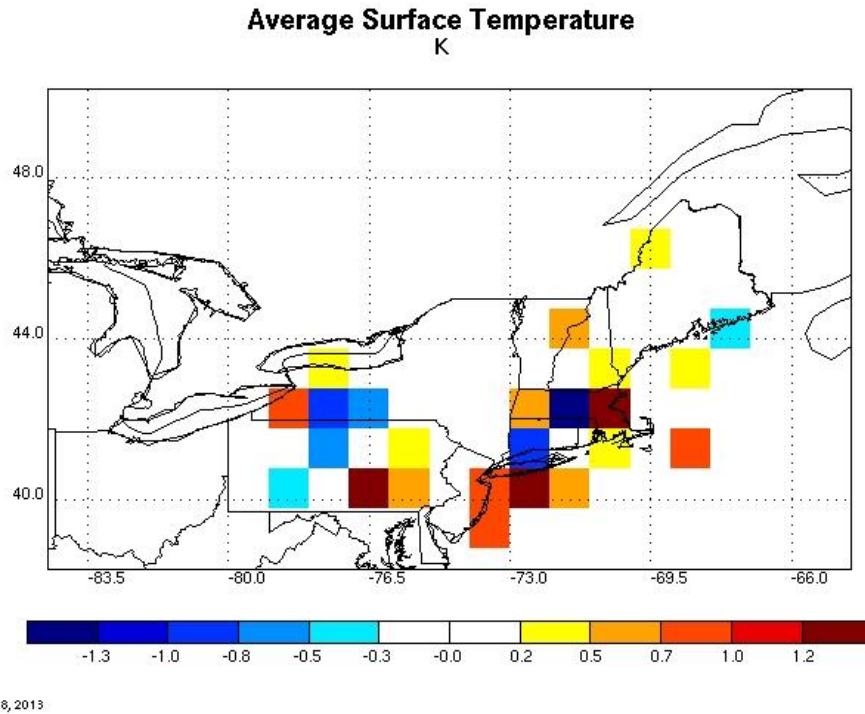


Figure 3.6 Changes in average JJA surface temperature (K) between the 2005-2010 time period and the 1950-1955 time period.

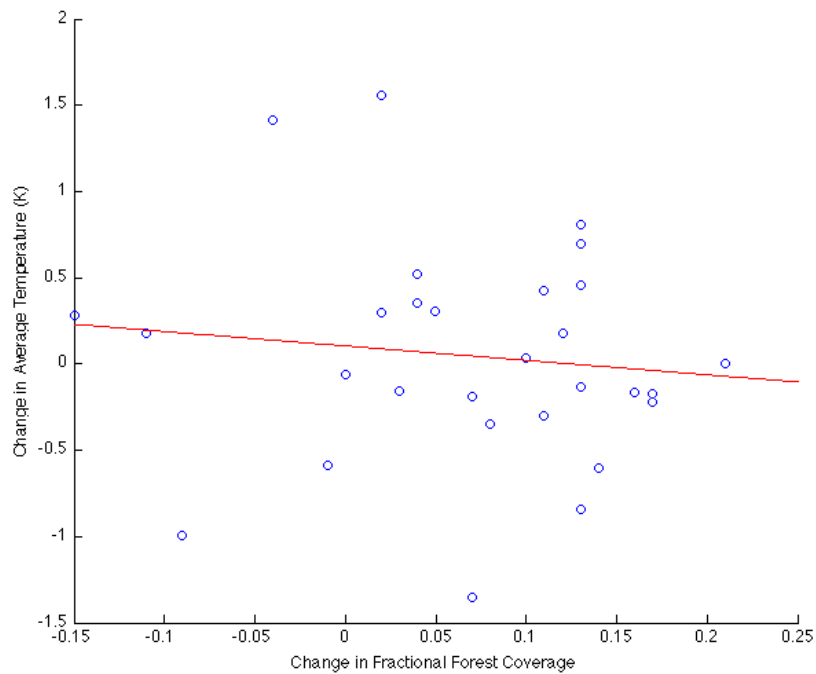


Figure 3.7 Change in average JJA surface temperature (K) versus the absolute change in fractional tree coverage. The red line is the linear regression of the plotted data, and is equal to $y = -0.84x + 0,1$ (as in equation 3.4).

The changes in the average JJA daily maximum and minimum surface temperatures were also analyzed. Both variables increased on average over the area of interest. Average daily maximum surface temperature increased by 0.08 K (figure 3.8). The majority of the large increases, including changes as large as 4.98 K, were found in eastern Pennsylvania and along the eastern coast of Connecticut, Rhode Island, and Massachusetts. Small decreases were located in southern New York and coastal Maine. The largest negative shifts in maximum temperatures, on the order of 1.76 K, were in New York (figure 3.8), in the same region as large relative shifts in fractional forest coverage (figure 3.2). As in average surface temperature, none of the changes in average daily maximum temperature were significant at the 95% level.

A weak negative correlation existed between average JJA daily maximum temperatures and absolute (relative) fractional forest coverage. Both correlations were equal to -0.20, and both comparisons had a negative linear relationship (equation 3.3. for daily maximum temperature and absolute fractional forest coverage) between the temperature and forest coverage variables (figure 3.9).

$$y = -2.6x + 0.23 \quad \text{(Equation 3.5)}$$

Overall, there was a positive linear relationship between daily minimum surface temperatures changes and fractional forest changes (figure 3.11, equation 3.5).

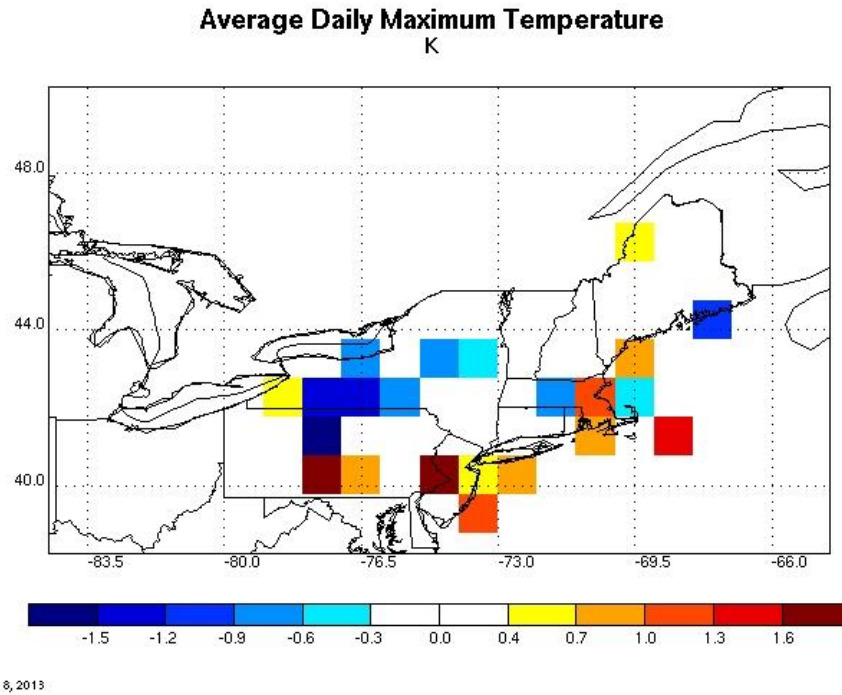


Figure 3.8 Changes in average JJA daily maximum temperature (K) between the 2005-2010 time period and the 1950-1955 time period.

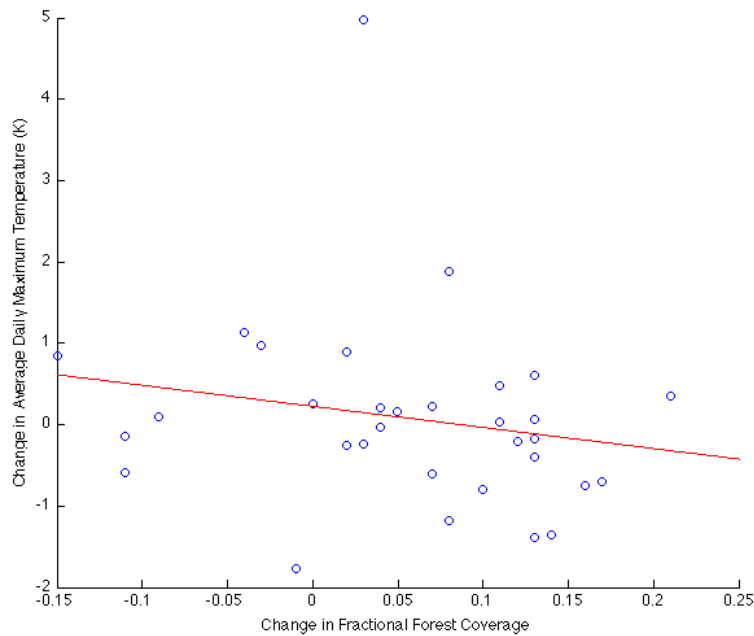


Figure 3.9 Change in average JJA surface daily maximum (K) versus the absolute change in fractional tree coverage. The red line is the linear regression of the plotted data, and is equal to $y = -2.6x + 0.23$ (as in equation 3.5).

Overall, average surface daily minimum temperatures increased in the modern time period relative to the historical time period. The largest increases were in south-central Pennsylvania and western Massachusetts, with the greatest shifts around 2.5 K, or half of the scale of the maximum changes in daily maximum temperatures. Decreases in minimum surface temperatures were not located in the same areas as the decreases in maximum daily temperature or average surface temperature, while there were common increases in all three variables in southern Pennsylvania. The largest decreases were on the order of 3 K. In New York, while areas of increased temperatures corresponded to regions of increased forest coverage, there was typically no connection between the magnitude of forest coverage alteration and temperature shifts. The average increase in minimum temperatures, at 0.36 K, was larger than the increase in daily maximum temperatures. Again, the changes in daily minimum temperature were not significant at the 95% confidence level.

Out of the three temperature variables analyzed, average daily minimum temperature had the strongest connection with absolute and relative changes in forest coverage (figure 3.11). Between daily minimum surface temperature and absolute forest changes, the spatial correlation was 0.43, while the correlation was slightly lower between minimum surface temperature shifts and relative forest changes at 0.38.

$$y = 4.7x + 0.086 \quad \text{(Equation 3.6)}$$

The linear relationship between the summer season daily minimum temperatures and absolute fractional forest change was positive (equation 3.6, figure 3.11). There was also a

positive relationship between temperatures and relative forest changes that was weaker than in equation 3.6.

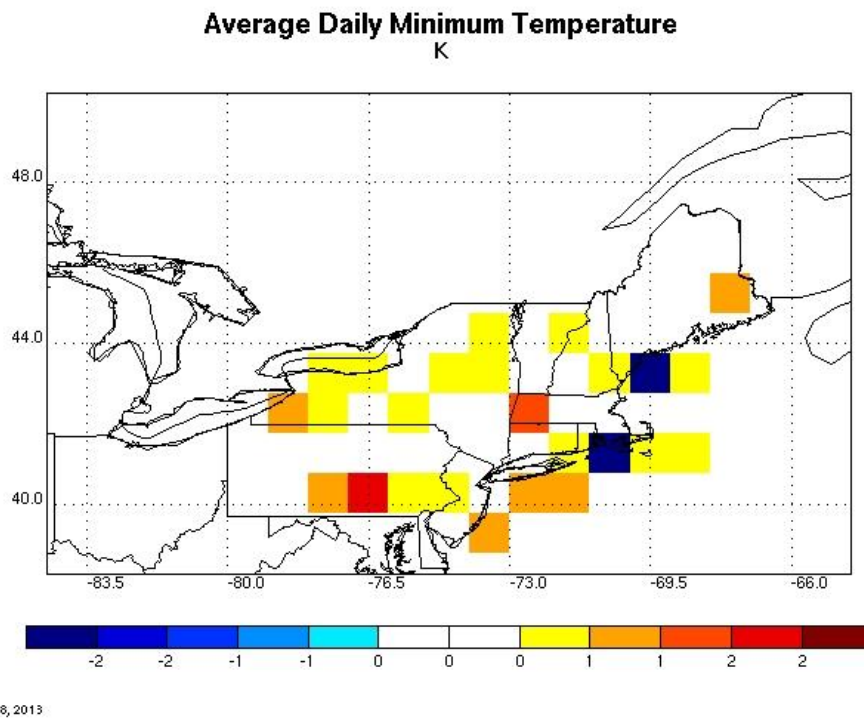


Figure 3.10 Changes in average JJA daily minimum temperature (K) between the 2005-2010 time period and the 1950-1955 time period.

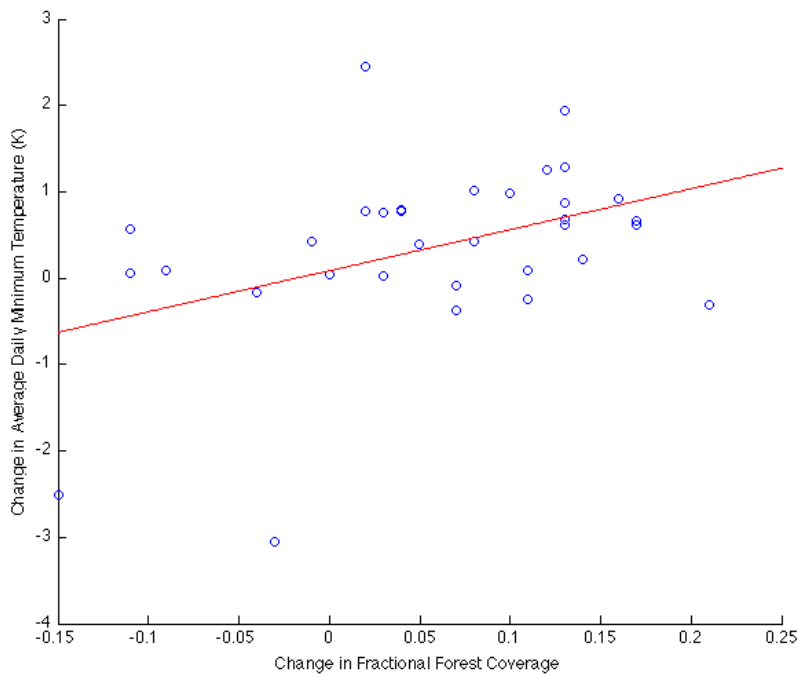


Figure 3.11 Change in average JJA surface daily minimum temperature (K) versus the absolute change in fractional tree coverage. The red line is the linear regression of the plotted data, and is equal to $y=4.7x+0.086$ (as in equation 3.6).

3.4. Summary

In the time between the mid-20th century (1950-1955) and modern (2005 – 2010) years, there was considerable regrowth in northeastern United States’ forests. A majority of the area of study had a positive change in fractional forest coverage. Only Massachusetts, Connecticut, and Rhode Island alone had deforestation during this time period. The largest reforestation occurred in central New York, with some counties more than doubling the amount of land area covered by forests in the 2000s compared to the 1950s. Typically, reforestation was modest and on the scale of a relative increase of 20%. Most of the computed relationships between fractional forest coverage change and

atmospheric quantities were weak. There was no connection between average JJA surface temperature and the observed forest coverage change. Between average daily maximum surface temperatures, there was a weak negative relationship, with most changes in temperature found the southern part of the area of interest. In general, daily minimum average temperature increased in time with increases located across the entire domain, with spatial correlation of 0.4, which was not expected. Overall, there were few strong changes in temperature, with the averages of the three variables all close to 0, between the historical and modern time periods in the United States. While no significant changes in temperature variables were seen in the observations, there were significant shifts in monthly precipitation totals. Most negative shifts in monthly precipitation occurred in Pennsylvania, Vermont, and New Hampshire and increases in Maine and New York. When analyzing all changes in the region, there was a slight decrease in precipitation between the two time periods and a weak positive relationship between precipitation totals and fractional forest coverage, similar to results from studies such as Strack et al. (2008). However, when the changes are constrained those significant at the 95% confidence level, there were moderate decreases (increases) in monthly precipitation totals in PA (NY) and there was a strong positive relationship between the two. The strongest connections were between forest coverage and precipitation changes significant at the 95% confidence level and forest coverage and average daily minimum temperatures.

A summary of the comparison between the modern and historical eras for monthly precipitation, average surface temperature, and average daily maximum and minimum surface temperature was included in table 3.1.

Table 3.1: Summary of relationships between listed variables and the fractional forest cover change between the present (2005-2010) and the 1950s (1950-1955).

	Modern - Historical Comparison
Monthly Precipitation Total	Weak positive
Significant Monthly Precipitation Total Changes	Strong positive
Average Surface Temperature	No relationship
Average Daily Maximum Surface Temperature	Weak negative
Average Daily Minimum Surface Temperature	Weak positive

A summary of relationships between listed variables and the fractional forest cover change between the present (2005-2010) and the 1950s (1950-1955) is presented in table 3.1. Each relationship was described as strong positive (negative), weak positive (negative), or no relationship. For example, having a 'strong positive' relationship indicated that a variable increased as forest coverage increased. A strong relationship was defined as having a positive (negative) regression coefficient and a correlation coefficient with an absolute value greater than 0.5. A weak relationship was defined as having a positive (negative) regression coefficient and a correlation coefficient with an absolute value between 0.2 and 0.5. Having no relationship was defined as having a correlation coefficient with an absolute value less than 0.2.

Chapter 4: Results of Model Analysis

4.1. Analysis of the Effects of Ground Cover on Atmospheric Quantities

In the figures, all areas shaded in are significant at the 95% confidence level as computed with the difference of means t-test (equations 3.1, 3.2) with an n-value of 15, based on the number of months included in each five-year sample. For all comparisons, data was averaged over the summer season of June, July, and August. In this analysis, the differences between the forest and grasslands simulation (FG comparison), the forest and control simulations (CF comparison), and the control and grasslands run (CG comparison) were analyzed. When comparing two different simulations, the less forested simulation was always subtracted from the more forested run so as to show the impact of reforestation on each selected variable.

4.2. Surface Fluxes

Significant changes in surface latent heat fluxes over the entire globe are displayed in figure 4.1 (top) and significant changes in the northeastern United States in figure 4.1 (bottom). Overall, the significant changes in latent heat flux scattered across the globe. Positive changes in latent heat flux are located in the Pacific Ocean between 15 and 30 degrees south latitude and smaller positive changes in South America. These increases in latent heat flux may be due to shifts in planetary wave locations. However, while the changes are significant, it is unlikely that the changes outside the study region are

meaningful. Here, a positive difference in latent heat flux indicates that the forested run had higher fluxes of latent heat compared to the grassland run. Out of the 39 grid cells in the study region, all had an increase in surface latent heat flux. The change in latent heat flux over the study region ranged from approximately 40.02 W/m^2 to 66.99 W/m^2 with an average increase of 54.16 W/m^2 . Smaller increases in latent heat were located in eastern Pennsylvania, southeastern New York, and along the eastern coast of Maine. The largest increases in latent heat flux were found in Rhode Island and northern New York and Vermont (figure 4.1 bottom). There was no distinct spatial pattern in the increases of latent heat fluxes.

When comparing the completely reforested run and the control run, the overall global pattern was similar (figure 4.2 top). The change in surface latent heat flux was about half compared to the change in the forest-grasslands comparison, but qualitatively the pattern was similar. Pockets of increased and decreased surface latent heat fluxes were found across South America and the Pacific Ocean, as in the previous comparison. A large positive change was located in the southern Pacific Ocean (figure 4.2 top). In the region of study, only 23% of the grid cells had a significant latent heat flux change. The changes in the control run compared to the reforested run were smaller than in the FG comparison, but the shift in the CG comparison was still large. The maximum change was an increase of 41.63 W/m^2 and the average change was 18.42 W/m^2 (figure 4.2 bottom). The greatest increase in surface latent heat flux did not occur in the same grid cell as the maximum change in the FG comparison. A decrease in surface latent heat flux of 14.52 W/m^2 was found in south-central Pennsylvania. In contrast, when comparing the control simulation to the grasslands run (CG), nearly the entire study region had a significant increase in

surface latent heat flux. The changes in the CG comparison similar to the changes in the forest-to-grasslands comparison; here, the maximum increase was 62.96 W/m^2 , the average was 48.43 W/m^2 , and the minimum was 20.98 W/m^2 (figure 4.3 bottom). However, there were fewer significant changes around the world in the CG comparison. The global pattern was dominated by the changes in the study region and, for example, the large increase in latent heat fluxes in the Pacific Ocean was not seen in this comparison (figure 4.3 top).

On a global scale, the majority of significant changes in surface sensible heat fluxes were found in the northeastern United States as well (figure 4.4 top). There were slight increases in sensible heat flux in the extratropical Pacific Ocean, sporadically located across the United States and South America, and in Siberia. When focusing in on the northeastern United States, again, all thirty-nine altered grid cells had a negative change in sensible heat flux. Thus, in this region, the reforestation represented by the all forested run decreased the amount of sensible heat fluxes. Overall, the impact on sensible heat fluxes was smaller than the impact on the latent heat fluxes. Decreases in the sensible heat flux in the study region averaged 21.18 W/m^2 , with a range of 32.27 W/m^2 to 10.48 W/m^2 (figure 4.4 bottom). The smallest changes in sensible heat fluxes were located in northern and central Pennsylvania, central New York, and southern Maine. Off the coast of Maine, there were slight significant increases of sensible heat flux on the order of 10 W/m^2 (figure 4.4 bottom).

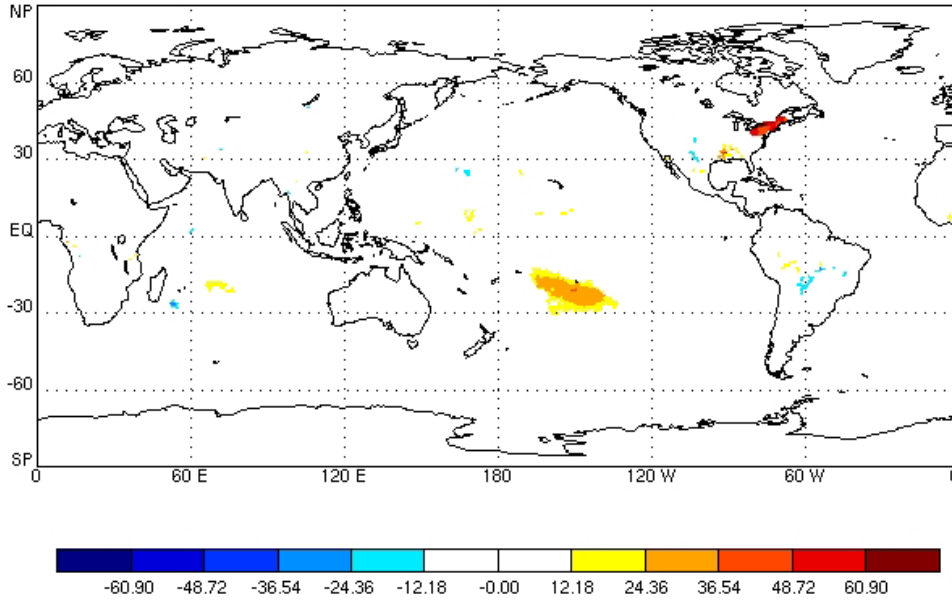
Similar changes in surface heat flux are seen when comparing the control run to the grasslands run. 87% of the cells had a significant decrease of surface sensible heat fluxes

when the amount of tree coverage increases. For this comparison, the average decrease was 21.18 W/m^2 (figure 4.6 bottom). The maximum decrease was 38.15 W/m^2 ; the largest decreases were located in southern Pennsylvania and upstate New York. The smallest decreases, including the minimum decrease of 11.53 W/m^2 , were found in central New York, Rhode Island, and eastern Maine (figure 4.6 bottom). Overall, the most striking changes occurred in the study region. In addition, a small decrease in surface sensible heat flux over Louisiana and scattered increase through the midwest United States, Russia, and Brazil (figure 4.6 top). In comparison, when looking at the difference between the forest and control runs, the global changes were similar to the forest-grassland comparison. An increase in sensible heat fluxes in the southern Pacific Ocean was the largest response on the global scale (figure 4.5 top) as a majority of the significant changes are scattered across the Americas and Europe instead of forming a cohesive pattern. Again, only 21% of the cells located in the study region had a significant change in surface sensible heat fluxes. In southern Pennsylvania, there was a significant increase in the flux, with a maximum of 21.9 W/m^2 , while all other changes were a decrease in sensible heat flux (figure 4.5 bottom). The largest decrease in sensible heat flux, approximately -38 W/m^2 , was located in eastern Maine (figure 4.5 bottom). The significant decreases in sensible heat flux were primarily found along bodies of water, such as the coasts of Maine and Rhode Island and along Lakes Erie and Ontario. Overall, the average change in sensible heat flux when comparing the control to the completely reforested run was -8.57 W/m^2 (figure 4.5 bottom).

FOREST - GRASSLAND COMPARISON

Surface Latent Heat Flux

W/m²



Surface Latent Heat Flux

W/m²

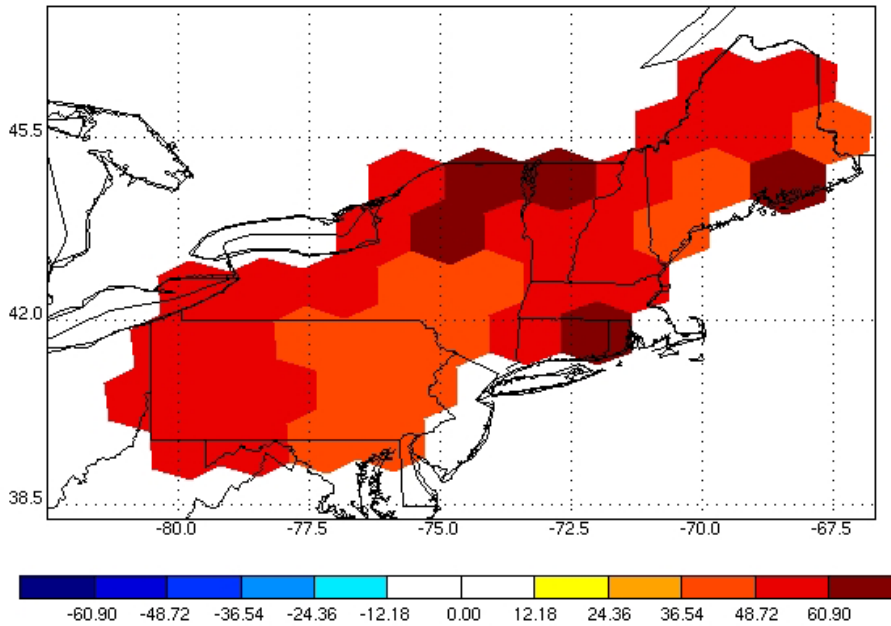
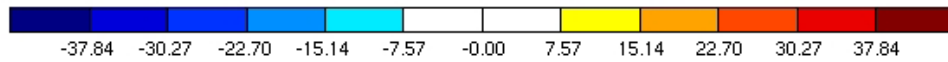
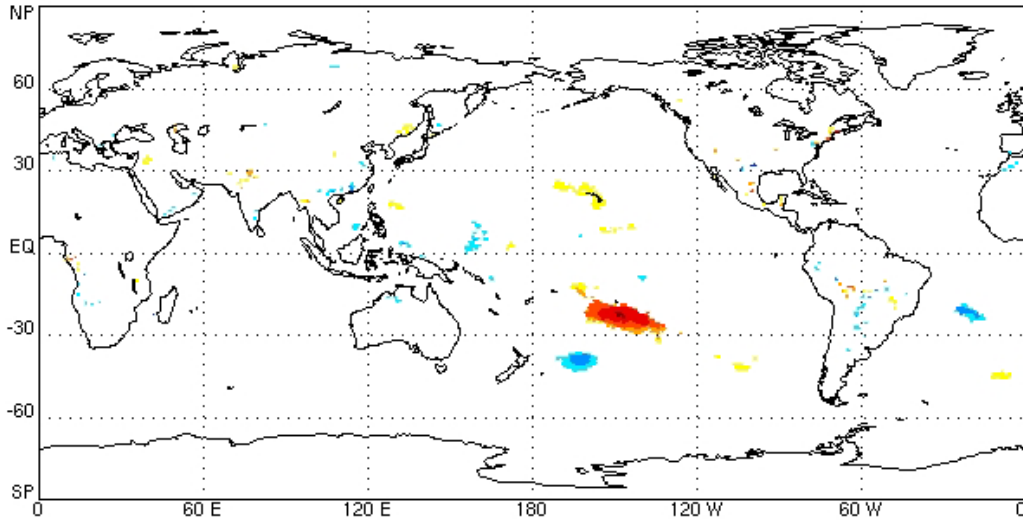


Figure 4.1 Changes globally (top) and in the study region (bottom) in average JJA surface latent heat fluxes (W/m^2) between the entirely forested run and the grassland run. All colored areas are a change significant at the 95% confidence level.

FOREST - CONTROL COMPARISON

Surface Latent Heat Flux

W/m^2



Surface Latent Heat Flux

W/m^2

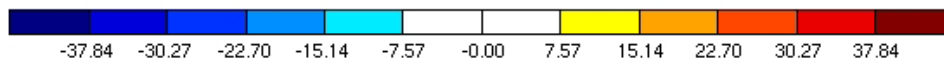
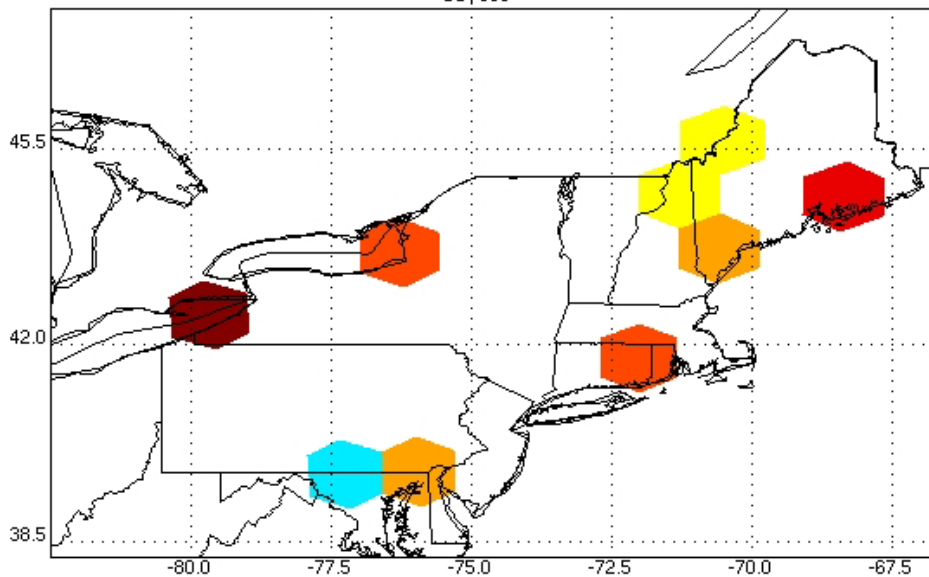
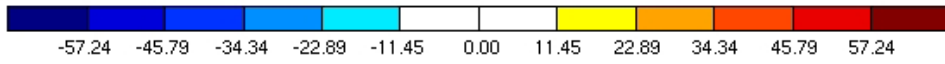
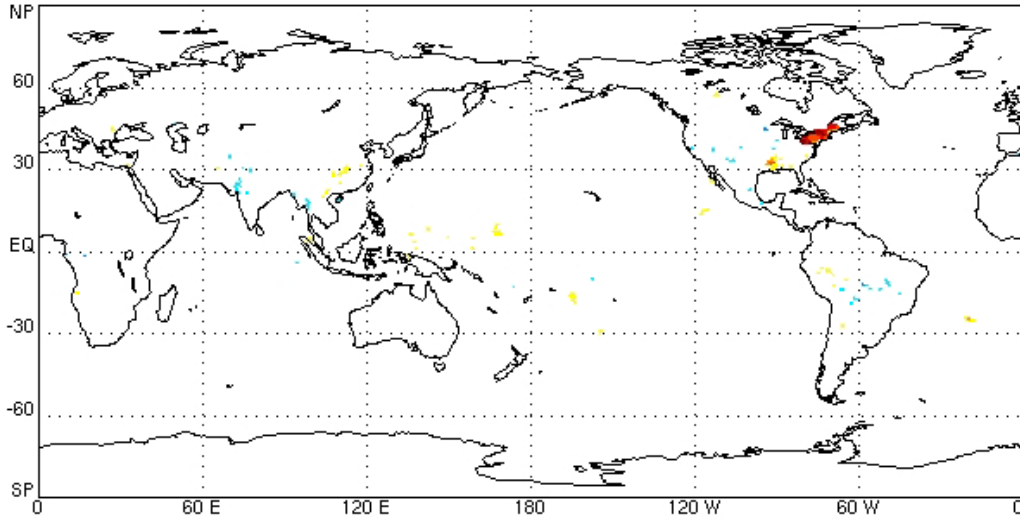


Figure 4.2 Changes globally (top) and in the study region (bottom) in average JJA surface latent heat fluxes (W/m^2) between the entirely forested run and the control run. All colored areas are a change significant at the 95% confidence level.

CONTROL - GRASSLAND COMPARISON
Surface Latent Heat Flux
W/m²



Surface Latent Heat Flux
W/m²

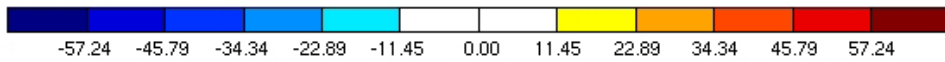
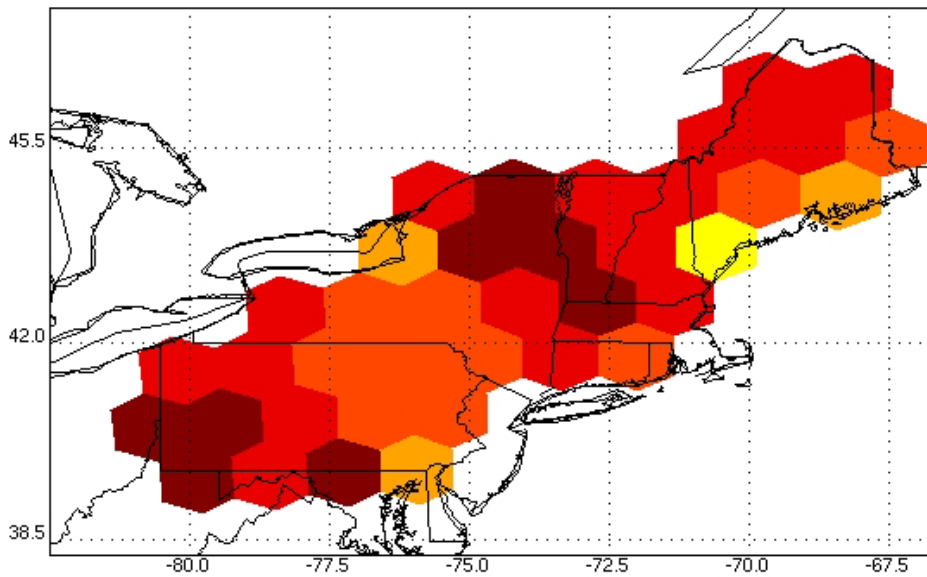
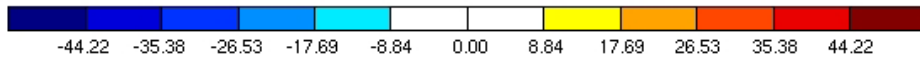
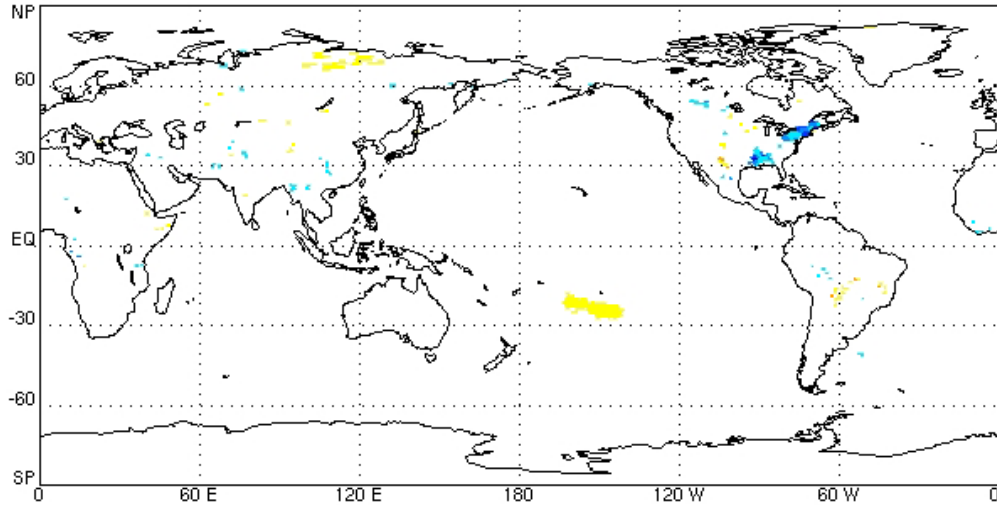


Figure 4.3 Changes globally (top) and in the study region (bottom) in average JJA surface latent heat fluxes (W/m²) between the control run and the grassland run. All colored areas are a change significant at the 95% confidence level.

FOREST - GRASSLAND COMPARISON

Surface Sensible Heat Flux

W/m^2



Surface Sensible Heat Flux

W/m^2

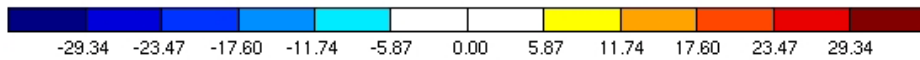
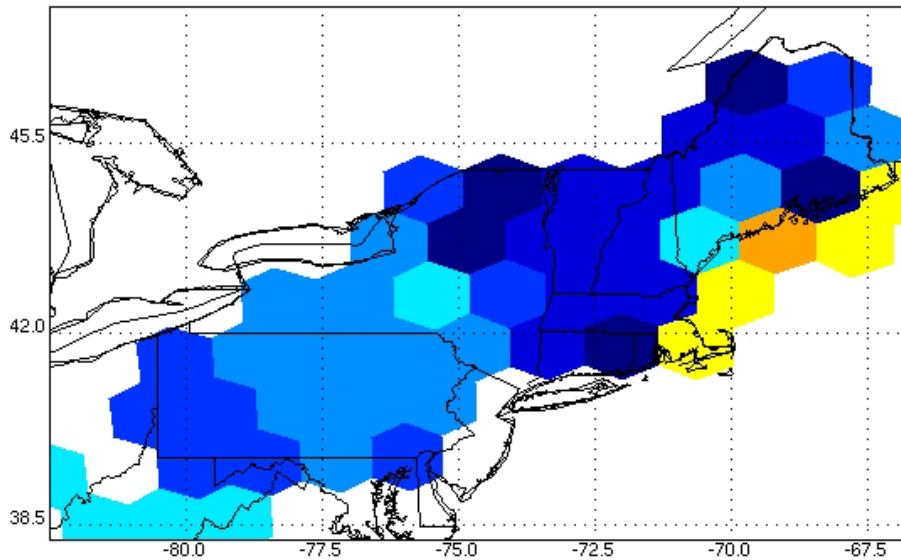
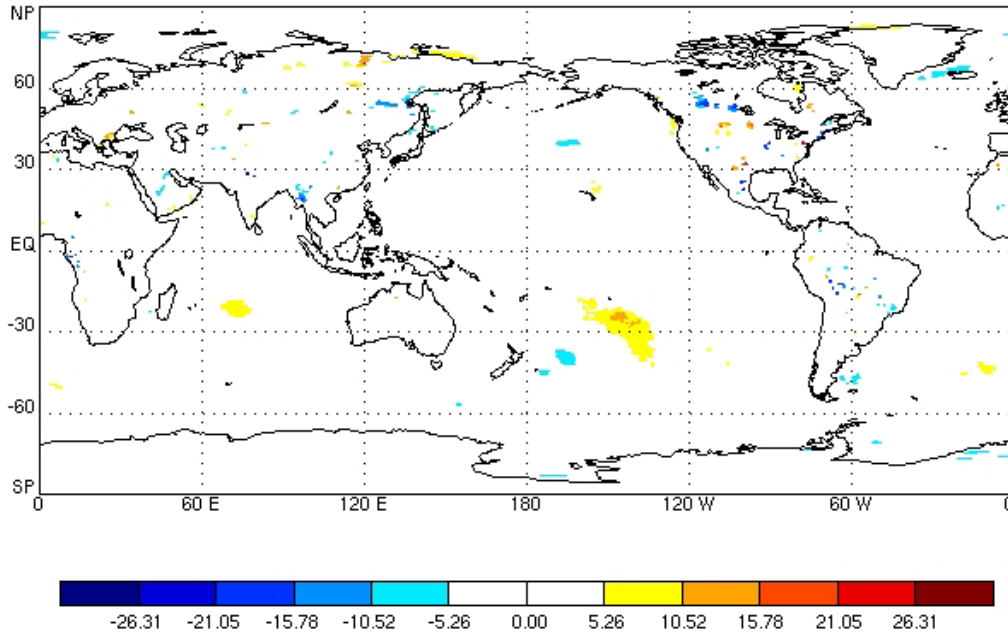


Figure 4.4 Changes globally (top) and in the study region (bottom) in average JJA surface sensible heat fluxes (W/m^2) between the entirely forested run and the grassland run. All colored areas are a change significant at the 95% confidence level.

FOREST - CONTROL COMPARISON

Surface Sensible Heat Flux

W/m^2



Surface Sensible Heat Flux

W/m^2

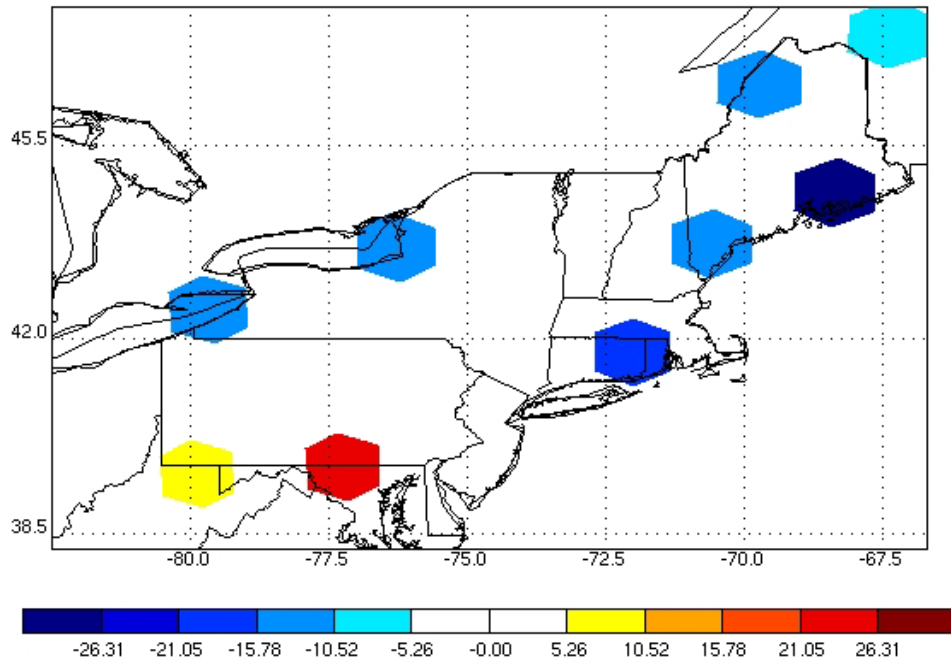
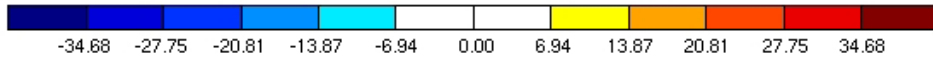
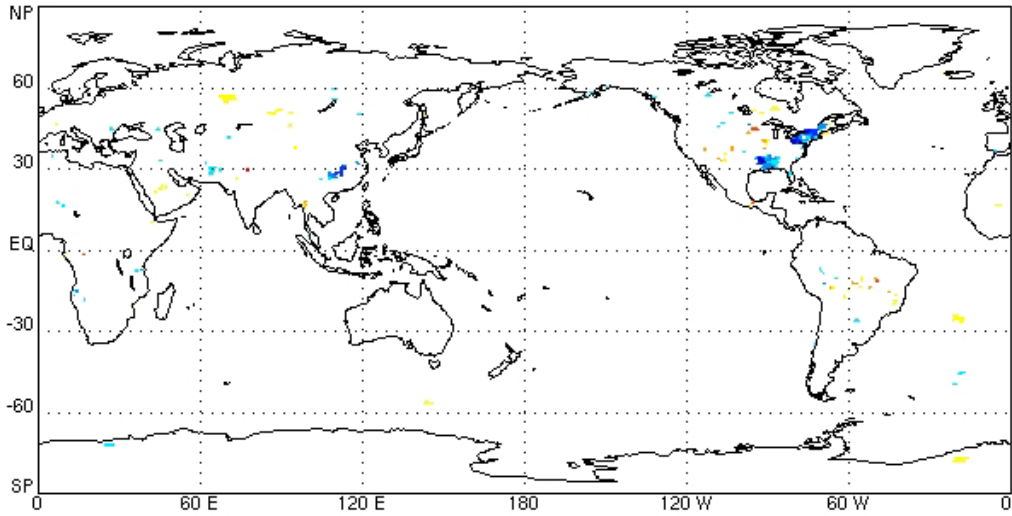


Figure 4.5 Changes globally (top) and in the study region (bottom) in average JJA surface sensible heat fluxes (W/m^2) between the entirely forested run and the control run. All colored areas are a change significant at the 95% confidence level.

CONTROL - GRASSLAND COMPARISON
Surface Sensible Heat Flux
 W/m^2



Surface Sensible Heat Flux
 W/m^2

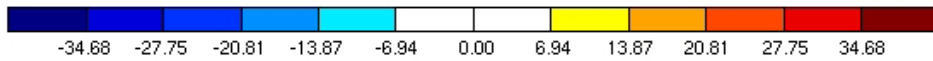
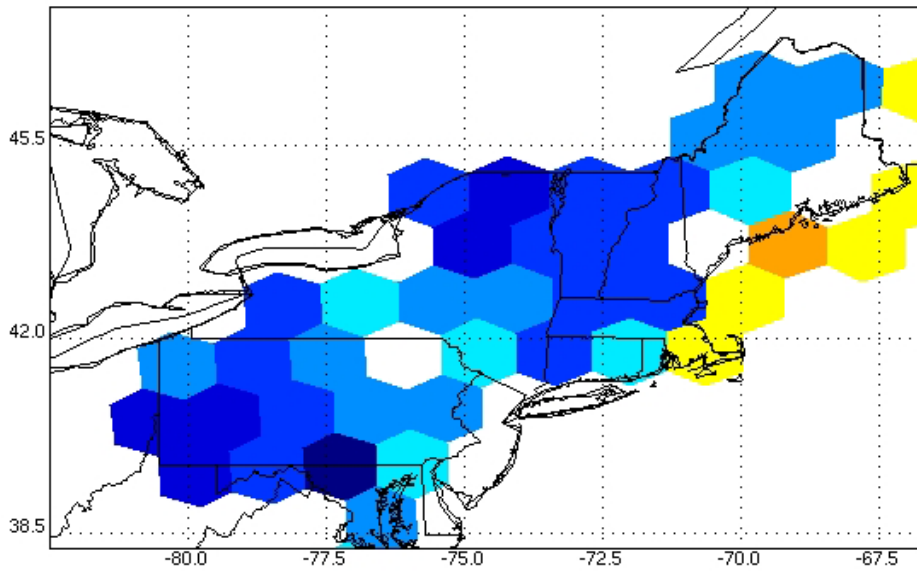


Figure 4.6 Changes globally (top) and in the study region (bottom) in average JJA surface sensible heat fluxes (W/m^2) between the control run and the grassland run. All colored areas are a change significant at the 95% confidence level.

4.3. Temperature

For the average summer season temperature, the global map of changes between the forested and grassland run, the dominant change was a major decrease in temperatures over the northeast United States. There were very few other significant changes, including slight decreases in the northern high latitudes (figure 4.7 top). When comparing the control and grassland runs, a similar dominant change in temperatures over the northeast United States was seen (figure 4.10 top). There are few other significant differences in temperatures between the control and grassland runs. In comparison, when comparing temperatures from the forested and control runs, there are few significant differences (figure 4.9 top). The large changes over the northeast United States are not present.

In the region of study, all grid boxes had a significant decrease in average JJA temperature when comparing the forested and grasslands run (figure 4.7 bottom). The spatial distribution pattern of the cooling was not similar to the changes in latent or sensible heat flux. There was an average cooling of -1.91 K in the area of study, with a maximum decrease of -2.63 K and a minimum decrease of -1.06 K (figure 4.7 bottom). The smallest changes were found in the Lake Ontario region where there were small decreases in sensible heat and moderate increases in latent heat fluxes. The largest decreases in temperature were found in western Pennsylvania. In contrast, when comparing the forested and control runs, only Rhode Island had a significant change in temperature of -1 K (figure 4.9 bottom). The differences between the control and grassland runs were on a scale similar to the changes between the forested and grassland runs (figure 4.10 bottom). The average change in the CG comparison was -1.78K, with changes ranging from -2.50K to -1.05K. However, the spatial pattern of the temperature changes differed from the FG

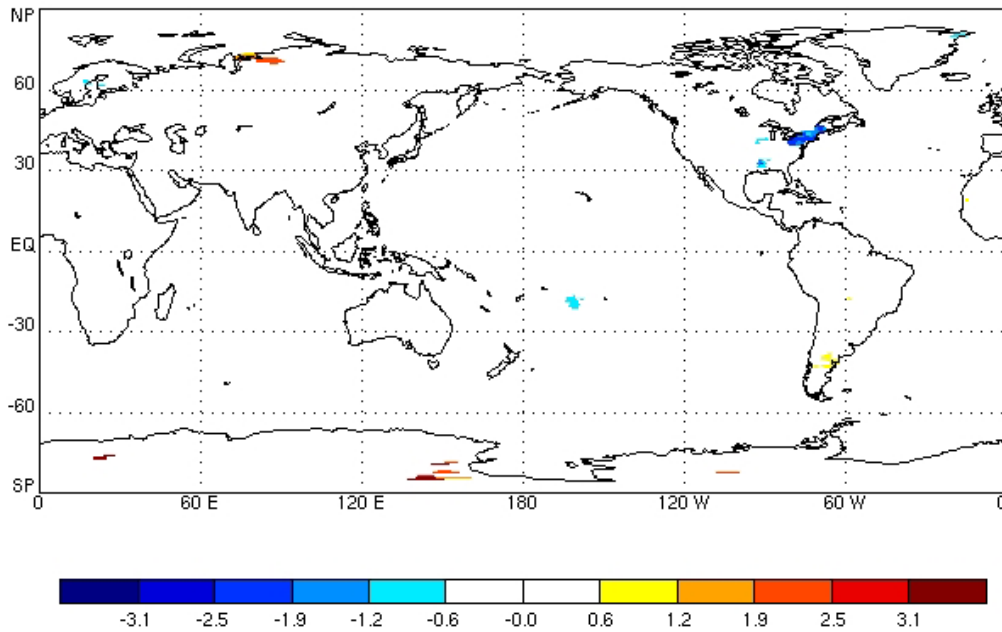
comparison. While the changes in Maine's temperature were similar between the two, the CG comparison had relatively larger temperature decreases concentrated in Pennsylvania, New York, and Vermont, with no distinct change around the Great Lakes region.

Daily maximum and minimum temperatures, averaged over the summer season, were also computed (figure 4.8). Here, the maximum (minimum) temperature was defined as the highest (lowest) temperature in each 24-hour period within the sample. All maximum (minimum) temperatures were then averaged together to compute the average daily maximum (minimum) temperature. When comparing the forest and grasslands runs, 30% of the study region had a significant change in the maximum surface temperature. A majority of these changes were found in Maine, central Pennsylvania, and Connecticut. All cells had a decrease in maximum temperature, with the average change being smaller than the decrease in average temperature. Decreases ranged from -0.87K to -0.56K, with the average change in the region of -0.65K (figure 4.8 bottom). There was also an overall decrease in surface minimum temperatures, with an average decrease of -0.41K in the area of study (figure 4.8 top). While the changes in minimum surface temperature were approximately twice as large in the changes in average temperatures, the two spatial patterns are qualitatively similar. Features such as a minimum change north of Lake Ontario, a maximum decrease south of Lake Erie, and moderate decreases across Pennsylvania and New York are a commonality between the two fields. However, the spatial correlation between the CG comparison and FG comparison was only 0.29. In contrast, no significant changes in maximum or minimum temperatures were found when comparing the two extreme case simulations to the control run.

FOREST - GRASSLAND COMPARISON

Surface Temperature

K



Surface Temperature

K

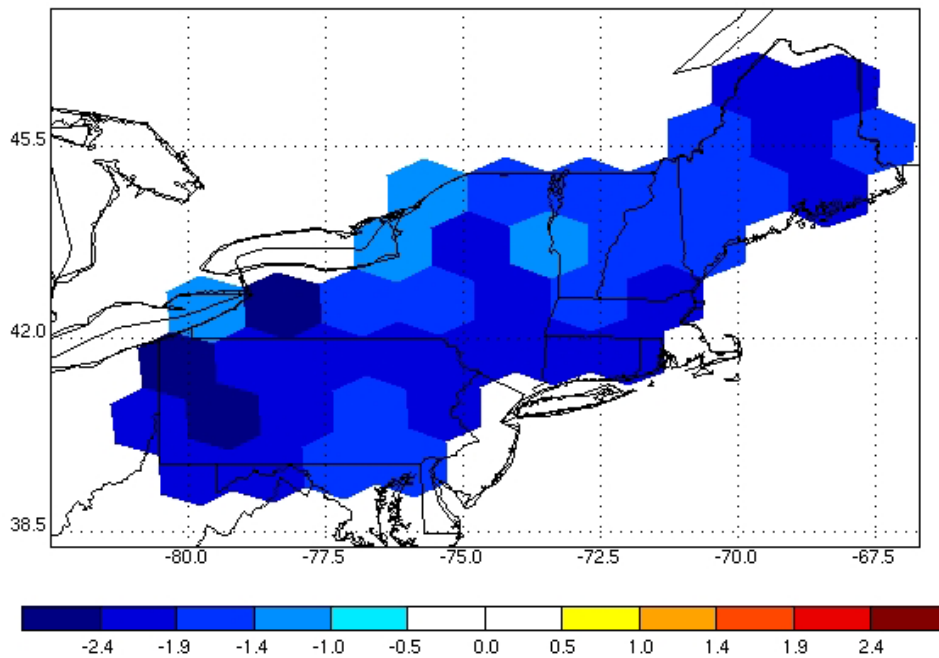
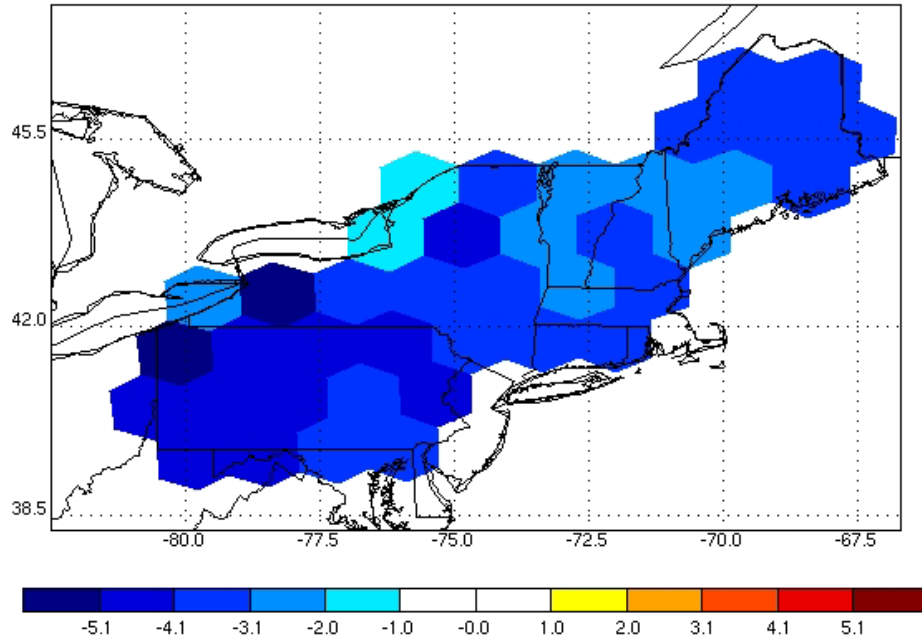


Figure 4.7 Changes globally (top) and in the study region (bottom) in average JJA surface temperature (K) between the entirely forested run and the grassland run. All colored areas are a change significant at the 95% confidence level.

FOREST - GRASSLAND COMPARISON

Surface Daily Minimum Temperature

K



Surface Daily Maximum Temperature

K

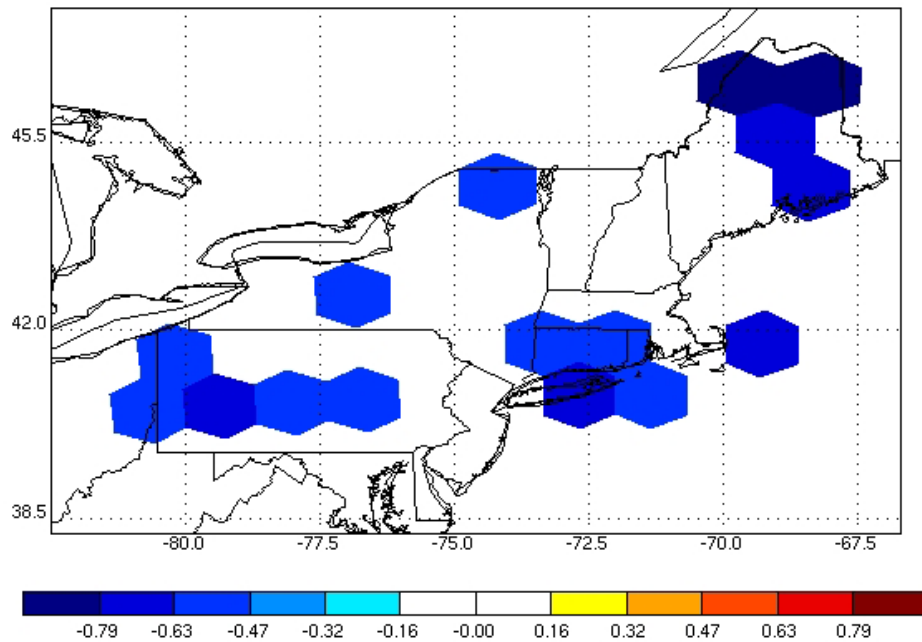
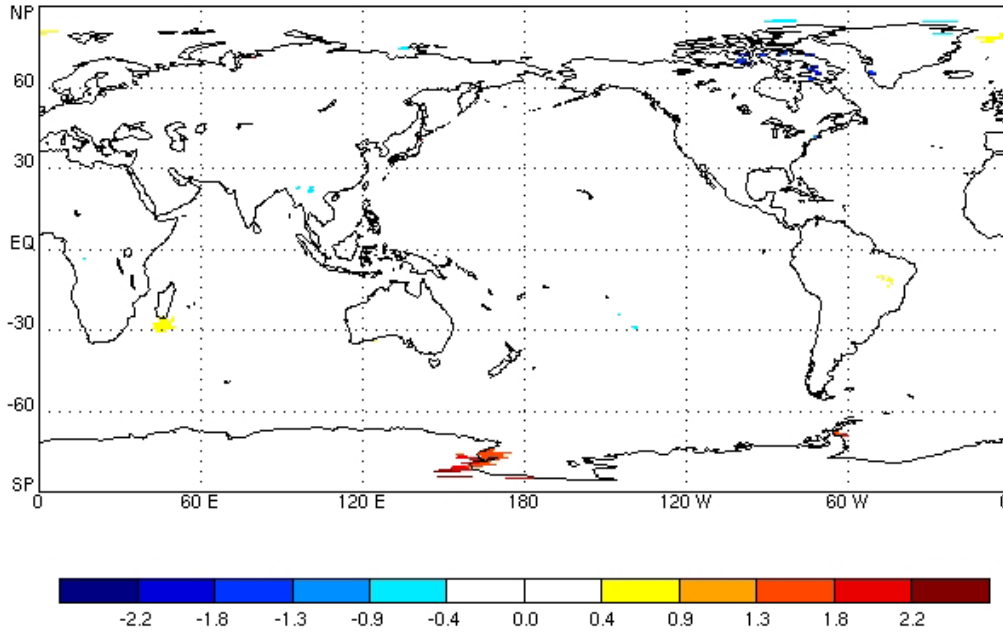


Figure 4.8 Changes in the study region in average JJA surface daily minimum surface temperature (K, top) and average JJA surface daily maximum surface temperature (K, bottom) between the entirely forested run and the grassland run. All colored areas are a change significant at the 95% confidence level.

FOREST - CONTROL COMPARISON

Surface Temperature

K



Surface Temperature

K

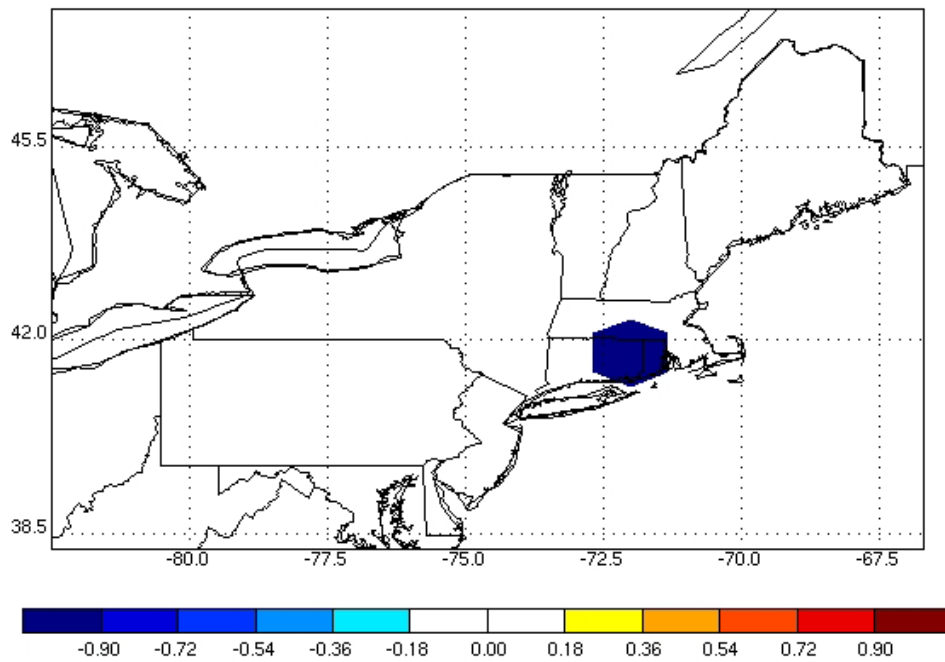
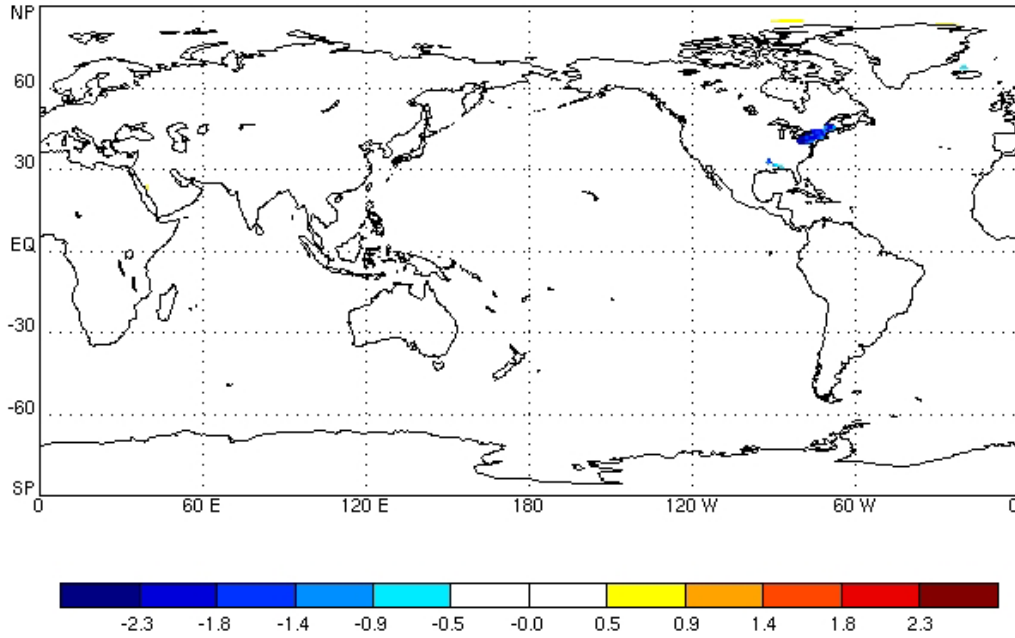


Figure 4.9 Changes globally (top) and in the study region (bottom) in average JJA surface temperature (K) between the entirely forested run and the control run. All colored areas are a change significant at the 95% confidence level.

CONTROL - GRASSLAND COMPARISON

Surface Temperature

K



Surface Temperature

K

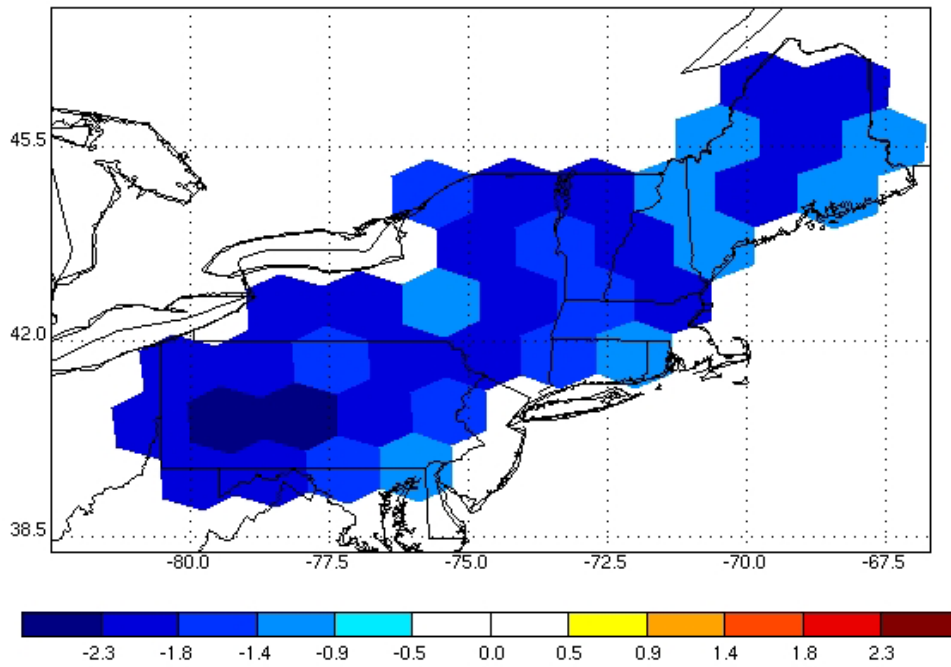


Figure 4.10 Changes globally (top) and in the study region (bottom) in average JJA surface temperature (K) between the entirely forested run and the grassland run. All colored areas are a change significant at the 95% confidence level.

4.4. Precipitation

The global changes in precipitation rates for all three comparisons had very little structure (figures 4.11, 4.12, 4.13 top). A majority of the significant differences in precipitation were found in the Pacific Ocean and in the northeast United States. In all comparisons, there were both positive and negative changes in the Pacific Ocean and the significant changes were concentrated in the western Pacific. The comparison between the forested and control run did not have a significant structure in the northeast United States. Only two grid cells in the region of study had a significant difference in precipitation rate (figure 4.12 bottom). Both cells, in which the averaged precipitation rate increased, were located in Maine. For this comparison, the change in precipitation ranged from 1.53 to 1.73 mm/day (figure 4.12 bottom).

The FG and CG comparisons both had significant changes in total precipitation rate. In the forest-grassland comparison, 30% of the grid cells had a significant increase in precipitation rate. Thus, in a reforested scenario in western and northern Pennsylvania, southeastern New York, and Connecticut, the precipitation rate increased. The average increase was 2.46 mm/day with a maximum of 3.13 mm/day and a minimum of 1.85 mm/day (figure 4.11 bottom). The largest increases were located on the New York-Pennsylvania border. Decreases on a similar scale were located in the Atlantic Ocean, just west of Pennsylvania, forming a dipole structure (figure 4.11 top). This pattern was only seen in the FG comparison. In the control-grassland comparison, only 15% of the grid cells included in the study region had a significant change in precipitation rate. These grid cells were located primarily in southern Pennsylvania with additional significant changes

occurring in grid cell outside of the study area, primarily in Maryland and New Jersey. In this situation, all cells had an increase in precipitation rates but the increases were smaller than in the FG comparison. Here, the average change in the study region was 2.29 mm/day with a maximum 2.71 mm/day and a minimum of 1.93 mm/day (figure 4.13 bottom). Additionally, the cells that had the largest increase in precipitation in the FG comparison typically did not have a significant change in precipitation in the CG comparison. Instead, the maximum changes were in southeastern Pennsylvania and in southern New Jersey.

Fields of evaporation minus precipitation were also analyzed. Similarly to global changes in precipitation, there was little structure in the Evaporation minus Precipitation changes on a global scale. In all three comparisons, most of the significant changes were found in the western Pacific Ocean (figures 4.14 top, 4.15, 4.16 top). Here, areas of increased and decreased evaporation minus precipitation were scattered from Australia to Japan. There was no dominant structure over the northeast United States as in the global maps of surface latent and sensible heat fluxes. For this analysis, as the evaporation minus precipitation increased (e.g., became more positive), evaporation increased relative to precipitation. In the control-reforested comparison, there were no significant changes in evaporation minus precipitation in the area of interest. Differences between the control and grasslands run in evaporation minus precipitation are plotted in figure 4.16 (bottom). In this comparison, 23% of the grid cells in the area of interest had a significant change. All of these cells had a positive change in evaporation minus precipitation in the control run relative to the grasslands run. The average change was 1.99 mm/day, with a minimum change of 1.40 mm/day and a maximum change of 2.91 mm/day (figure 4.16 bottom). Most of the cells with a significant change were located in northern Maine; the largest

increases were found in this region. In New Jersey, southern Maryland, and northern West Virginia, there were regions of decreased evaporation minus precipitation. When comparing the reforested run to the grasslands run, the cells with significant changes, only 17% of the total study area, all had an increase in evaporation minus precipitation (figure 4.14 bottom). As in the CG comparison, outside the study region in West Virginia, New York, and Canada, there were areas of decreased evaporation minus precipitation. The average change in evaporation minus precipitation was 1.89 mm/day, with a minimum of 1.31 mm/day. The largest changes, with a maximum of 2.48 mm/day, were located on the coast of Maine and Massachusetts (figure 4.14 bottom). For the FG comparison, a relative majority of the significant grid cells was located in northern New York, north of Lake Ontario.

4.5. Circulation Changes

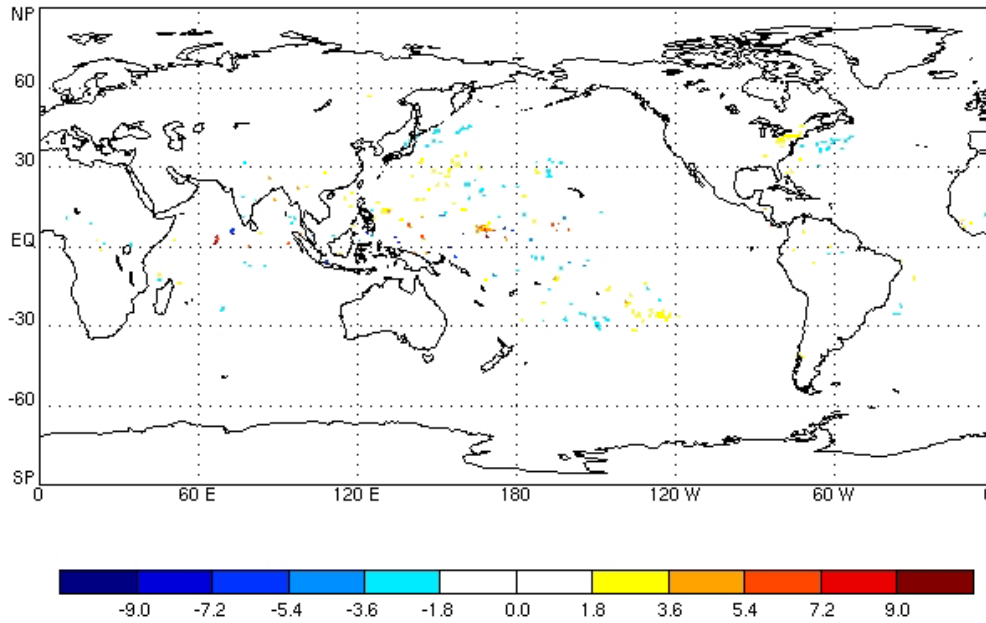
4.5.1. Winds

The dominant change in 10m wind speed in the forest-grassland comparison was in the region of study (figure 4.17 top). Other changes globally were enhancements of the surface wind speed across the Pacific Ocean and south of 60 degrees south latitude. Overall, these decreases were less than 2 m/s (figure 4.17 top). In the northeast United States, the average change was a decrease of 1.87 m/s, with anomalies ranging from -3.48 to -0.53 m/s (figure 4.17 bottom). 90% of the grid cells had a significant decrease in surface wind speeds and additional cells off the eastern coast of Maine, Massachusetts, and Connecticut had significant decreases. The largest decreases were located in Maine and

FOREST - GRASSLAND COMPARISON

Total Precipitation Rate

mm/day



Total Precipitation Rate

mm/day

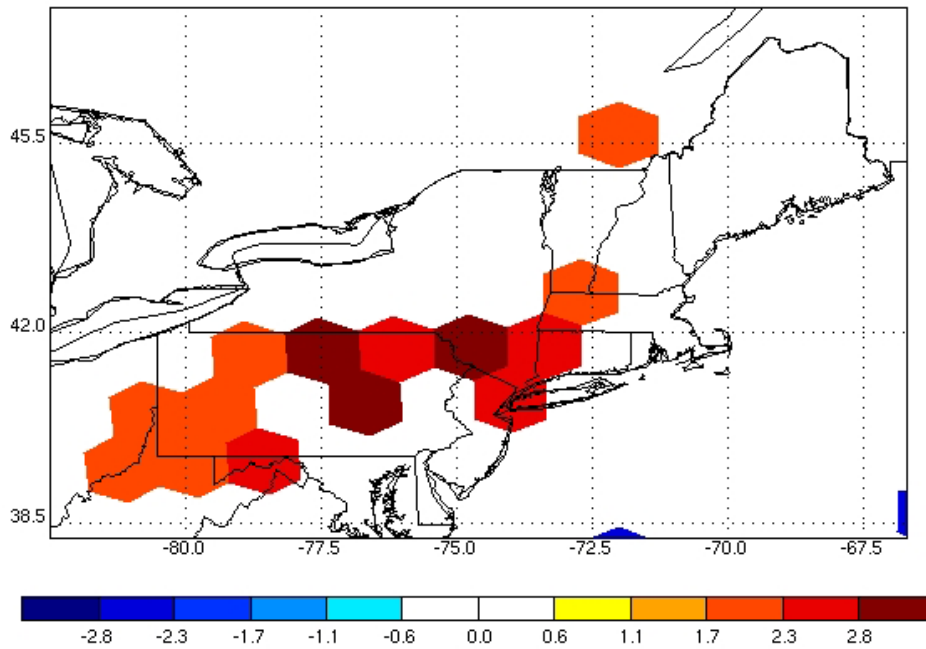
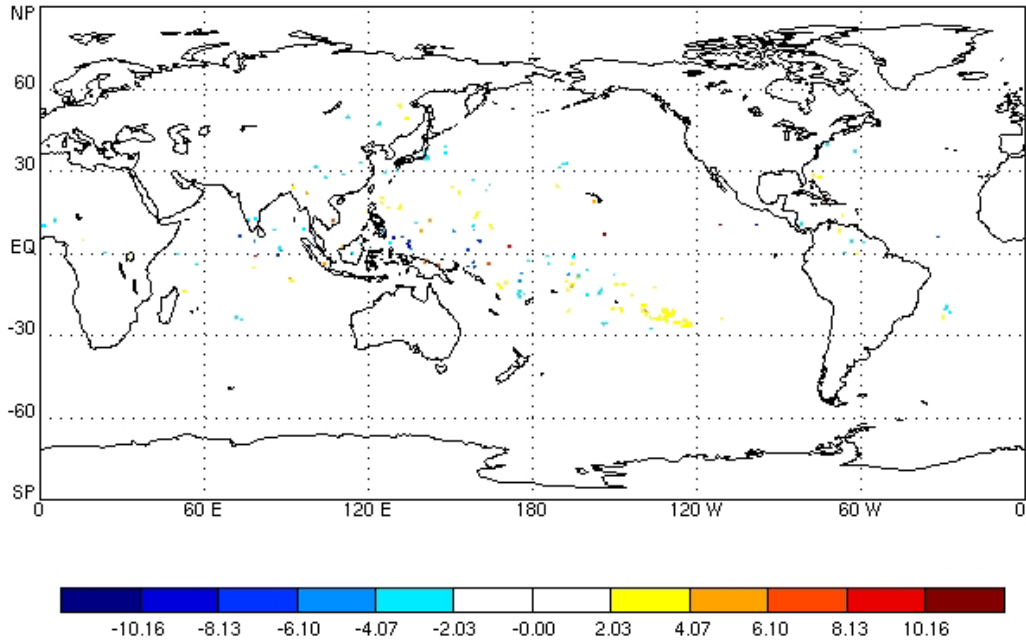


Figure 4.11 Changes globally (top) and in the study region (bottom) in average JJA total precipitation rate (mm/day) between the entirely forested run and the grassland run. All colored areas are a change significant at the 95% confidence level.

FOREST - CONTROL COMPARISON

Total Precipitation Rate

mm/day



Total Precipitation Rate

mm/day

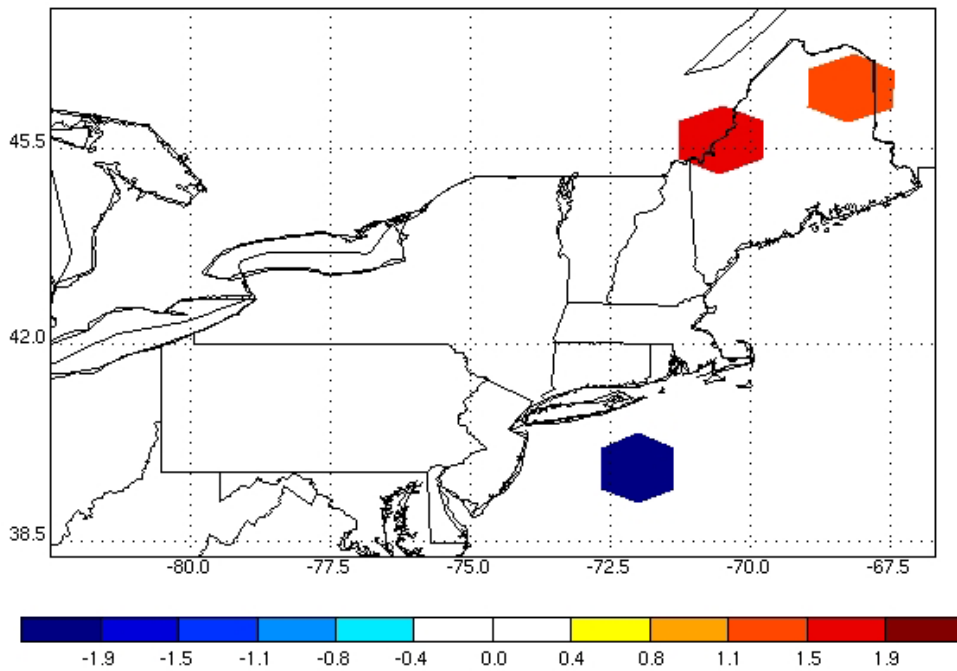
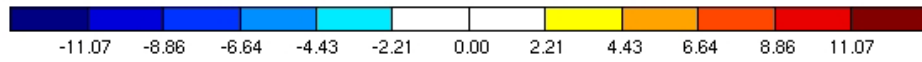
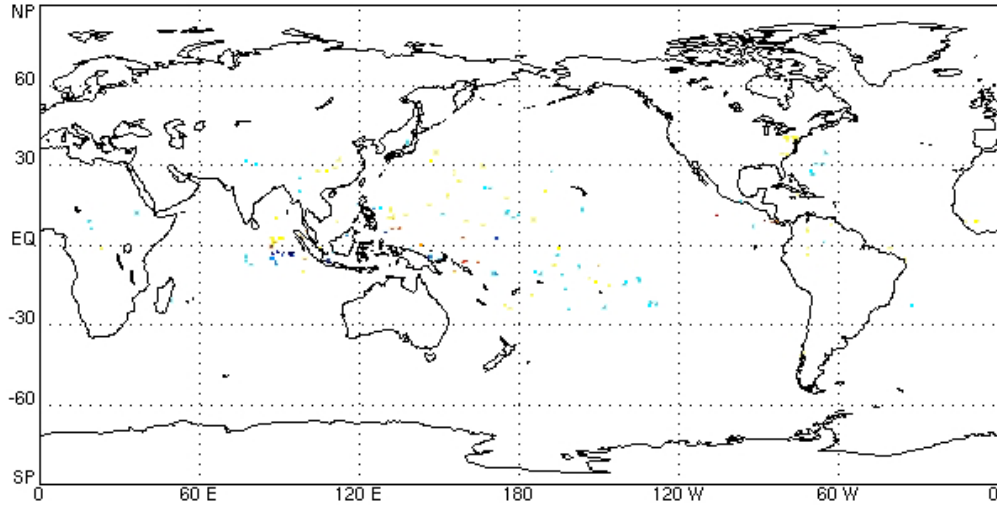


Figure 4.12 Changes globally (top) and in the study region (bottom) in average JJA total precipitation rate (mm/day) between the entirely forested run and the control run. All colored areas are a change significant at the 95% confidence level.

CONTROL - GRASSLAND COMPARISON

Total Precipitation Rate

mm/day



Total Precipitation Rate

mm/day

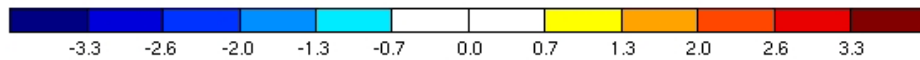
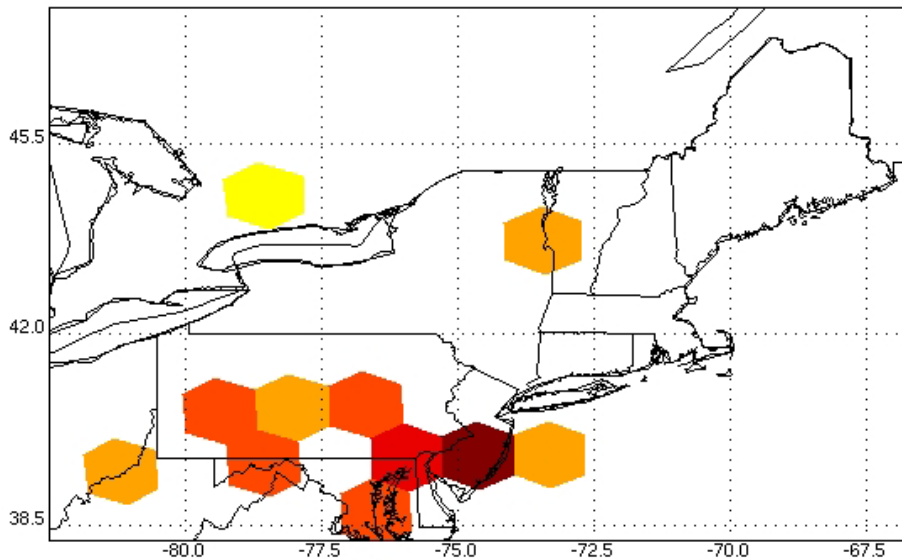
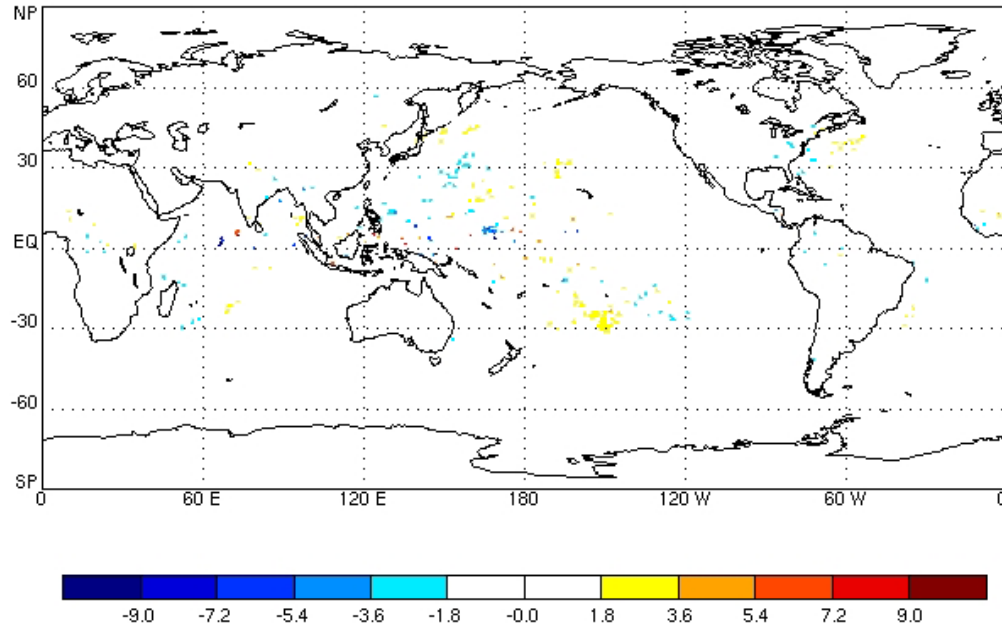


Figure 4.13 Changes globally (top) and in the study region (bottom) in average JJA total precipitation rate (mm/day) between the control run and the grassland run. All colored areas are a change significant at the 95% confidence level.

FOREST - GRASSLAND COMPARISON

Evaporation - Precipitation

mm/day



Evaporation - Precipitation

mm/day

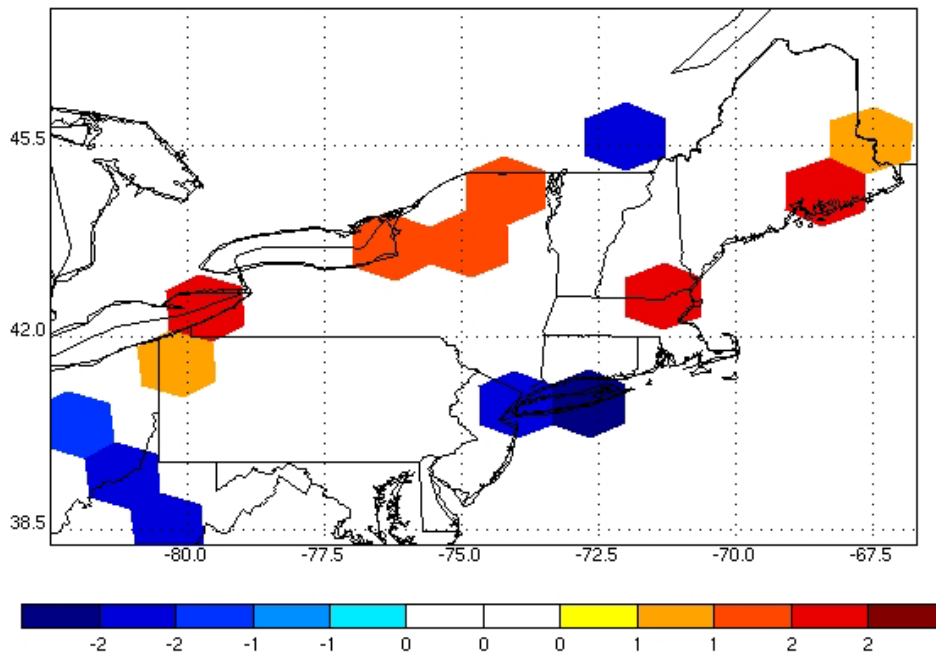


Figure 4.14 Changes globally (top) and in the study region (bottom) in average JJA evaporation - precipitation (mm/day) between the entirely forested run and the grassland run. All colored areas are a change significant at the 95% confidence level.

FOREST - CONTROL COMPARISON
Evaporation - Precipitation
mm/day

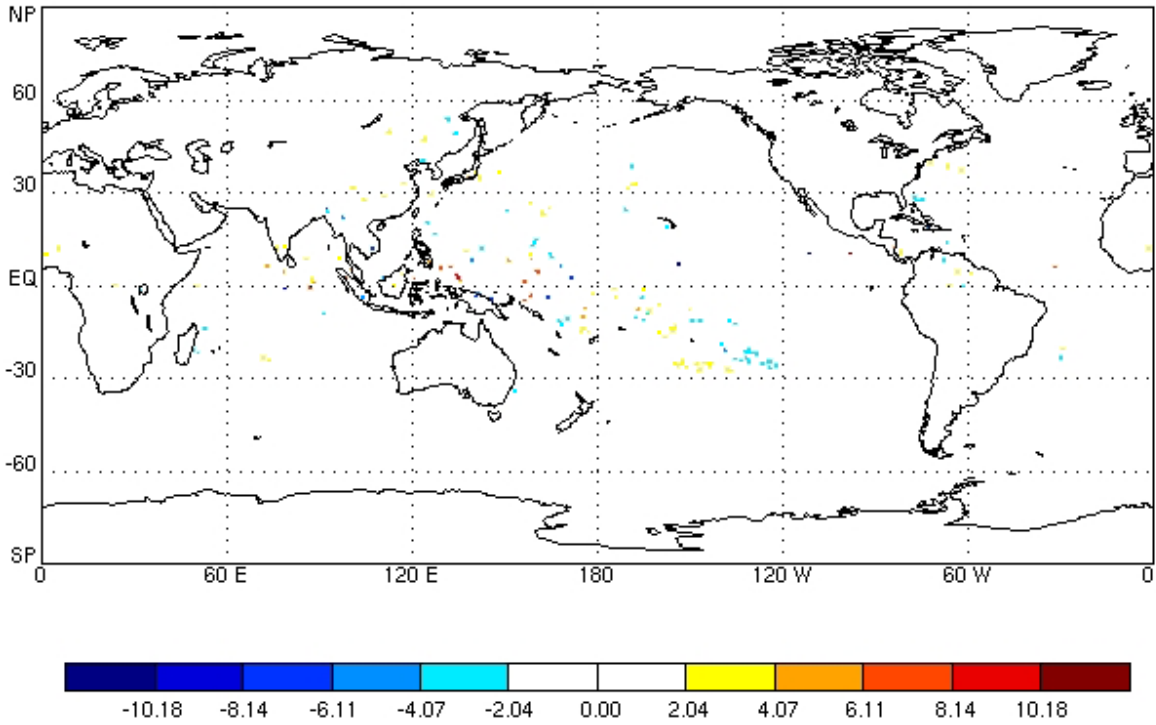
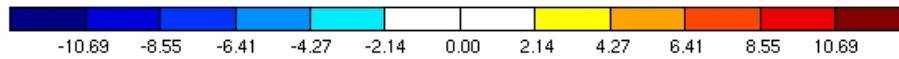
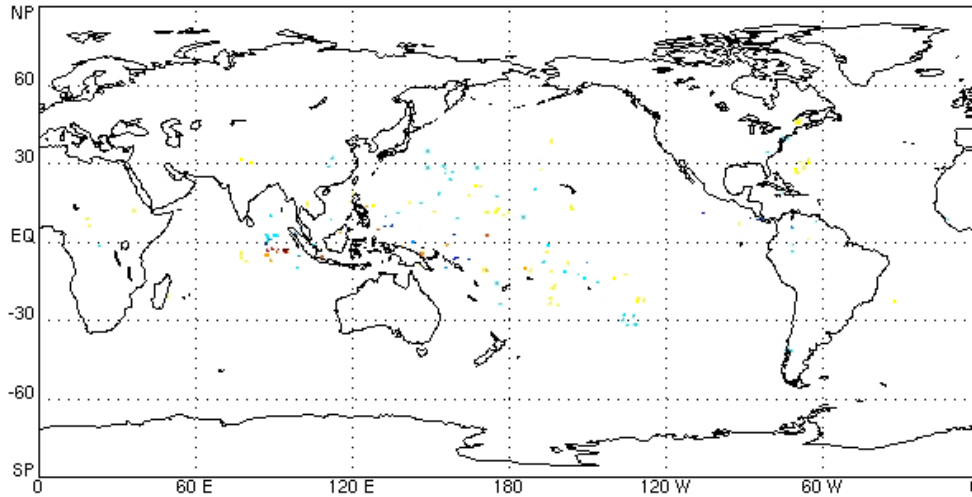


Figure 4.15 Changes globally in average JJA evaporation - precipitation (mm/day) between the entirely forested run and the control run. All colored areas are a change significant at the 95% confidence level.

CONTROL - GRASSLAND COMPARISON

Evaporation - Precipitation

mm/day



Evaporation - Precipitation

mm/day

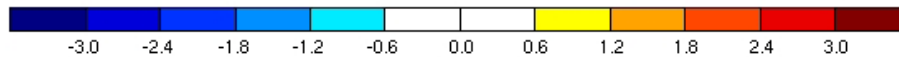
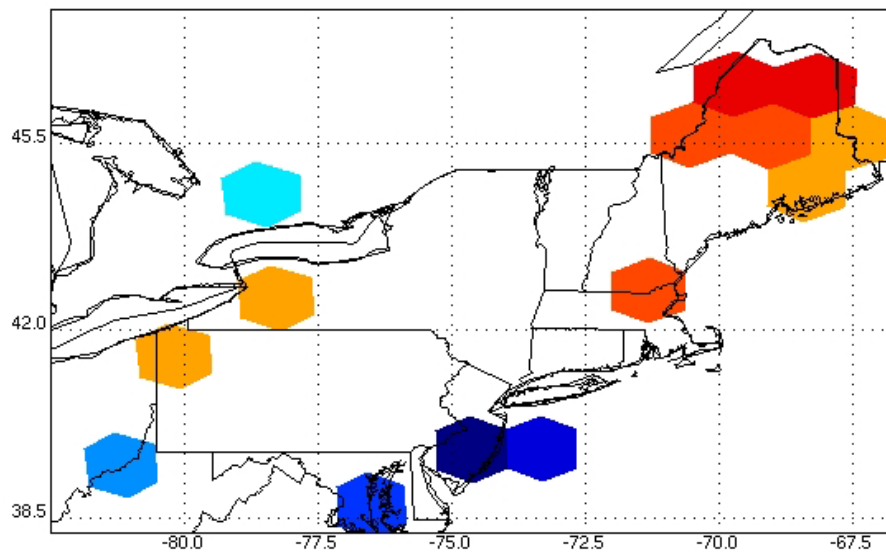


Figure 4.16 Changes globally (top) and in the study region (bottom) in average JJA evaporation - precipitation (mm/day) between the control run and the grassland run. All colored areas are a change significant at the 95% confidence level.

along the coast. In comparison, smaller decreases were found primarily in Pennsylvania and New York. There were no significant shifts in wind direction between the two simulations.

In contrast, there were fewer shifts in wind speed in the area of interest in the forest-control comparison. On a global scale, changes were qualitatively similar, with increases of approximately 2 m/s in the Pacific Ocean. There were additional negative anomalies over the northern polar region and positive anomalies at 60 degrees north latitude (figure 4.18 top). In the northeast United States, the only significant changes in wind speed were found in southern Maine and north central Pennsylvania, with less than 10 grid cells with significant changes (figure 4.18 bottom). Changes were small, typically less than -1m/s. There was also no negative shift off the eastern coast as there was in the forest-grassland comparison. Instead, there were significant positive increases in surface wind speed in New Jersey and northern Virginia. Additionally, the changes in wind speed over Pennsylvania were similar in scale to the changes in Maine, unlike in the forest-grassland comparison. However, there was also no change in surface wind direction globally and in the area of interest.

The comparison between the control and grassland simulations was similar to the forest-grassland comparison, particularly in the region of study (figure 4.19). On a global scale, there were fewer areas with a significant change in surface wind speed. Once again, the changes in the northeast United States were the dominant feature. There were small regions of positive increases in surface wind speed scattered across the Pacific Ocean from 60 degrees south to 45 degrees north. Additional pockets of isolated wind speed

enhancements were located in the northern polar region, with decreases similar in scale in southern Greenland. In the northeast United States, there was an average decrease in surface wind speeds of 1.85 m/s. 80% of the region had a significant change and there was also, as in the forest-grassland comparison, significant decreases in surface wind speed along the Atlantic coastline (figure 4.19 bottom). As well, the largest decreases, with a maximum of -3,42 m/s, were found east of the Appalachian Mountains in Maine and in the eastern part of the region. The smallest decreases were again found in Pennsylvania and New York, with a minimum change of -0.70 m/s (figure 4.19 bottom). There were also no changes in wind direction, as in the forest-grassland and forest-control comparisons.

4.5.2. Pressure

In none of the three comparisons were there any significant changes in JJA averaged mean sea level pressures in the region of study. However there were regions of altered pressure on the global scale, none of which exceeded 500Pa. In the FG comparison, there was a significant increase in pressure off the east coast of the United States and in the polar region (figure 4.20). In contrast, there were little changes in the summer season averaged mean sea level pressure between the entirely forested run and the control run (figure 4.21). Anomalous areas of lowered pressure occurred around 60N, over Greenland and northern Canada and north of Japan. An additional region of higher pressure existed over 30S latitude in the central Pacific Ocean (figure 4.21). The changes in pressure between the control and grasslands run were opposite the changes in the FG comparison. Where before pressures over the Atlantic Ocean increased, now in this comparison pressures were

lowered by approximately 200Pa (figure 4.22). Additionally, anomalously low pressures occurred at 30S latitude. This region of significant change, while opposite in sign and closer to South America to the change at 30S found in the FC comparison, was similar in magnitude (figure 4.22).

4.5.3. Empirical Orthogonal Function Analysis

To further investigate the influence of land cover change on mean sea level pressure and circulation patterns, empirical orthogonal function (EOF) analysis was used (appendix A). As shown above, by altering the forest coverage in the northeast United States, latent and sensible heat fluxes are significantly affected. Changing the rates of surface moisture and heat fluxes to the atmosphere have been shown to change rates of momentum convergence, to shift circulation patterns, and, in the Southern Hemisphere, to increase the tendency towards a positive Southern Annular Mode (e.g., Deser et al. 2004). First in the analysis, the change in mean sea level pressure between the forested run JJA season and the grassland run's JJA season was defined as the response to the land cover changes (figure 4.24a). In this analysis, the area of study was expanded to include all area between 20 and 90N latitude and all longitudes. Major features in the response include an increase in sea level pressures to north of Greenland, with the center located approximately over the North Pole. A corresponding decrease in sea level pressures, smaller in magnitude, was located to the south of Greenland and was spread over 225 to 360 longitude. An additional region of small decreases in mean sea level pressure began in the Midwest United States,

continued up to the northeast United States, and continued through the Atlantic Ocean (figure 4.24a).

As detailed in appendix A, the EOFs of the entirely forested run were computed, with the variance explained by the first ten EOFs plotted in figure 4.23. The leading EOF only described approximately 6.5% of the variance in the data and none of the EOFs were well separated (figure 4.23). Accordingly, there was little structure in the pressure variances in the time domain. The differences between the response and the leading EOF were still examined. This was accomplished by first projecting the response onto the first EOF with a spatial linear regression (as in figure 4.24b, scaled by the regression coefficients). The full hemispheric domain was included in the regression calculation. The residual was then computed by subtracting the projection from the response (figure 4.24c). As seen in the residual, the main features of the projection and response were not tied together. Instead, the residual response consisted of an anomalous ridge west of Alaska, continuing to the North Pole and an anomalous trough over Europe. There was an additional slight trough over eastern United States and Atlantic Ocean but it was not the major feature of the residual. Thus, the forcing enacted by the land cover did not cause a discernible direct forcing on the atmosphere.

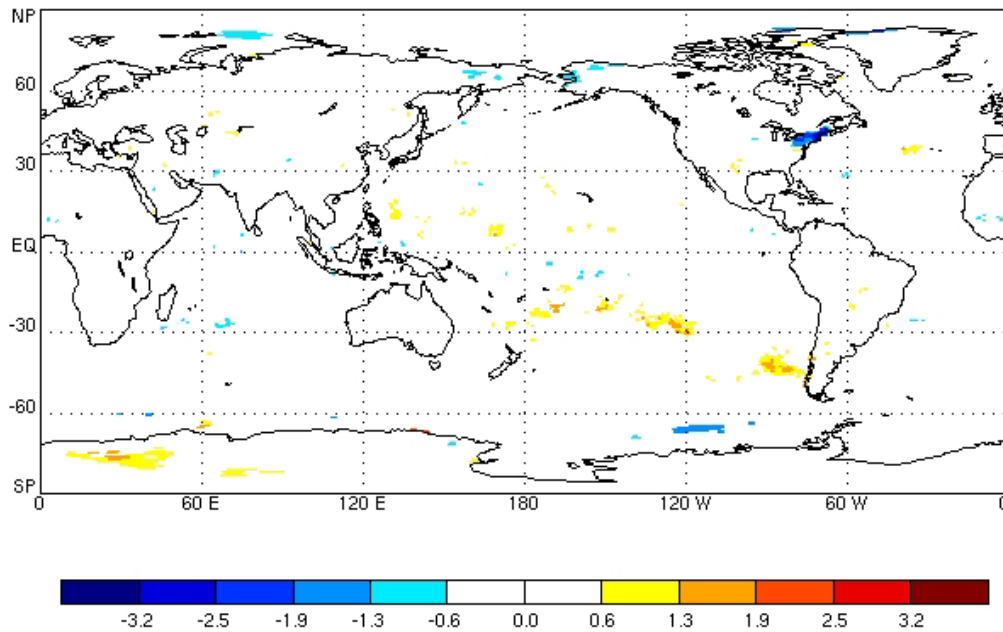
4.6. Summary

In the model analysis, three five-year simulations were run, one was a control run with forest coverage mimicking modern day coverage, one where the northeast United States was entirely reforested and one where the United States was completely covered

FOREST - GRASSLAND COMPARISON

Surface Wind Speed

m/s



Surface Wind Speed

m/s

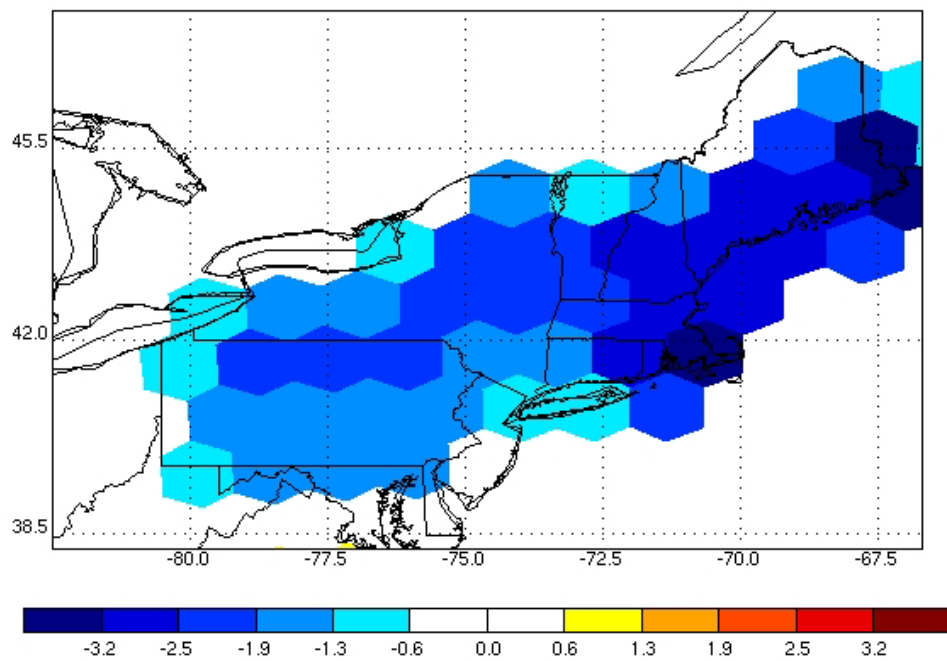
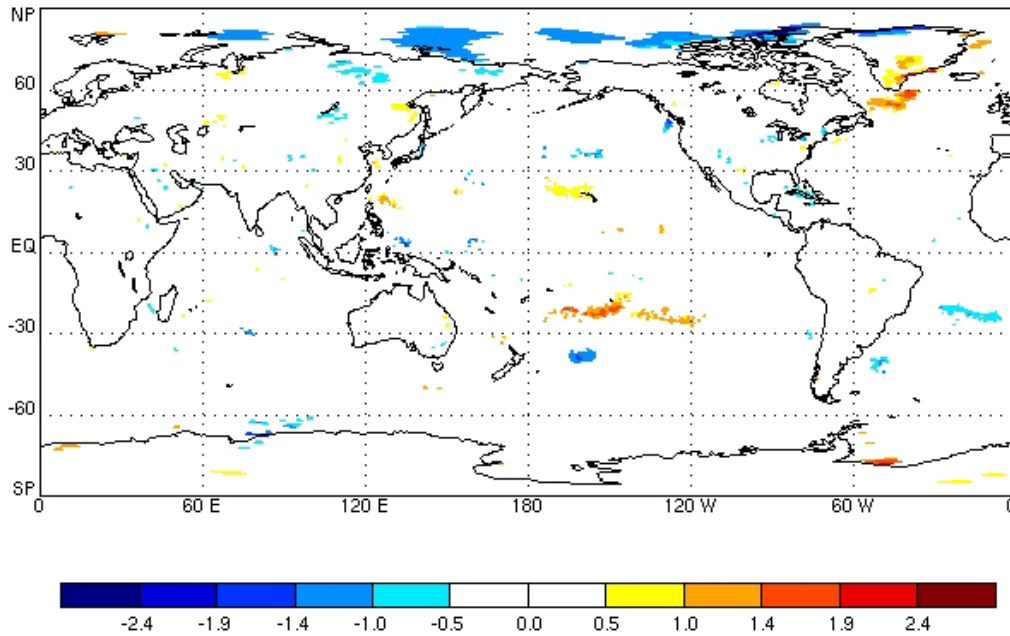


Figure 4.17 Changes globally (top) and in the study region (bottom) in average JJA surface wind speed (m/s) between the entirely forested run and the grassland run. All colored areas are a change significant at the 95% confidence level.

FOREST - CONTROL COMPARISON

Surface Wind Speed

m/s



Surface Wind Speed

m/s

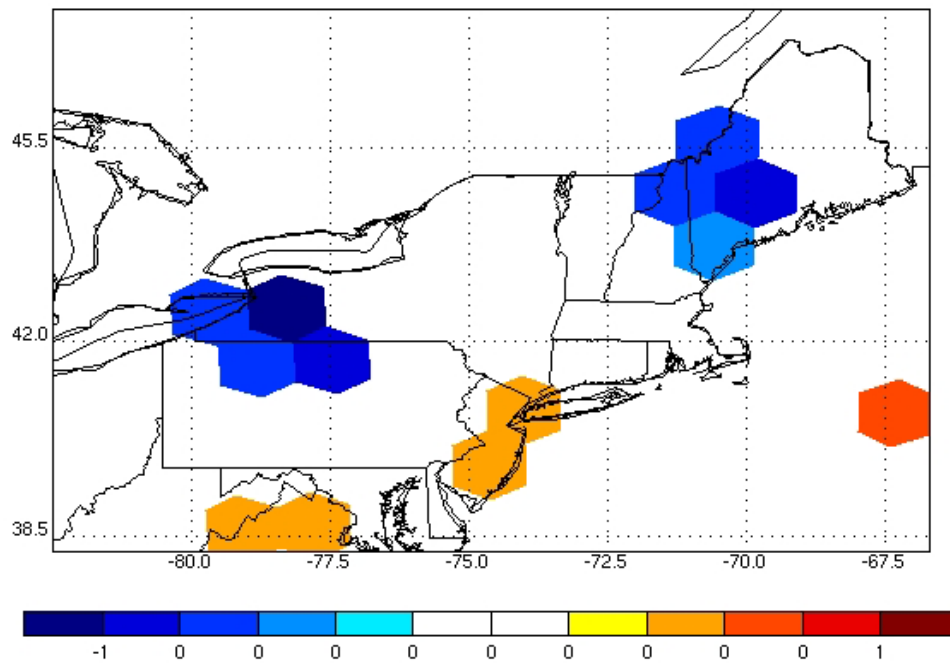
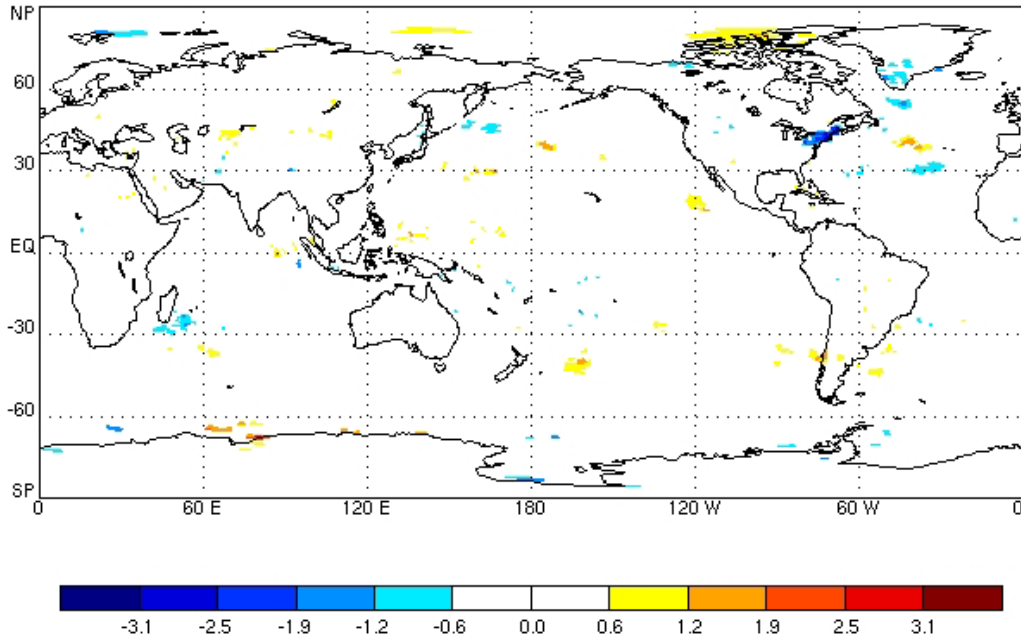


Figure 4.18 Changes globally (top) and in the study region (bottom) in average JJA surface wind speed (m/s) between the entirely forested run and the control run. All colored areas are a change significant at the 95% confidence level.

CONTROL - GRASSLAND COMPARISON

Surface Wind Speed

m/s



Surface Wind Speed

m/s

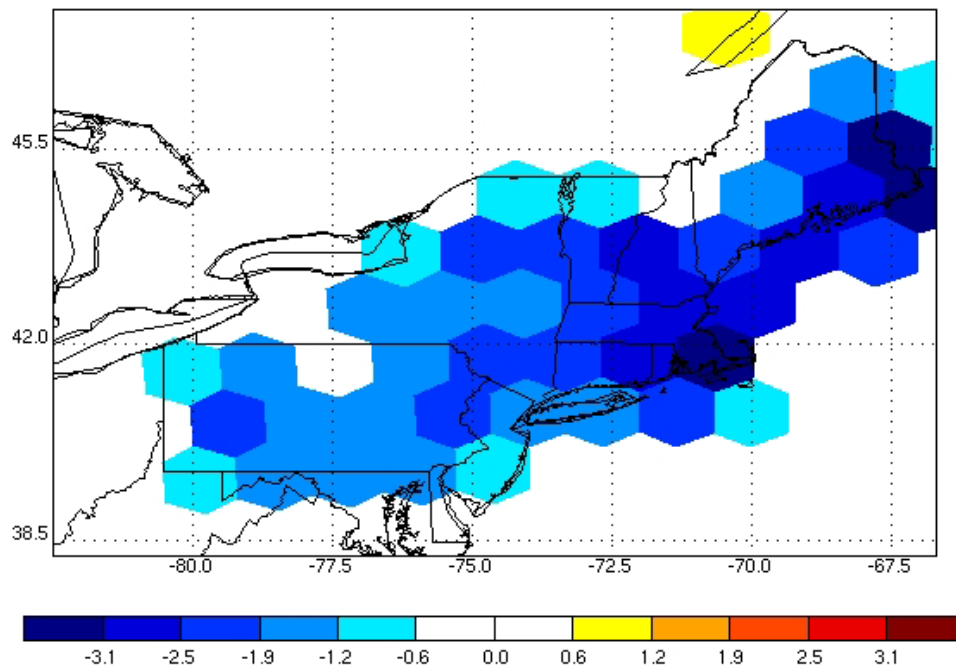


Figure 4.19 Changes globally (top) and in the study region (bottom) in average JJA surface wind speed (m/s) between the control run and the grassland run. All colored areas are a change significant at the 95% confidence level.

FOREST - GRASSLAND COMPARISON

Mean Sea Level Pressure

Pa

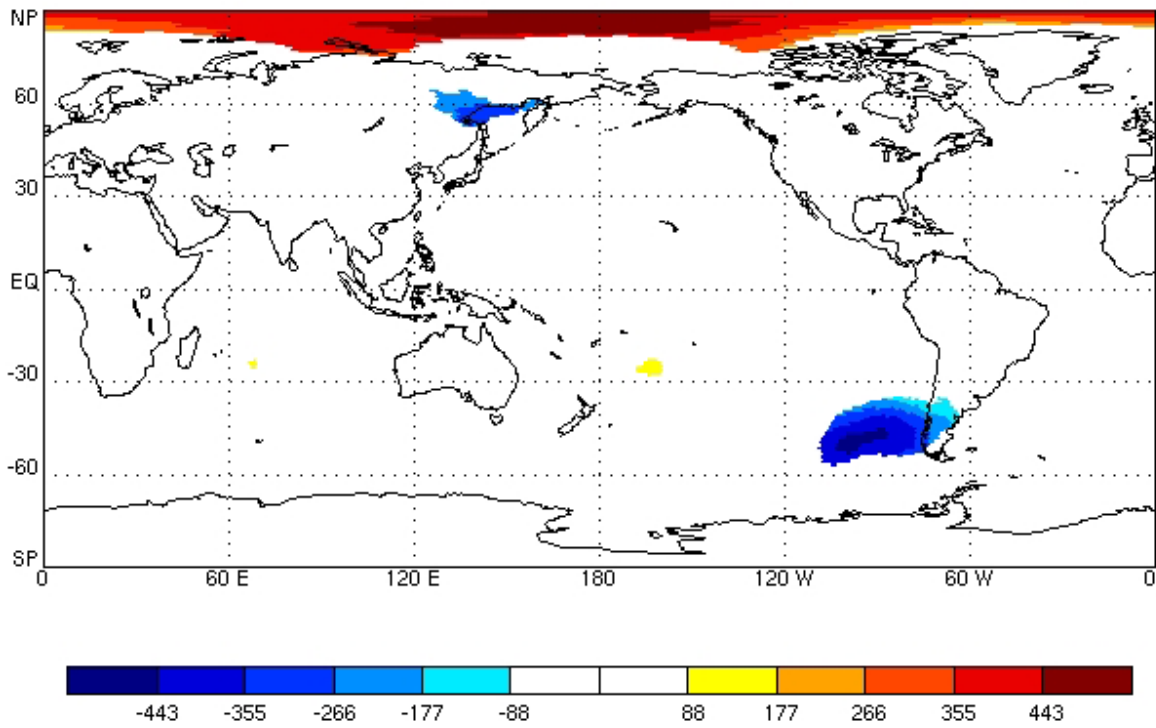


Figure 4.20 Changes globally in average JJA sea level pressure (Pa) between the entirely forested run and the grassland run. All colored areas are a change significant at the 95% confidence level.

FOREST - CONTROL COMPARISON
Mean Sea-Level Pressure
Pa

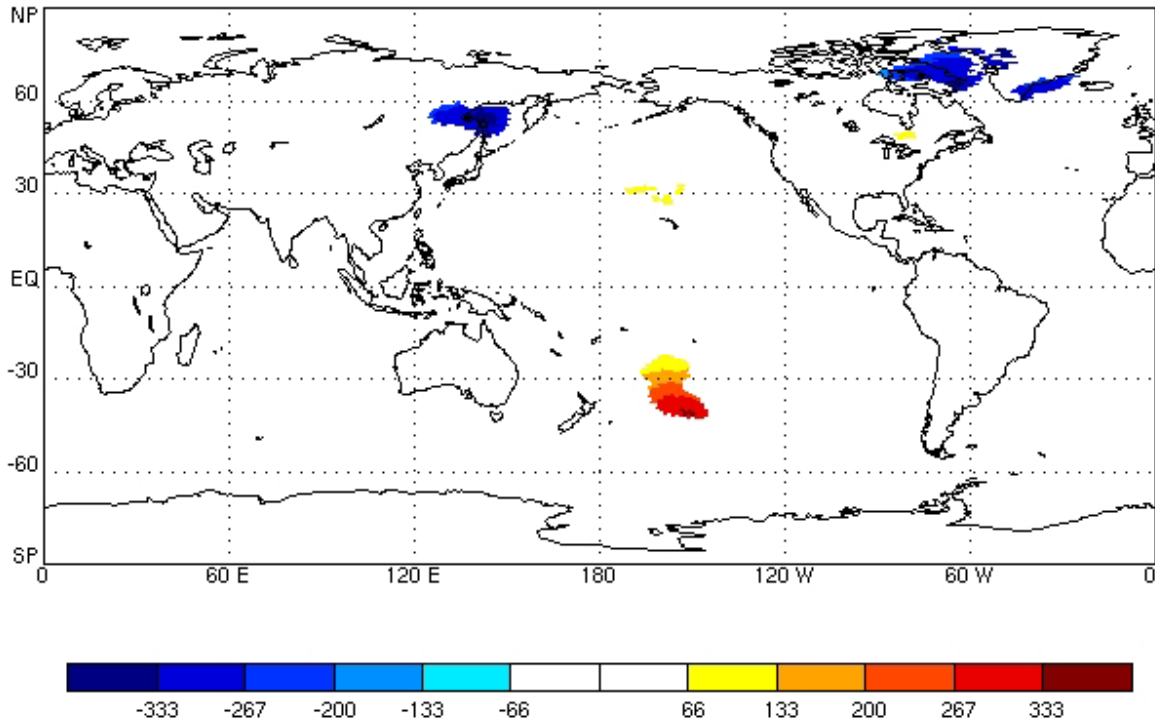


Figure 4.21 Changes globally in average JJA sea level pressure (Pa) between the entirely forested run and the control run. All colored areas are a change significant at the 95% confidence level.

CONTROL - GRASSLAND COMPARISON
Surface Pressure
Pa

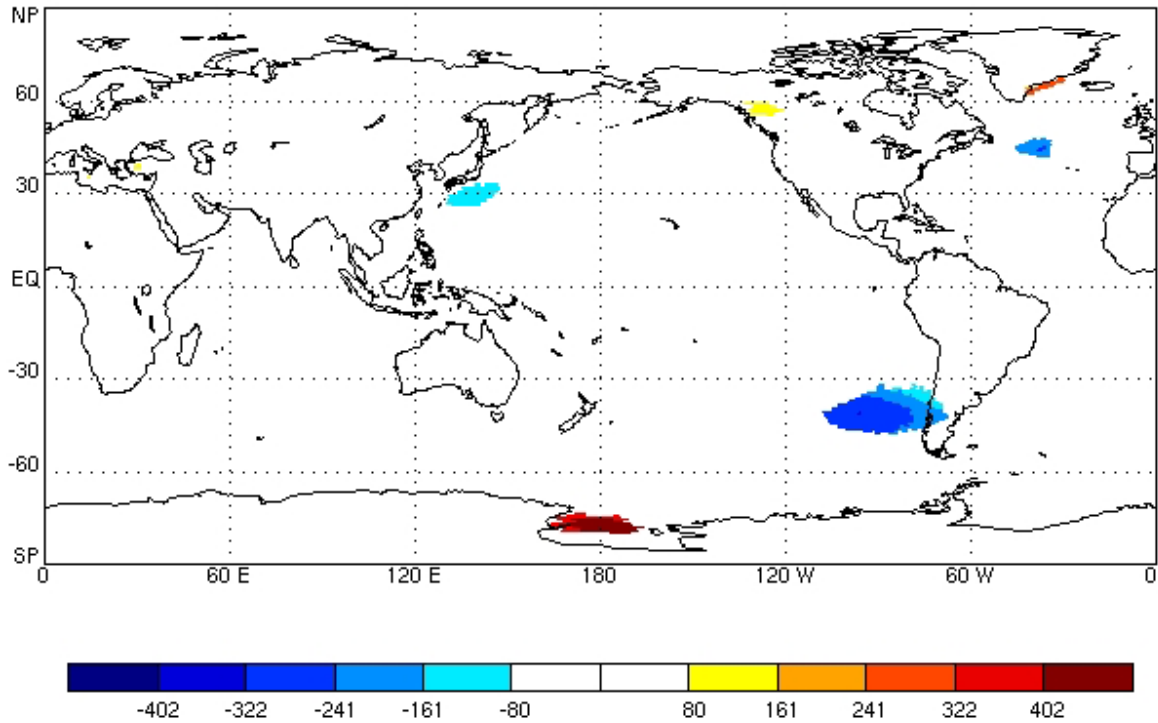


Figure 4.22 Changes globally in average JJA sea level pressure (Pa) between the control run and the grassland run. All colored areas are a change significant at the 95% confidence level.

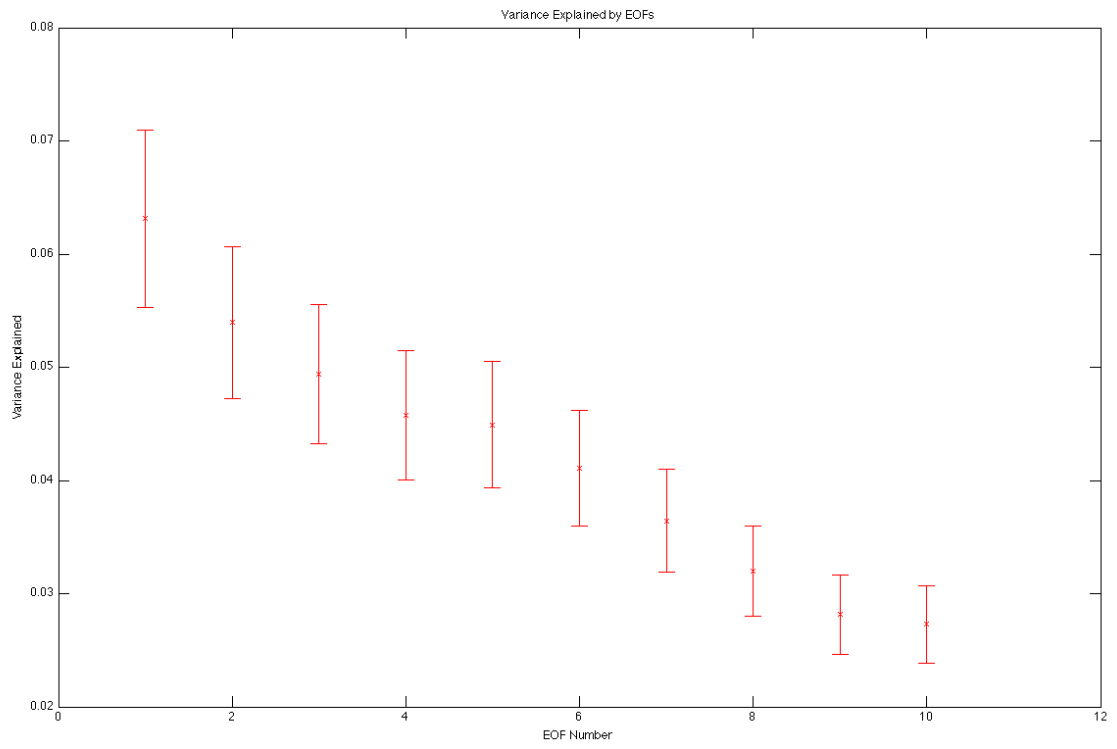


Figure 4.23 Variance explained by the first ten EOFs.

Response to Forcing

Pa

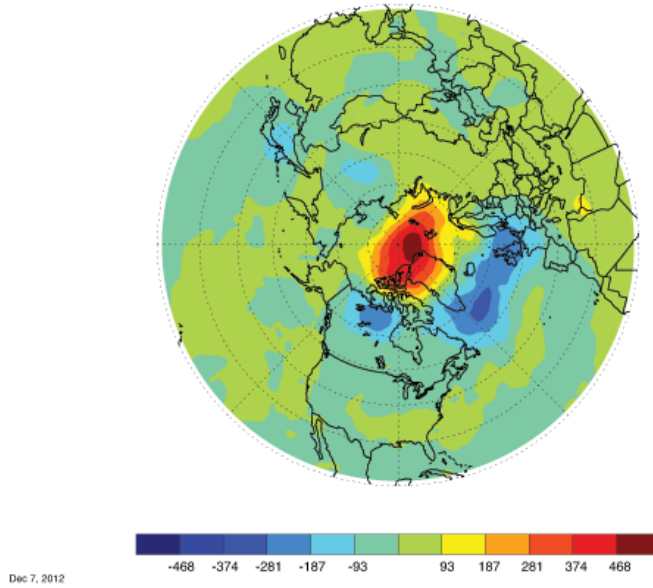


Figure 4.24a The response of mean sea level pressure to change in ground cover, calculated by the averaged JJA mean sea level pressure subtracted from the averaged JJA mean sea level pressure from the forested run for the area of 20 latitude to 90 latitude.

Projection of 1st EOF

Pa

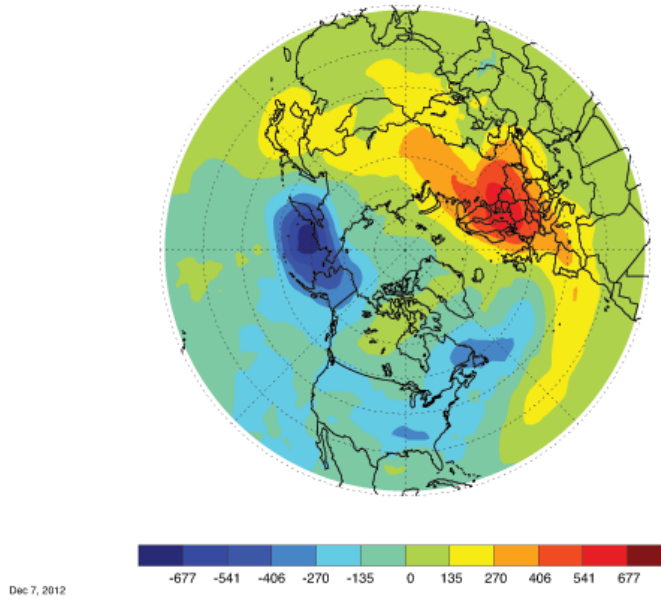


Figure 4.24b The first EOF, as computed in appendix A, projected onto the response in 4.24a

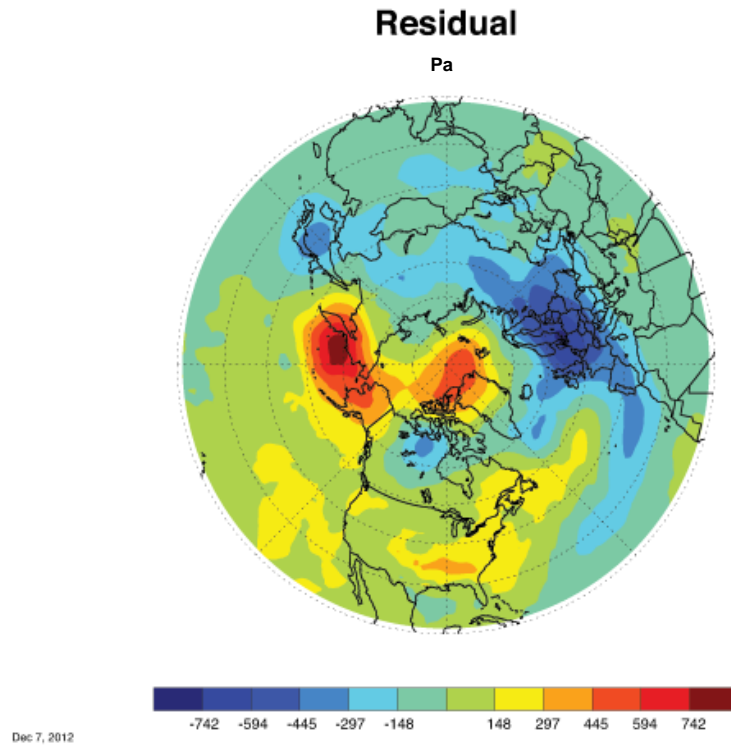


Figure 4.24c The residual, calculated by subtracting the projection from the response. All plots are in units Pa and the 95% confidence level filter was not applied.

with grassland. When comparing the three prescribed land coverages, the control and the entirely forested simulations were the most similar (figure 2.4). When comparing the impacts of the prescribed ground change, the entirely forested to grassland comparison typically had the greatest change, then control – grassland change, and finally entirely forested to control comparison. For example, in all three comparisons surface latent and sensible heat fluxes reacted to ground cover change as was hypothesized. However, in the forest-control comparison, there were only significant changes in surface latent and sensible heat fluxes on the edges of the domain. In the other two comparisons, the shifts were observed across the entire domain. Overall, the forest-grassland and control-grassland comparisons were similar with connections of the same sign between an atmospheric variable and the forest coverage increase, with a greater magnitude in the changes and number of grid cells with significant changes in the forest-grass comparison. There were significant alterations in average daily maximum and minimum temperatures in the forest-grassland comparison. In this scenario, both temperature variables decreased as forest coverage increased (table 4.1). For both the forest-grassland and control-grassland comparisons, average JJA surface temperatures across the domain were lower by approximately 2 Kelvin in the more heavily forested simulation. Additionally, monthly precipitation rates increased, primarily in Pennsylvania, by 2.5 mm/day, (2.29 mm/day) in the FG comparison (CG comparison). As expected, wind speeds at 10m decreased in all three comparisons. There were no significant changes in the area of interest in wind direction or surface pressure in any of the comparisons. However, there were shifts in mean sea level pressure outside the area of interest.

Additional analysis of changes between the entirely forested and grassland simulations in the surface pressured field in the entire northern hemisphere was also completed with the use of empirical orthogonal function (EOF) analysis. This was modeled off of studies such as Deser et. al. (2004). In these studies, the amount and sources of heat and moisture fluxes was altered through ground cover changes such as increased sea ice. Through EOF analysis, the indirect effects (large scale variability such as the North Atlantic Oscillation) and direct effects ('hotspots' in pressure variability directly over the area of changed ground cover) were identified. In this study, there were no significant, distinct EOFs that were identifiable, and thus no distinct indirect effects (figure 4.23). When the first EOF was removed from the change in surface pressure between the entirely forested run and grasslands runs, there was no dominant pattern of variability over the area with prescribed forest coverage changes (figure 4.24). Thus, in the time span of the simulations, any changes in surface pressure can only be attributed to noise inherent to the model.

A summary of the relationships between the analyzed variables and ground cover change for each comparison was listed in table 4.1

Table 4.1: Summary of relationships between listed variables and the prescribed ground cover change in the forest-grass comparison, forest-control comparison, and control-grassland comparison.

	Forest-Grass Comparison	Forest-Control Comparison	Control-Grassland Comparison
Surface Latent Heat Flux	Strong positive	Weak positive	Strong positive
Surface Sensible Heat Flux	Strong negative	Weak negative	Strong negative
Average Surface Temperature	Strong negative	No relationship	Strong negative
Average Daily Maximum Surface Temperature	Weak negative	No relationship	No relationship
Average Daily Minimum Surface Temperature	Strong negative	No relationship	No relationship
Total Precipitation Rate	Weak positive	No relationship	Weak positive
Evaporation – Precipitation	Weak positive	No relationship	Weak positive
Surface Wind Speed	Strong negative	No relationship	Strong negative
Surface Pressure	No relationship	No relationship	No relationship

A summary of relationships between listed variables and the prescribed ground cover change in the forest-grass comparison, forest-control comparison, and control-grassland comparison is presented in table 4.1. In this analysis, surface latent heat fluxes, surface sensible heat fluxes, total precipitation rate, evaporation minus precipitation, average surface temperature, average daily maximum surface temperature, average daily minimum surface temperature, surface wind speed, and surface pressure, all averaged over the JJA season, were studied. Each relationship was described as strong positive (negative), weak positive (negative), or no relationship. For example, having a ‘strong positive’ relationship in the forest-grassland comparison indicated that a variable increased as forest coverage increased. A strong relationship was defined as over 75% of grid cells in the study region had a significant positive (negative) change. A weak relationship was defined as between 20 and 75% of grid cells had a significant positive (negative) change. Having no relationship was defined as less than 20% of grid cells had a significant change.

Chapter 5: Discussion

5.1. Discussion

Between the mid-twentieth century and modern times, the northeast United States had a relative increase in forestland of approximately 20% on average. The comparison between the forest and grassland simulations, in comparison, represented a 100% reforestation rate, 5 times the amount of reforestation actually observed. Overall, the comparison between the forest-control simulations had a change in forest coverage most similar to the change seen in observations. Most areas in the northeast United States had an absolute increase in forest coverage of around 0.30 (1) in the FC (FG) comparison. Additionally, there were regions of deforestation in the observations, unlike in the model simulations. Both qualitative and quantitative comparisons of the results of the forest-control comparison and the modern-historical observation comparisons will be undertaken.

In both observational analysis and comparison between the forested and control simulations, there was no relationship between average JJA surface temperature forest change. However, in the model simulation, there were no significant changes in surface temperature. In observational studies, there were both positive and negative temperature anomalies scattered throughout the northeast United States. These changes were not significant at the 95% level and had no discernible structure that could be tied to variables such as forest changes or topography. Other model comparisons also did not agree with

observational changes in average surface temperature; in both the forest-grassland and control-grassland comparisons, average surface temperatures decreased across the entire domain. Additionally, changes in average temperature were much larger in the model simulations. In both the FG and CG comparisons, the average changes in average temperature were more than 30 times larger. In contrast, there was only a 6% difference in average shift in average temperatures between the FG and CG comparisons. Thus, another issue, not represented in the model simulations, was influencing minimum temperatures, such as increased carbon dioxide amounts (i.e., IPCC 2007). Thus, to explain changes in temperature in observations other variables must be considered. While there was no significant change in average daily minimum and maximum temperatures between the entirely forested and control runs, in the observational comparison, weak relationships were recorded. In average daily maximum temperature, a weak negative relationship was computed between temperature and fractional forest coverage. However, in the observations, as forest coverage increased in time, so did the average daily minimum temperature, opposite what was noted in the forest-control comparison. The change in maximum temperature was similar to the change between modern and 1920s temperature reported in Strack et al. (2008). However, in the Strack study, modern minimum temperatures also decreased, similar to the relationships found in the FG comparisons. However, the magnitudes of the changes in minimum and maximum daily temperatures were much larger in the FG comparison than in observations. In the comparison, the average change in maximum (minimum) temperatures was 8 (1.14) times larger than in the observations. When comparing the maximum and minimum temperatures in the observations to the FG comparison, there was a large difference in how much larger the

change in maximum temperature was. This implies that after reforestation, different processes will influence night and daytime temperatures and the variables should be considered separately.

In the entirely forested–control comparison, there were only significant changes in precipitation in northern Maine and no noted relationship between forest coverage and precipitation. In observations, there was a weak positive relationship between fractional forest coverage and all precipitation changes and a strong positive relationship between fractional forest coverage and significant precipitation changes. This positive relationship was expected from the results of previous studies (e.g., Malhi et al. 2008), but was stronger than the relationship noted in other studies in the region (Asner et al. 2004, Strack et al. 2008, Bounua et al. 2000). In the observations, significant changes in monthly precipitation totals occurred in Maine and the Appalachian region of Pennsylvania. In Pennsylvania observations, decreases in monthly precipitation coincided with small decreases in forest coverage. In both the forest-grassland and control-grassland comparison, this region was reforested and had significant increases in precipitation. While in Pennsylvania, all significant changes occurred in a mountainous region, this was not true in the rest of domain, making it unclear the exact amount of influence topography exerted on precipitation changes. Overall, changes in precipitation in the observations were much smaller than in the model simulations. The average change in precipitation in the FG (CG) comparison was 16 (15) times larger than the change in the observations. Even in the FC comparison, precipitation changes were 10 times greater than in the observations. So while the models and the observations had a relationship between

reforestation and precipitation of the same sign, there are other factors influencing the real precipitation rates that are not accounted for in the simulations.

The model analysis results for changes in wind speed, surface latent heat flux, and surface sensible heat flux qualitatively agreed with theory and previous studies (e.g., Pielke 2011, Pielke 2001, Schrieber et al. 1996, Ban-Weiss et al. 2011). When the amount of forests in this study region increased, wind speeds and surface heat fluxes decreased and surface latent heat fluxes increased. The magnitude of these changes was dependent on the amount of reforestation. For example, both the average change in wind speeds and the range of changes was approximately the same in both the FG and CG comparisons. However, the changes in surface latent heat fluxes were 3 (1.11) times greater in the FG comparison than the FC (CG) comparison. The range of changes in surface latent heat flux was largest in the FC comparison; the other two comparisons had ranges approximately half as large. It was similar in surface sensible heat flux; the average change in surface sensible heat fluxes was largest in the FG comparison. The FC comparison had an average shift that was 40% as big, while the shifts in CG approximately the same. Here, the range of change in surface sensible heat flux in the FG (CG) comparison was still 50% (82%) the range in the FC comparison. Thus, as the amount of reforestation was increased, the average changes in surface fluxes increased by approximately the same factor. Changes in wind speeds were about the same in the FG and CG comparisons despite the FG comparison having approximately 1.3 times the amount of reforestation in the CG comparisons. The shifts in surface fluxes did not result in changes in surface temperature and precipitation rates of similar magnitude and spatial scales. For example, in the forest-grassland comparison, surface latent heat fluxes increased an average of 51 W/m² in every grid cell in

the study region. However, only in Pennsylvania, southern New York, and western Connecticut and Massachusetts were increases in the average precipitation rate recorded. These were locations that did not have the largest shifts in latent heat fluxes, and there was a missing connection between the increase of moisture to the atmosphere and precipitation that was not studied in this analysis. Thus, while there were qualitative agreements on connections between precipitation and forest coverage, the relationship cannot be fully described based on this analysis. Additionally, while the comparisons between the control and entirely forested simulations were the most similar to changes seen in observations, an analysis of the changes between extreme forest coverage scenarios also can be used to better understand impacts of reforestation in the northeast United States.

5.2. Future Work

To improve the viability and applications of the current experiment design to possible future developments, several extensions could be made. First, this analysis was applied solely to the northern hemisphere summer season. By extending the temporal domain to include the entire year, the location, magnitude, and possible sources of changes in atmospheric characteristics between, for example, summer and winter seasons could be compared. Additionally, the analysis used a five-year model simulation; by conducting a longer simulation (e.g., extend to 10 or 20 years) to further explore climatological trends in not only the variables analyzed here, but additional characteristics such as cloud cover and upper atmospheric quantities to clarify the influences of altered heat and moisture fluxes. Expanding both the length the simulations ran and the months included in the sample

would also be used to further the EOF analysis. There was no structure in the variability of the surface pressure field and changes between simulations were just noise; with a larger time sample, try to find the signal of major trends in atmospheric circulation (i.e., the North Atlantic Oscillation) and possible influences of ground cover changes on these patterns.

Another way to analyze the impacts of ground cover change on global circulations would be to change the area of interest. Instead of study focusing on the northeast United States, the entire United States or North American continent would be reforested (deforested). By moving to a more global scale of ground cover change, the influence of isolated changes on one continent on other locations can be analyzed. While in this study, the only significant changes outside of the region of interest were in wind speed, the size of ground cover change needed for wide-reaching impacts could be determined. As well, this would determine if the influences on these regions on a similar scale to the changes and due to similar processes as in the chosen area of change. Increasing the spatial domain would also increase the number of observational samples, to allow for comparisons in how different geographic locations influence changes on surface temperature and precipitation.

References

Abiodun, Babatunde J., Zachariah D. Adeyewa, Philip G. Oguntunde, Ayobami T. Salami, and Vincent O. Ajayi, 2012: Modeling the impacts of reforestation on future climate in West Africa. *Theor. Appl. Climatol.*, doi: 10.1007/s00704-012-0614-1.

Alerich, Carol L., 1993: Forest statistics for Pennsylvania: 1978 and 1989. *Res. Bulletin NE-126*, U. S. Department of Agriculture, Forest Service, Northeastern Forest Experiment Station.

Alerich, Carol L. and David A. Drake, 1995: Forest statistics for New York: 1980 and 1993. *Res. Bulletin NE-132*, U. S. Department of Agriculture, Forest Service, Northeastern Forest Experiment Station.

Alerich, Carol L., 2000a: Forest statistics for Connecticut: 1985 and 1998. U.S. Department of Agriculture, Forest Service, Northeastern Forest Experiment Station.

Alerich, Carol L., 2000b: Forest statistics for Massachusetts: 1985 and 1998. *Resource Bulletin NE-148*. U. S. Department of Agriculture, Forest Service, Northeastern Research Station.

Alerich, Carol L., 2000c: Forest statistics for Rhode Island: 1985 and 1998. *Res. Bull. NE-149*, U. S. Department of Agriculture, Forest Service, Northeastern Research Station.

Alpert P., and M. Mandel, 1986: Wind variability – An indicator for mesoclimatic change in Israel. *J. Climate Appl. Meteor.*, **25**, 1568-1576.

Armstrong, George R, and John C. Bjorkbom, 1956: The timber resources of New York. U. S. Department of Agriculture, Forest Service, Northeastern Forest Experiment Station.

Asner, G. P., A. J. Elmore, L. P. Olander, R. E. Martin, and A. Harris, 2004: Grazing systems, ecosystem responses, and global change. *Ann. Rev. Environ. Resources*, **29**, 261-299.

Avissar, Roni and David Werth, 2004: Global hydroclimatological teleconnections resulting from tropical deforestation. *J. of Hydrometeorology*, **6**, 134-145.

Ban-Weiss, George A., Bala Govindasamy, Long Cao, Julia Pongratz, and Ken Caleira, 2011: Climate forcing and response to idealized changes in surface latent and sensible heat. *Environmental Research Letters*, **6**. doi: 10.1088/1748-9326/6/3/034032.

Bonan, Gordon B., 2008: Forests and climate change: forcings, feedbacks and the climate benefits of forests. *Science*, **380**, 1444-1449. doi: 10.1126/science.1155121.

Bounua, L., G. J. Collatz, S. O. Los, P. J. Sellers, D. A. Dazlich, C. J. Tucker, and D. A. Randall, 2000: Sensitivity of climate to changes in NDVI. *J. of Clim.*, **13**, 2277-2292.

Brooks, Robert T., David B. Kittredge, and Carol L. Alerich, 1993: Forest resources of southern New England. *Res. Bull. NE-127*, U. S. Department of Agriculture, Forest Service, Northeastern Forest Experiment Station.

Butler, B. J., G. Boyce, W. McWilliams, B. O'Connell, 2010a: Massachusetts' forest resources 2007. *Resource Note NRS-46*. U. S. Department of Agriculture, Forest Service, Northern Research Station.

Butler, B. J., W. McWilliams, B. O'Connell, and B. Payton, 2010b: Rhode Island's forest resources, 2007. *Res. Note NRS-48*, U. S. Department of Agriculture, Forest Service, Northern Research Station.

Butler, Brett J., Cassandra Kurtz, Christopher Martin, and W. Keith Moser, 2011: Connecticut's forest resources 2010. *Res-Note NRS-107*, U. S. Department of Agriculture, Forest Service, Northern Research Station.

Claussen M., Brovkin V, and Ganopolski A, 2001: Biogeophysical versus biogeochemical feedbacks of large scale land cover change. *Geophys. Res. Lett.*, **28**, 1011-1014.

Davin, E, and de Noblet Ducloudre N, 2010: Climatic impact of global-scale deforestation: radiative versus nonradiative processes. *J. Clim.*, **23**, 97-112.

DeFries, R, Bounoua L, and Collatz G, 2002: Human modification of the landscape and surface climate in the next fifty years. *Glob. Change Biol.*, **8**, 438-458.

Deser, C., G. Magnusdottir, R. Saravanan, and A. Phillips, 2004: The effects of North Atlantic SST and sea-ice anomalies on the winter circulation in CCM3, Part II: Direct and indirect components of the response. *J. Climate*, **17**, 877-889.

Dickson, David R. and Carol L. McAfee, 1988a: Forest statistics for Connecticut – 1972 and 1985. *Resource Bulletin NE-105*, U.S. Department of Agriculture, Forest Service, Northeastern Forest Experiment Station

Dickson, David R. and Carol L. McAfee, 1988b: Forest statistics for Massachusetts – 1972 and 1985. *Resource Bulletin NE-106*, U.S. Department of Agriculture, Forest Service, Northeastern Forest Experiment Station.

Dickson, David R. and Carol L. McAfee, 1988c: Forest Statistics for Rhode Island – 1972 and 1985. *Res. Bull. NE-104*, U. S. Department of Agriculture, Forest Service, Northeastern Forest Experiment Station.

Diffenbaugh, Noah S., 2009: Influence of modern land cover on the climate of the United States. *Clim. Dyn.*, **33**, 945-958. doi: 10.1007/s00382-009-0566-z.

Duriex, L., L. Machado, and H. Laurent, 2003: The impact of deforestation on cloud cover over the Amazon arc of deforestation. *Remote Sensing of Environment*, **86**, 132-140.

Enger, L. and M. Tjernstrom, 1991: Estimating the effects on the precipitation climate in a semiarid region caused by an artificial lake using a mesoscale model. *J. Appl. Meteorol.*, **30**, 227-250.

Ferguson, Roland H. and Milford C. Howard, 1956: A report on the timber resources of Rhode Island. U.S. Department of Agriculture, Forest Service, Northeastern Forest Experiment Station.

Ferguson, Roland H. and John R. McGuire, 1957: A report on the timber resources of Massachusetts. U.S. Department of Agriculture, Forest Service, Northeastern Forest Experiment Station.

Ferguson, Roland H., 1958: A report on the timber resource of Maine. U.S. Department of Agriculture, Forest Service, Northeastern Forest Experiment Station.

Ferguson, Roland H. and Franklin R. Longwood, 1960: A report on the timber resources of Pennsylvania. U.S. Department of Agriculture, Forest Service, Northeastern Forest Experiment Station.

Ferguson, Roland H. and Victor S. Jensen, 1963: The timber resources of New Hampshire. *Forest Resource Report NE-1*, U. S. Department of Agriculture, Forest Service, Northeastern Forest Experiment Station.

Ferguson, Roland H., 1968: The timber resources of Pennsylvania. *Res. Bulletin NE-8*, U. S. Department of Agriculture, Forest Service, Northeastern Forest Experiment Station.

Ferguson, Roland H. and Carl E. Mayer, 1970: The timber resources of New York. *Resource Bulletin NE-20*, U. S. Department of Agriculture, Forest Service, Northeastern Forest Service Experiment Station.

Ferguson, Roland H. and Neal P. Kingsley, 1972: The timber resources of Maine. U.S. Department of Agriculture, Forest Service, Northeastern Forest Experiment Station.

Forster P, Ramaswamy V, Artaxo P, Berntsen T, Betts R, Fahey DW, Haywood J, Lean J, Lowe DC, Myhre G, et al., 2007: Radiative forcing of climate change. *Climate Change 2007: The Physical Science Basis. Contribution of Working Group I to the Fourth Assessment Report of the Intergovernmental Panel on Climate Change*. Cambridge and New York, NY: Cambridge University Press, 129-234.

Frieswyk, Thomas S. and Anne M. Malley, 1985a: Forest statistics for New Hampshire: 1973 and 1983. *Resource Bulletin NE-88*, U. S. Department of Agriculture, Forest Service, Northeastern Station.

Frieswyk, Thomas S. and Anne M. Malley, 1985b: Forest statistics for Vermont: 1973 and 1983. *Res. Bull. NE-87*, U. S. Department of Agriculture, Forest Service, Northeastern Station.

Frieswyk, Thomas and Richard Widmann, 2000a: Forest statistics for New Hampshire: 1983 and 1997. *Resource Bulletin NE-146*, U. S. Department of Agriculture, Forest Service, Northeastern Research Station.

Frieswyk, Thomas and Richard Widmann, 2000b: Forest statistics for Vermont: 1983 and 1997. *Res. Bull. NE-145*, U. S. Department of Agriculture, Forest Service, Northeastern Research Station.

Gash, J. H. C. and C. A. Nobre, 1997: Climatic effect of Amazonian deforestation: some results from ABRACOS. *Bull. Amer. Meteorol. Soc.*, **78**, 823-830. Doi: 10.1175/1520-0477(1997)078<0823:CEOADS>2.0.CO;2.

Griffith, Douglas M. and Carol L. Alerich, 1996: Forest Statistics for Maine, 1995. *Resource Bulletin NE-135*, U.S. Department of Agriculture, Forest Service, Northeastern Station.

Griswold, Norman B. and Roland H. Ferguson, 1957: A report on the timber resource in Massachusetts. U.S. Department of Agriculture, Forest Service, Northeastern Forest Experiment Station.

Hurrell, James W., James J. Hack, Dennis Shea, Julie M. Caron, and James Rosinski, 2008: A new sea surface temperature and sea ice boundary dataset for the community atmosphere model. *J. Climate*, **21**, 5145-5153.

IPCC, 2007: Climate change 2007: impacts, adaptation, and vulnerability. In: Parry ML, Canziani OF, Palutik JP, van der Linden PJ, Hanson CE (eds). *Contribution of Working Group II to the Fourth Assessment Report of the Intergovernmental Panel on Climate Change*. Cambridge University Press, Cambridge, 976.

Kingsley, Neal P. and Joseph E. Barnard, 1968: The timber resources of Vermont. *Res. Bull. NE-12*, U. S. Department of Agriculture, Forest Service, Northeastern Forest Experiment Station.

Kingsley, Neal P., 1976: The forestland owners of southern New England, *Res. Bull. NE-41*, U.S. Department of Agriculture, Forest Service, Northeastern Research Station.

Larson, E. vH., J. C. Rettie, A. M. Gilbert, and J. R. McGuire, 1954: The Forest Resources of New Hampshire. *Forest Resource Report 8*, U. S. Department of Agriculture, Forest Service, Northeastern Forest Experiment Station.

Los, S. O., C. O. Justice, and C. J. Tucker, 1994: A global 1 by 1 degree NDVI data set for climate studies derived from the GIMMS continental NDVI data. *International Journal of Remote Sensing*, **15**, 3493-3518.

Lyons, T.J., P. Schwerdtfeger, J. M. Hacker, I. J. Foter, R. C. G. Smith, and X. Huang, 1993: Land atmosphere interaction in a semiarid region: the bunny fence experiment, *Bull. Am. Meterol. Soc.*, **74**, 1327-1334.

Lyons, T. J., 2002: Clouds prefer native vegetation. *Meteorol. Atmos. Physics*, **80**, 131-140. doi: 10.1007/s007030200020.

Malhi, Yadvinder et al., 2008: Climate change, deforestation, and the fate of the Amazon. *Science*, **319**, 169-172. doi: 10.1126/science.1146961.

Meher-Homiji, V. M., 1991: Probable impact of deforestation on hydrological processes. *Climate Change*, **19**, 163-173.

McCaskill, G. L., W. H. McWilliams, B. J. Butler, D. M. Meneguzzo, C. J. Barnett, M. H. Hansen, 2011: Pennsylvania's forest resources 2009. *Res. Note NRS-90*, U. S. Department of Agriculture, Forest Service, Northern Research Station.

McGuire, John R. and Robert D. Wray, 1952: Forest statistics for Vermont. U. S. Department of Agriculture, Forest Service, Northeastern Forest Experiment Station.

McWilliams, W. H., B. J. Butler, D. M. Griffith, M. L. Hoppus, A. J. Lister, T. W. Lister, R. S. Morin, L. B. Stewart, and J. A. Westall, 2005: The forests of Maine: 2003. *Resource Bulletin NE-164*, U. S. Department of Agriculture, Forest Service, Northeastern Research Station.

McWilliams, W. H., S. P. Cassell, C. L. Alerich, B. J. Butler, M. L. Hoppus, S. B. Horsley, A. J. Lister, T. W. Lister, R. S. Morris, C. H. Perry, J. A. Westall, E. H. Wharton, C. W. Woodall, 2007: Pennsylvania's forests, 2004. *Res. Bull. NRS-20*, U. S. Department of Agriculture, Forest Service, Northern Research Station.

Morin, R. S., G. M. McCaskill, W. McWilliams, M. Tansey, 2010: New Hampshire's forest resources 2007. *Res. Note. NRS-56*, U. S. Department of Agriculture, Forest Service.

Morin, R. S., M. Nelson, and R. De Geus, 2011: Vermont's forest resources 2010. *Res. Note NRS-105*, U. S. Department of Agriculture, Forest Service, Northern Research Station.

Nair, Udaysankar S., Y. Wu, J. Kala, T. J. Lyons, R. A. Pielke Sr., and J. M. Hacker, 2011: The role of land use change on the development and evolution of the west coast trough, convective clouds, and precipitation in southwest Australia. *J. of Geophys. Res.*, **116**. doi: 10.1029/2010JD014950.

Otterman, J., D. O' C Starr, A. Manes, A. Rubin, and P. Alpert, 1990: An increase of early rains in southern Israel following land-use change? *Boundary-Layer Meteor.*, **53**, 333-351.

Pielke Sr., Roger A, 2001: Influence of the spatial distribution of vegetation and soils on the prediction of cumulus convective rainfall. *Review of Geophysics*, **39**, 151-177.

Pielke Sr., R. A., J. Adegoke, A. Beltran-Przekurat, C. A. Hiemstra, J. Lin U. S. Nair, D. Niyogi, and T. E. Nobis, 2007: An overview of regional land-use and land-cover impacts on rainfall. *Tellus*, **59B**, 587-601.

Pielke Sr., Roger A. et al., 2011: Land use/land cover changes and climate: modeling analysis and observational evidence. *WIREs Clim Change*, **2**: 828-850. doi: 10.1002/wcc.144

Pinty, J.-P., P. Mascart, E. Richard, and R. Rosset, 1989: An investigation of mesoscale flows induced by vegetation in homogeneities using an evapotranspiration model calibrated against HAPEX-MOBILHY data. *J. Appl. Meteor.*, **28**, 976-992.

Pitman, A. J., G. T. Narisma, R. A. Pielke Sr., N. J. Holbrook, 2004: Impact of land cover change on the climate of southwest Western Australia. *J. of Geophys. Res.*, **109**. doi: 10.1029/2003JD004347.

Powell, Douglas S. and David R. Dickson, 1984: Forest statistics for Maine: 1972 and 1982. *Resource Bulletin NE-81*, U.S. Department of Agriculture, Forest Service, Northeastern Station.

Powell, Douglas S., 1985: Forest Composition of Maine: An Analysis Using Number of Trees. *Resource Bulletin NE-85*, U.S. Department of Agriculture, Forest Service, Northeastern Station.

Rabin, Robert M., Steven Stadler, Peter J. Wetzler, David J. Stensrud, and Mark Gregory, 1990: Observed effects of landscape variability on convective clouds. *Bull. of the Am. Met. Soc.*, **71**, 272-280.

Randall, D. A., D. A. Dazlich, C. Zhang, A. S. Denning, P. J. Sellers, C. J. Tucker, L. Bounoua, J. A. Berry, G. J. Collatz, C. B. Field, S. O. Los, C. O. Justice, and I. Fung, 1996: A revised land surface parameterization (SiB2) for GCMs. Part III: The Greening of the Colorado State University General Circulation Model. *J. Climate*, **9**, 738-763.

Ray, D. K., U. S. Nair, R. O. Lawton, R. M. Welch, and R. A. Pielke, Sr., 2006: Impact of land use on Costa Rican tropical montane cloud forests: Sensitivity of orographic cloud formation to deforestation in the plains. *J. Geophys. Res.*, **111**, d020108. doi: 10.1029/2005JD006096.

de Ridder, Koen and Hubert Gallée, 1998: Land surface-induced regional climate change in Southern Israel. *J. of App. Meteorol.*, **37**, 1470-1485.

Russell, Emily W.B. and Ronald B. Davis, 2001: Five centuries of changing forest vegetation in the Northeastern United States. *Plant Ecology*, **155**, 1-13.

Schrieber, Kelly, Roland Stull, and Qing Zhang, 1996: Distributions of surface-layer buoyancy versus lifting condensation level over a heterogeneous land surface. *J. of the Atms. Sci.*, **53**, 1086-1107.

Sellers, Piers J., Sietse O. Los, Compton J. Tucker, Christopher O. Justice, Donald A. Dazlich, G. James Collatz, and David A. Randall, 1996a: A revised land surface parameterization (SiB2) for atmospheric GCMs, Part II: The generation of global fields of terrestrial biophysical parameters from satellite data. *J. of Clim.*, **9**, 706-737.

Stebbing, E. P., 1935: The encroaching Sahara. *J. Geogr.*, **86**, 509-516.

Steyaert, Louis T. and Robert G. Knox, 2008: Reconstructed historical land cover and biophysical parameters for studies of land-atmosphere interactions within the eastern United States. *J. of Geophys. Res.*, **113**, D02101. doi: 10.1029/2006JD008277.

Strack, John E., Roger A. Pielke Sr., Louis T. Steyaert, and Robert G. Knox, 2008: Sensitivity of June near-surface temperatures and precipitation in the eastern United States to historical land cover changes since European settlement. *Water Resources Research*, **44**, W11401. doi: 10.1029/2007WR006546.

Sud, Y.C., R. Yang, and G. K. Walker, 1996: Impact of in situ deforestation in Amazonia on the regional climate: General circulation model simulation study. *J. of Geophys. Res.*, **101**, 7095-7109.

Swank, W. T. and J. M. Vose, 1994: Long-term hydrologic and stream chemistry responses of southern Appalachian catchments following conversion from mixed hardwoods to white pine. *Hydrologie kleiner Einzugsgebiete*, **35**, 164-172.

Veen, Arthur W. L., Wim Klaasen, Bart Kruijt, and Ronald W.A. Hutjes, 1996: Forest edges and the soil-vegetation-atmosphere interaction at the landscape scale: the state of affairs. *Progress in Physical Geography*, **20**, 292. doi: 10.1177/030-13339602000303.

Wharton, Eric H., Richard H. Widmann, Carol L. Alerich, Charles J. Barnett, Andrew J. Lister, Tonya W. Lister, Don Smith, and Fred Borman, 2004: The Forests of Connecticut. *Resource Bulletin NE-105*, U.S. Department of Agriculture, Forest Service, Northeastern Research Station.

Widmann, R. H., B. J. Butler, and S. Crawford, 2010: New York's forest resources 2008. *Res Note NRS-66*, U. S. Department of Agriculture, Forest Service, Northern Research Station.

Xue, Yongkang, Michael J. Fennessy, and Piers J. Sellers, 1996: Impact of vegetation properties on U. S. summer weather prediction. *J. of Geophys. Res.*, **101**, 7419-7430.

Appendix A: Empirical Orthogonal Function Analysis

Large scale changes in ground cover can alter the location and sources of moisture and heat to the atmosphere (e.g. Pielke et al. 2011, Ban-Weiss 2011, Pielke 2001, Lyons et al. 1993, 2002). Empirical orthogonal function (EOF) analysis was used to investigate potential shifts in spatial variability of mean sea level pressure that resulted from changes in forestation in the northeastern United States locally and throughout the northern Hemisphere. Here, mean sea level pressure was used as a proxy for circulation patterns.

Mean sea level pressure data from two different runs of the BUGS global climate model were used in the EOF analysis. In the model, values were written out every six hours. The time domain was constrained to the summer months (June, July, August). The same five-year model runs as discussed in section 2 were used; for the purposes of this analysis, the entirely forested case study was used in computing the EOFs. The region of interest was expanded for the EOF analysis to 20 to 90 degrees in latitude. All longitudes were included (e.g., figure 4.28). This domain was selected based on the scale of dominant pressure patterns observed in the raw data.

To complete the analysis, matrix A was defined as all mean sea level pressure data in the region of interest from the five summer seasons. The seasonal cycle was then removed from all data in preparation for the analysis. The mean of each month was computed and then removed from all data in each of the occurrences of that month. For example, for the June data, the mean was first computed based on all data from all five June months in the

time domain. This mean value was then subtracted from each data point represented in those five months.

Using singular value decomposition, matrix A was decomposed into the product of three matrices:

$$A = U\Sigma V^T \quad (2.1)$$

The rows of the V^T matrix represented the EOFs of the original matrix A. The columns of the U matrix were the principal component (PC) time series of the data matrix. These time series described the temporal evolution of the corresponding EOF. EOFs significant at the 95% confidence levels and distinct from the other EOFs were used to identify the significant patterns in atmospheric circulations.